Aus dem Bereich Physiologie

Theoretische Medizin und Biowissenschaften

der Medizinischen Fakultät

der Universität des Saarlandes, Homburg/Saar

CAPS (Ca^{2+}-dependent Activator Protein for Secretion) Promotes Maturation of Large Dense Core Vesicles in Adrenal Medulla

Dissertation zur Erlangung des Grades eines Doktors der Naturwissenschaften

der Medizinischen Fakultät

der UNIVERSITÄT DES SAARLANDES

2010

vorgelegt von: Yuanyuan Liu

geb.am: 13.08.1981, in Hubei, China

Tag des Promotionskolloquiums: _____

Dekan: _____

Vorsitzender: _____

Berichterstatter: _____

_____

_____

Acknowledgements

---------- List of Contents ----------

LIST OF CONTENTS

---------- List of Contents ----------

Zusammenfassung

Die regulierte Exozytose von Neurotransmittern und vieler Hormone erfolgt an spezialisierten sekretorischen Komplexen über Ca^{2+}-vermittelte Fusion sekretorischer Vesikel mit der Plasmamembran. Der molekulare Mechanismus der Neurotransmitter- und Hormonausschüttung steht im Focus intensiver Forschung. Viele Proteine, die eine Rolle spielen könnten in der regulierten Form der Exozytose, wurden isoliert. CAPS (calcium-activator protein of secretion) ist ein zytosolisches Protein, das mit large dense core Vesikeln assoziiert ist und an ihrer Sekretion beteiligt ist. Säugetiere exprimieren zwei CAPS-Isoformen mit ähnlicher Domain-Struktur, die unter anderem eine Munc13 Homologie Domaine (MHD) beinhalten, die für das „Priming" von sekretorischen Vesikeln verantwortlich sein soll. Wo CAPS im sekretorischen Prozess agiert ist noch unklar. Wir untersuchten die Sekretion von CAPS-2 KO Chromaffinzellen, die eine ähnliche Sekretion zeigten wie Wildtyp-Zellen. Anschließend untersuchten wir die Sekretion von Chromaffinzellen in denen beide CAPS-Gene deletiert wurden mit dem Ziel die Funktion von CAPS in der regulierten Exozytose zu entschlüsseln.

Die Deletion beider CAPS Isoformen führte zu einer Reduktion des „rapidly releasable pools" der Chromaffingranulen und des „sustained release" bei weiterer Stimulation. Die ähnliche Verteilung von LDCV in CAPS DKO und Wildtypzellen schließt die Möglichkeit aus, dass die verminderte Sekretion in CAPS DKO Zellen durch einen Defekt im „docking" der LDCV hervorgerufen wird. Doppel-Flash-Experimente zeigen, dass nach starker sekretorischer Aktivität in CAPS DKO Zellen im Vergleich zu Wildtyp-Zellen, die Wiederherstellung des RRP stark reduziert ist, aber das Auffüllen des SRP normal bleibt. Die Calcium-Sensitivität der Exozytose wurden durch „calcium ramp" Experimente und die Fusionskinetik durch Einzelspikeanalyse untersucht. Durch die Deletion von CAPS wurde die Calcium-Sensitivität oder die Kinetik der Fusion der einzelnen Vesikel während der Sekretion nicht verändert.

Sowohl CAPS1 als auch CAPS2 können die Sekretion in Zellen, denen beide CAPS-Isoformen fehlen, wiederherstellen. Zusätzlich kann durch die konstitutiv

---------- ZUSAMMENFASSUNG ----------

offene Form von Syntaxin der Verlust des Readily releasable LDCV Pools bei Verlust von CAPS wiederhergestellt werden. Munc13-1 jedoch, ein Priming-Protein, das die Umformung von Syntaxin in die offene Konformation vereinfacht, hat keinen Effekt. Wir schließen daraus, dass CAPS für das Auffüllen und/oder die Erhaltung des rapidly releasable Pools benötigt wird und eher stromabwärts von Munc13s wirkt. Eine funktionelle Interaktion zwischen diesen beiden Proteinen scheint während des gesamten LDCV-Priming Prozesses nötig zu sein, einschließlich der Öffnung von Syntaxin.

Abbreviations

$[Ca^{2+}]_i$	Intracellular calcium concentration
ATP	Adenosine Triphosphate
BHK	Syrian Hamster Kidney
BoNT	Botulinum Toxin
Bp	Base pair
BSA	Bovine Serum Albumin
C. elegans	Caenorhabditis elegans
Ca^{2+}	Calcium
cAMP	Cyclic adenosine monophosphate
CAPS	Calcium-dependent activator protein for secretion
C_m	Membrane capacitance
DAG	Diacylglycerol
dATP	Deoxyriboadenosine Triphosphate
DEPC	Diethylpyrocarbonate
DMEM	Dulbecco's Modified Eagle's Medium
DMSO	Dimethylsulphoxide
DNA	Deoxyribonuleotide
dNTP	Desoxyribonucleotide
DKO	CAPS-1/CAPS-2 double knock-out
DPTA	1,3-Diamino-2-propanol-N,N,N,N-tetraacetic acid
DTT	1,4-Dithiotheritol
ECL	Enhanced Chemiluminescence
EDTA	Ethylene Diamine Tetra-Acetic Acid
EGFP	Enhanced Green Fluorescent Protein
EGTA	Ethylene bis-(oxyethylenenitrilo)-tetraacetic acid
EM	Electron Microscope
ER	Endoplasmic Reticulum
FCS	Fetal Calf Serum
fF	Femtofarad

---------- Abbreviations ----------

Fig	Figure
GA	Golgi apparatus
GFP	Green Fluorescent Protein
GTP	Guanidine Triphosphate
H_2O	Water
HEPES	4-(2-hydroxyethyl)-1-piperazineethanesulfonic acid
IRES	Internal Ribosome Entry Site
K_d	Dissociation constant
KDa	Kilo Dalton
KHz	Kilohertz
LDCV	Large Dense-Core vesicle
MHD	Munc Homology Domain
mOsm	Milliosmol
MSD	Mean Square Displacement
n	Number of measured cells
N	Number of measured mice
NGS	Normal Goat Serum
NP-EGTA	Nitrophenyl-EGTA
NPY	Neuro-peptide Y
nS	nano Siemens
NSF	N-ethylmaleimide sensitive factor
PBS	Phosphate Buffered Saline
PC-12 cells	Pheochromocytoma cells
PCR	Polymerase Chain Reaction
pH	Potential hydrogen
PKA	Protein kinase A
PKC	Protein kinase C
PM	Plasma Membrane
PMA	Phorbol-12-myristate-13-acetate
PV	Polyvirus
R_m	Membrane resistance (resistance of the cell)

---------- Abbreviations ----------

RNA	Ribonucleic acid
RNase	Ribonuclease
RPM	Revolutions per minute
RRP	Rapidly-releasable pool
R_s	Series Resistance (pipette resistance)
RT	Room Temperature
S	Siemens
SDS	Sodium Dodecyl Sulfate
SEM	Standard Error of Mean
SFV	Semliki Forest Virus
SNAP-25	Synaptosome Associated Protein of 25 kD
SNARE	Soluble NSF Attachment Protein Receptor
SRP	Slowly releasable pool
SV	Synaptic Vesicle
TAE-Buffer	Tris acetate EDTA buffer
TeNt	Tetanus Toxin
TGN	Trans-Golgi network
Tris	2-Amino-2(hydroxymethyl)-1,3-propanediol
U	Voltage
UPP	Unprimed Pool
UV	Ultra violet
VAMP	Vesicle Associated Membrane Protein
α-SNAP	α-Soluble NSF Attachment Protein
μL	Microliter

1. Introduction

1.1 Regulated exocytosis and neurotransmitter release

Exocytosis is an important pathway for the movement of substances across membranes. Two distinct pathways use exocytosis to release materials into the extracellular space, a constitutive exocytotic pathway and a non-constitutive regulated exocytotic pathway. Constitutive exocytosis, present in all eukaryotic cells, mediates the transport of soluble proteins and other materials from Golgi complex to the cell surface, supplies newly synthesized lipid and membrane protein to the plasma membrane, and provides nutrients to cells. It is essential for the maintenance and reconstitution of cells. There is no evidence that constitutive exocytosis requires a stimulatory signal.

Regulated exocytosis is present in some more specialized cells, such as neurons and neuroendocrine cells. In contrast to constitutive exocytosis, regulated exocytosis requires a stimulus to induce secretion. This stimulus varies according to cell type. The secretory products for regulated exocytosis are concentrated and packed into specialized membrane-bound organelles, secretory granules, and these granules can be stored for long periods of time and thus can form a large intracellular pool of mature secretory products (Burgess and Kelly, 1987). Regulated exocytosis constitutes the basis of neurotransmission, and has been extensively studied in neurons and neuroendocrine cells. Two types of secretory granules are found, which differ in their contents. Vesicles containing classical neurotransmitters, which are released rapidly at synapses, are small clear vesicles (SCVs), while vesicles containing neuropeptides and neurotransmitters, exhibiting large dense core under electron microscope, are termed large dense core vesicles (LDCVs). LDCVs are larger than SCVs. Both SCVs and LDCVs are present in neurons and neuroendocrine cells.

Ca^{2+} evoked neurotransmitter release is temporally and spatially tightly regulated. According to the results from morphological studies, vesicles in the synapse are restricted to designated release sites at so-called active zones. Only a fraction of the

vesicles contacting the plasma membrane are readily releasable (Sudhof, 1995). In neuroendocrine cells such as adrenal chromaffin cells and pancreatic β cells, there is no active zone, but a fraction of vesicles also are found in close apposition to the plasma membrane. When an action potential occurs, Ca^{2+} influx through voltage-gated Ca^{2+} channel stimulates the fusion of vesicles containing neurotransmitter with the plasma membrane. Released neurotransmitters diffuse across the synaptic cleft and bind to postsynaptic receptors to produce a new electrical signal. This excitation coupled exocytosis is a very fast process occurring in less than 1ms (Borst and Sakmann, 1996). In cerebellar synapses, the delay between the Ca^{2+} influx and postsynaptic response is 60 µs (Sabatini and Regehr, 1996); in the giant terminals of the calyx of Held it is 300 µs (Bollmann et al., 2000). Ca^{2+} triggered secretion in adrenal chromaffin cells is slower than that in neurons and occurs within 1-20 ms (Voets, 2000). This rapid and precisely regulated exocytosis is tightly controlled by a sophisticated regulatory protein machinery which has been intensively studied.

The work presented here is focused on the role of CAPS (Ca^{2+}-dependent activator protein for secretion) in the regulated exocytosis of mouse chromaffin cells. CAPS is a cytosolic protein that associates with large dense core vesicles and is involved in their secretion. In this study, the role of CAPS in regulated exocytosis of mouse chromaffin cells was investigated using genetic and electrophysiological methods.

1.2 Key steps of regulated exocytosis

Before vesicles arrive at their destination and fuse with the membrane, they must undergo a series of maturation steps (Fig. 1). Synaptic vesicles bud from the early endosome, and are then filled with neurotransmitter by vesicular transporters which are driven by a proton gradient across the vesicular membrane (Tooze et al., 2001). Packed vesicles are delivered to the plasma membrane and cluster at the active zone. Vesicles are eventually tethered and held close to the membrane, which is called docking. Vesicles go through further maturation steps to become releasable and then are available for release when triggered by a rise in $[Ca^{2+}]_i$. The maturation to the releasable state is referred to as priming. Finally vesicles fuse with the

membrane upon an increase of the intracellular calcium. Secretory granules in chromaffin cells originate from the Trans-Golgi network (Burgoyne and Morgan, 2003). The uptake of the catecholamine into secretory granules relies on active transport driven by a proton gradient. Prior to exocytosis, secretory granules in chromaffin cells undergo the same sequential steps as synaptic vesicles. After exocytosis, vesicles can be retrieved by endocytosis via several pathways.
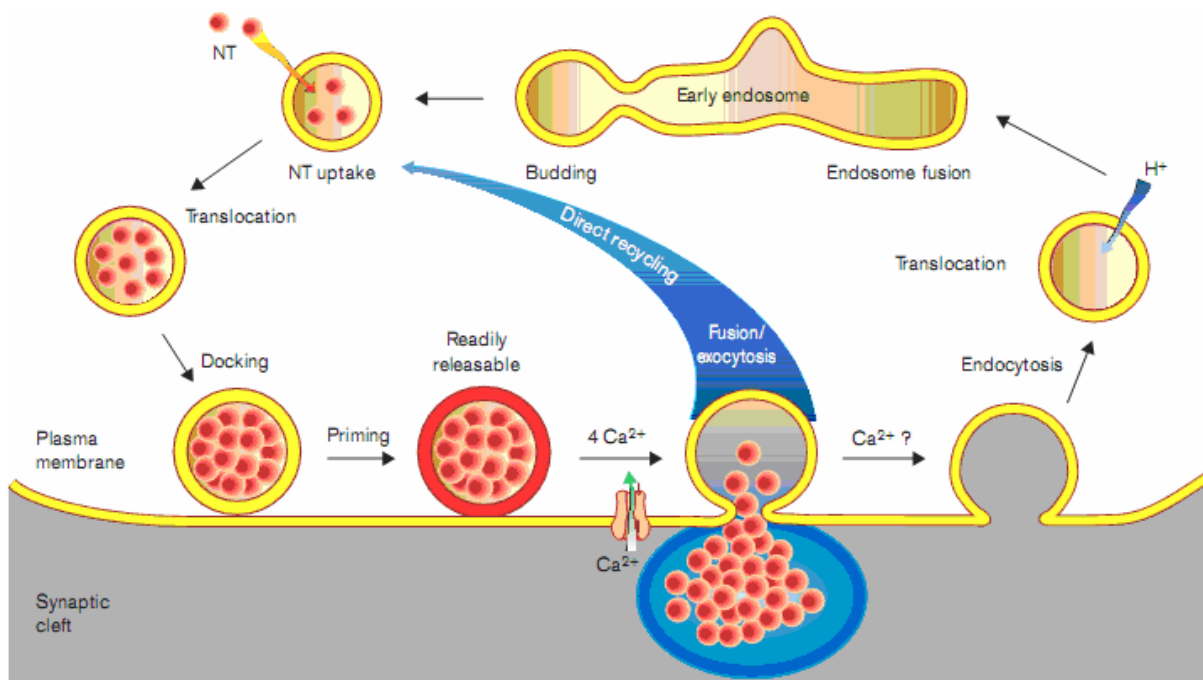
Figure 1. A general depict of vesicular recycling. (Modified from (Brose et al., 2000))

1.2.1 Docking

Docked vesicles are traditionally defined as those vesicles that appear closely apposed to the plasma membrane in electron micrographs (Verhage and Sorensen, 2008). Due to the definition of docking, docking has been studied mainly by electron microscopy. In neurons, vesicles are clearly visualized under the electron microscope and found accumulated at active zones. In chromaffin cells, secretory granules containing neuropeptides are easily identified by their large dense core. These vesicles distribute along the plasma membrane of the whole cell. The distribution of vesicles with respect to the plasma membrane is typically determined to examine docked vesicles. There are two different criteria to determine the docked vesicles. (1)

Vesicles within a distance from the plasma membrane are docked vesicles; normally this certain distance is smaller or equal to the average of a vesicle radius (Borisovska et al., 2005). (2) Vesicles in direct contact with the plasma membrane are docked vesicles, which means there is no measurable distance between the docked vesicles and the plasma membrane (Schikorski and Stevens, 2001). Both methods have flaws. The first method sets a large range for counting docked vesicles thus may overestimate the number of docked vesicles. The second method is quite stringent and thus underestimates the number of docked vesicles. The cumulative distance distribution of vesicles to the plasma membrane is used to estimate docked vesicles. If there was an augmentation or defect in docking, the plot of cumulative distance distribution will show a deviation at short distances from plasma membrane. Recently it has been suggested that conventional chemical fixation for electron microscopy might change the cell ultrastucture and cause modification of vesicle localization (Hammarlund et al., 2007). High-pressure freezing has been developed to improve sample preparation. The specimen is frozen by liquid nitrogen under high pressure (200 MPa) to avoid ice crystal formation in the cytoplasm (Studer et al., 2008). Cryofixation at high-pressure better preserves cell ultrastucture and circumvents artefacts caused by conventional chemical fixation. Electron microscopy combined with high-pressure freezing might allow high resolution imaging of vesicles in a close-to-native state. Its application has begun to change our view of the docked state. Although electron microscopy provides helpful information for investigation of docking, it delivers a static picture of vesicle distribution. Dynamic information of concerning changes in docking is more difficult to acquire. Total internal reflection fluorescence (TIRF) microscopy allows one to track vesicle movement near the target membrane. Vesicles are labelled by fluorescent cargo or fluorescent dye. As TIRF microscopy selectively excites the fluorophores in cellular environment very near to a solid surface (within ≤100 nm) (Axelrod, 2001), only vesicles that are very close to the membrane can be visualized. Docked vesicles are within this range, as they appear to be tethered to the plasma membrane (Toonen et al., 2006). Analysis of movements and mobility of vesicles may allow quantification of vesicles docking in living cells (Nofal et al., 2007). However TIRF microscopy can only track a fraction of

vesicles in a cell depending on how and what percent of vesicles are effectively labelled by fluorescent cargo or fluorescent dye. This makes it difficult to compare the results from electron microscopy and TIRF microscopy. TIRF microscopy supplements electron microscopy by giving dynamic information about single vesicle movement at the plasma membrane.

1.2.2 Priming

When $[Ca^{2+}]_i$ is suddenly increased from resting level (~ 100 nM) to tens of µM, vesicles are released as a rapid exocytotic burst. The exocytotic burst represents the secretion from primed vesicles in a readily releasable pool. If the calcium concentration remains high, releasable pools are rapidly emptied. However the number of vesicles in the readily releasable pool calculated from the amplitude of exocytotic burst, are much fewer than that of the docked vesicles recognized in electron micrographs (Steyer et al., 1997). This indicates that only a fraction of docked vesicles are fully mature and readily releasable. This is the primed pool of vesicles.

Upstream of the readily releasable pool is a Depot pool (DP) and the docked but unprimed pool (UPP). Vesicles from the Depot pool undergo docking to enter a docked but unprimed state, then prime into the readily releasable pool. The readily releasable pool can be further divided into a rapidly releasable pool (RRP) and a slowly releasable pool (SRP) distinguished by different release kinetics. Capacitance measurements combined with flash photolysis of caged calcium compounds are used to dissect the releasable pools. Vesicle fusion induces an increase of plasma membrane area which can be detected electrically as an increase of cell capacitance. Capacitance measurements allow high temporal resolution, and thus allow the accurate kinetic analysis of vesicle fusion. As Ca^{2+} is the messenger to trigger the exocytosis and the secretory rate is related to $[Ca^{2+}]_i$, different manipulations to increase $[Ca^{2+}]_i$ can affect the time course of exocytosis (Sorensen, 2004). Photolysis of Ca^{2+}-caged compounds provide a good way to control $[Ca^{2+}]_i$. Ca^{2+} bound to the calcium caging compounds, NP-EGTA (Nitrophenyl-EGTA) or DMN (DM-Nitrophen), is perfused into cells through a glass patch pipette. Upon UV illumination, the affinity

of NP-EGTA or DMN for Ca^{2+} is greatly reduced in a few microseconds. The intracellular free calcium concentration is quickly elevated throughout the cell. Using calcium-sensitive fluorescence dyes, $[Ca^{2+}]_i$ can be measured in real time before and after UV flash. In such a flash experiment shown in Fig. 2, $[Ca^{2+}]_i$ is raised from a base level of about 300 nM to near 20 µM in a bovine chromaffin cell, secretion is measured as the increase of capacitance, and released catecholamines are detected by amperometry. The capacitance trace can be fit as the sum of two exponentials and a linear component. The exponential component with a fast time constant, called the fast burst, represents the secretion from RRP; the slower exponential component is the slow burst and represents the secretion from SRP. The amplitudes of the fast and slow bursts estimate the size of RRP and SRP respectively. Voets showed that the RRP and SRP sizes are dependent upon the preflash $[Ca^{2+}]_i$ thus indicating that the priming process is Ca^{2+}-dependent (Voets, 2000). After the readily releasable pool is depleted, unprimed vesicles under sustained high $[Ca^{2+}]_i$ go through the priming reaction and then fuse with the plasma membrane. Thus the linear sustained phase following the fast exocytotic burst reflects priming, under high intracellular calcium concentration.

According to the electrophysiological data, priming is defined as a post-docking step, which results in vesicles becoming fusion competent. However studies from permeabilized PC12 cells indicate that Mg-ATP is necessary to support sustained secretion (Hay and Martin, 1992). This may indicate that the priming is ATP dependent. However these results come from biochemical experiments which are too slow to distinguish priming from release, and are rate-limited by several factors, for example, PIP_2 and SNARE proteins (Hay and Martin, 1993; Lang et al., 2002). To study the priming process, a high time resolution method is needed, which is best achieved by whole cell capacitance measurements.
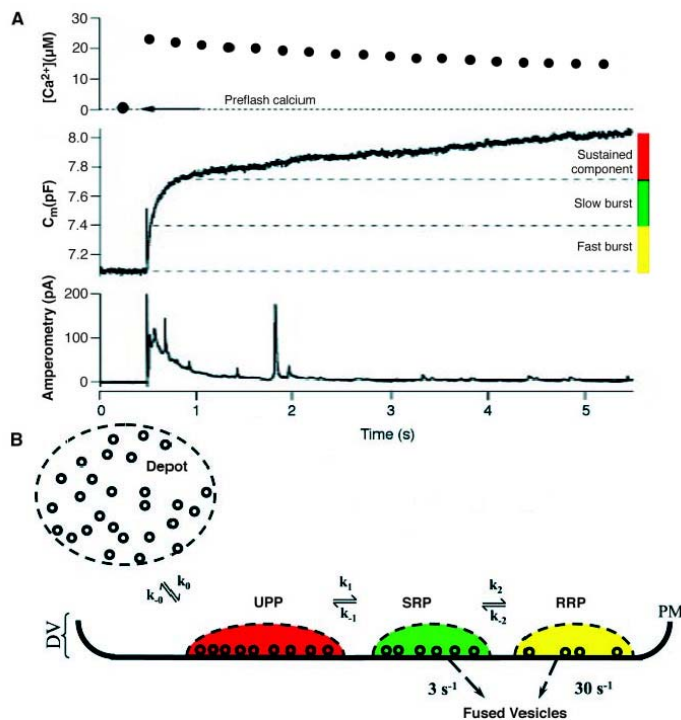
Figure 2. Vesicle pools and flash responses.
A. A typical flash photolysis response cooperated with carbon fibre microelectrode. Upper is a step increase of $[Ca^{2+}]_i$ from 300 nM (basic level) to 20 µM. Middle is the increase of membrane capacitance. Lower is the related change of amperometric signal.
B. Vesicles are depicted in four different states. In time sequence are Depot pool, UPP (red, unprimed vesicles pool), SRP (green, solid release pool) and RRP (yellow, ready release pool). (Modified from (Rettig and Neher, 2002))

1.2.3 Ca²⁺ triggering

Ca^{2+} has multiple roles in neurotransmitter release not only accelerating the recruitment of vesicles (priming) but also triggering the fusion of vesicles. Under physiological circumstances, neurotransmitter release is evoked by Ca^{2+} influx through the voltage-dependent Ca^{2+} channels during membrane depolarization. Depolarization studies in neuroendocrine cells show that short depolarizations induce the release of fewer vesicles than do long depolarizations, and indicate that there is an immediately releasable pool (Horrigan and Bookman, 1994; Moser and Neher, 1997). Comparison of the results obtained from depolarization and flash photolysis experiments reveal that only a small fraction of the vesicles in the RRP can be rapidly released in response to the brief depolarization (Voets et al., 1999). This indicates that vesicles in immediately releasable pool (IRP) exhibit fast fusion rates due to their close proximity to Ca^{2+} channels, rather than to a difference of fusion competence state or Ca^{2+} sensitivity. Depolarization induces Ca^{2+} influx though the voltage-dependent Ca^{2+} channels and produces a complicated spatial distribution of Ca^{2+} signal. Peak $[Ca^{2+}]_i$ within the microdomain of 10-20 nm around the Ca^{2+} channel can reach 100 µM or more in less than 100 µs after the channel has opened,

15

with a distance of 100-200 nm the peak values rise slowly and are only in the micromolar or tens of micromolar range (Neher, 1998). Because at different distances from Ca^{2+} channels, different calcium signals occur. Vesicles which are equally competent to fuse show different fusion rates. To circumvent this complication, and to establish the relationship between vesicle fusion rates and $[Ca^{2+}]_i$, photolysis of caged Ca^{2+} is used to produce spatially uniform $[Ca^{2+}]_i$ elevations which are measured fluometrically. Release rates are estimated on the basis of capacitance measurements. Two different methods are used to elevate $[Ca^{2+}]_i$, UV flash, and ramp experiments, respectively. In flash experiments, a stepwise increase of $[Ca^{2+}]_i$ triggers secretion, and time constants of the SRP and the RRP are referred as the secretory rates which are correlated to the postflash $[Ca^{2+}]_i$ with a three to four power relationship (Voets, 2000). In ramp experiments, $[Ca^{2+}]_i$ is elevated slowly by applying a series of illuminations altering between 350 nm and 380 nm, Ca^{2+}-dependence of the secretory rate is determined (Sorensen et al., 2001). Both flash and ramp experiments can be used to investigate the Ca^{2+}-dependence of secretion, however ramp experiments slowly elevate $[Ca^{2+}]_i$ from nM range to tens of µM thus allowing determination of the $[Ca^{2+}]_i$ threshold of secretion.

1.2.4 Fusion

Vesicle fusion with the plasma membrane is the final step of secretion. Fusion of lipid bilayers starts with close proximity of vesicles and plasma membrane. The boundary between the hydrophilic and hydrophobic portion of the bilayer is destabilized. The membranes form non-bilayer transition states and initiate the formation of an aqueous fusion pore (Jahn et al., 2003). The fusion pore was first investigated in mast cells by using quick-freezing and freeze-fracture techniques. It is a narrow-necked pore, 0.1 micrometer in diameter connecting the granule interior and the extracellular space (Chandler and Heuser, 1980). Electrophysiological studies in mast cells examined the conductance of fusion pore and revealed that the membrane fusion begins with the formation of a fusion pore and later the fusion pore dilates to allow the release of vesicle content (Breckenridge and Almers, 1987). Electrochemical methods are available to directly detect the transmitters released

from single cells (Leszczyszyn et al., 1990). Studies in chromaffin cells show that carbon-fibre electrodes are sensitive enough to detect catecholamines released from single granules and statistical analysis of these signals suggest quantal release of neurotransmitter. It is also shown that sometimes a small "foot" signal occurs preceding a large amperometrical spike, which may reflect the slow leak of catecholamine molecules out of narrow fusion pore before complete pore expansion and exocytosis (Chow et al., 1992). Whether the size of fusion pore can regulate the quantal neurotransmitter release is still under debate.

Electrochemical methods can be applied in various secretory cells. Patch-clamp experiments combined with electrochemical measurements in mouse mast cells indicate that fusion of secretory vesicles with plasma membrane does not always happen as an all-or-none event (Alvarez de Toledo et al., 1993). Measurements in chromaffin cells indicate that occasionally the narrow fusion pore allows complete transmitter release without full fusion of the vesicle with the plasma membrane (Albillos et al., 1997), which is termed as "kiss and run". The mechanism controlling "kiss and run" or full fusion is under investigation.

1.3 Molecular mechanism of exocytosis

The molecular mechanism of exocytosis has been intensively investigated in recent years, and has lead to the identification of many proteins involved in neurotransmitter release, for example SNARE proteins and SM proteins (Rizo and Rosenmund, 2008). SNARE complexes are the core machinery of exocytosis which not only execute the fast membrane fusion in synapses, but also drive much slower secretion in other tissues (Dietl et al., 2001; Sollner et al., 1993). To allow fast and accurate synaptic transmission, additional proteins are required to regulate speed, accuracy and plasticity at synapses (Wojcik and Brose, 2007). Munc13 is a priming factor for vesicle fusion (Ashery et al., 2000). CAPS was originally characterized as a brain cytosolic factor which reconstitutes regulated secretion in permeable neuroendocrine cells (Walent et al., 1992). In this work, the major interest is the role of CAPS in secretion.

1.3.1 SNARE proteins

SNARE proteins form a superfamily of small proteins which are conserved from yeast to humans and govern most types of intracellular membrane traffic (Bonifacino and Glick, 2004). There are 25 members of SNARE proteins found in *Saccharomyces cerevisiae*, 36 members in humans and 54 members in *Arabidopsis thaliana*. All SNAREs share an evolutionarily conserved stretch of 60-70 amino acids called the SNARE motif (Jahn and Scheller, 2006). Most SNAREs have variable domains positioned N-terminal to the SNARE motif and a single transmembrane domain connected with the SNARE motif by a short linker at the C-terminal (Jahn and Scheller, 2006). The SNARE motif contains periodically aligned hydrophobic residues and mediates the assembly of SNARE complex.

Different sets of SNAREs present in the two opposing membranes form a trimeric complex which is essential for vesicle fusion (Sollner et al., 1993). This leads to a functional classification of SNARE proteins as v-SNAREs (vesicle-membrane SNAREs) and t-SNAREs (target-membrane SNAREs) on the basis of their different localizations. Vesicle exocytosis in neurons and neuroendocrine cells is carried out by the v-SNARE synaptobrevin-2 (also known as VAMP 2) with syntaxin-1 and SNAP-25 as t-SNAREs on the target membrane. The three proteins, in a 1:1:1 stoichiometry, form a helical coil-coiled *trans*-SNARE complex which consists four α-helices, one from synaptobrevin-2, one from syntaxin-1 and two from SNAP-25 (Chapman et al., 1994). X-ray crystallography revealed that there are 16 highly conserved leucine-zipper-like layers of interacting amino acid side chains at the centre of the four-helix bundle (shown in Fig. 3; (Sutton et al., 1998)). These layers are largely hydrophobic except the central ionic "0" layer which contains three highly conserved glutamine (Q) residues and one highly conserved arginine (R) residue (Fasshauer et al., 1998b). This result leads to a reclassification of v-SNAREs and t-SNAREs as Qa-, Qb-, Qc- and R-SNAREs. The functional *trans*-SNARE complex mediates membrane fusion requiring one each of Qa-, Qb-, Qc- and R-SNARE motifs. After fusion, the SNARE complex is transformed from a *trans*- to *cis*- configuration and finally disassembled by ATPase N-ethylmaleimide-sensitive factor (NSF) and

18

soluble NSF attachment proteins (SNAPs) (Sollner et al., 1993). The free SNARE proteins then are available for the subsequent rounds of membrane fusion.

The essential role of SNARE proteins in exocytosis was first recognized when it was discovered that clostridial zinc proteases of the tetanus and botulinum neurotoxin family specifically cleave SNARE proteins and thus block neurotransmission (Blasi et al., 1993; Penner et al., 1986; Schiavo et al., 1992). The cleavage sites of SNARE proteins for tetanus and botulinum toxin are shown in Fig. 3. Treatment with different neurotoxins generates a variety of truncated SNARE proteins inducing distinct deficits in secretion. This has allowed study of the function of the various SNARE proteins (Xu et al., 1999). Genetic deletion of SNAREs blocks most but not all neurotransmitter release, indicating a degree of redundancy in function of these molecules (Scales et al., 2001; Sorensen et al., 2003).
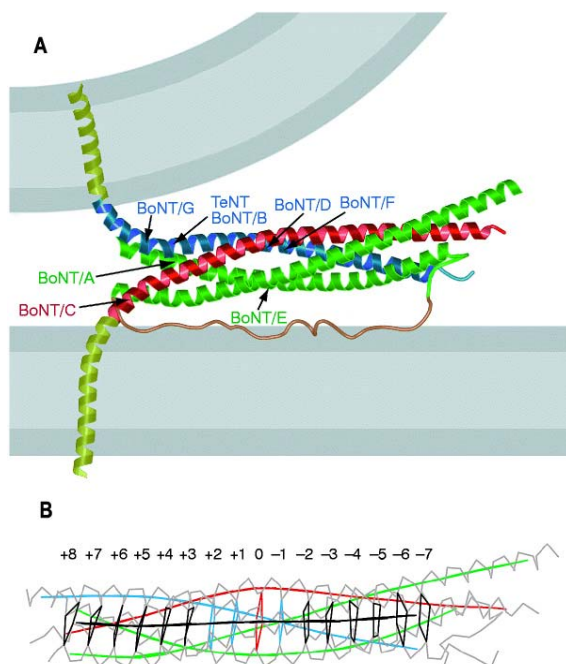
Figure 3. SNARE complex layers and neurotoxin cleavage sites.
A. Trans-SNARE complex connecting vesicle (curved) and plasma membrane (straight), consisting of synaptobrevin-2 (blue), syntaxin (red) and SNAP-25 (green). Arrows indicated neurotoxin cleavage sites.
B. Structural organization of the SNARE complex, hydrophobic layers are numbered. (Modified from (Sutton et al., 1998))

As the SNARE motifs of synaptobrevin and syntaxin are adjacent to their C-terminal transmembrane domain, formation of a bundle containing four parallel helices of the SNARE motifs should bring the vesicle and the plasma membrane into close proximity (Chen and Scheller, 2001; Rizo and Sudhof, 2002). Fully assembled SNARE complexes are extraordinarily stable and resistant to denaturation by heat

and SDS (Fasshauer et al., 1998a). It is believed that assembly of the SNARE complex provides the energy to overcome repulsive the electrostatic forces of membrane fusion. When t-SNAREs and v-SNAREs are incorporated into separate populations of liposomes, fusion occurs spontaneously. Reconstitution experiments indicate that the SNAREs alone are sufficient to promote liposomal fusion (Weber et al., 1998). However under these conditions, liposomal fusion is much slower, with time scales of hours, than the exocytosis observed in neurons. Removal of the N-terminal domain of syntaxin can dramatically increase the fusion rate of artificial bilayers, implying a negative regulatory role of the syntaxin N-terminal H_{abc} domain (Parlati et al., 1999). It has been shown that the syntaxin H_{abc} domain can fold back on itself and bind with syntaxin SNARE motif resulting in a so-called "closed conformation" that inhibits the assembly of the SNARE complex (Dulubova et al., 1999). Syntaxin and SNAP-25 tend to form a stable four-helix bundle in 2:1 stoichiometry in vitro, which can also hinder the SNARE complex assembly (Fasshauer et al., 1998b). Introduction of a short C- terminal stretch of the synaptobrevin SNARE motif prevents the formation of unproductive 2:1 syntaxin-1-SNAP-25 hetetrodimers and accelerates liposome fusion (Pobbati et al., 2006). This result supports the idea that the assembly of SNARE complex starts from the N-terminal and zippers up toward the C-terminal. Mutations in the N- and C-terminal SNARE motifs of SNAP-25 induce differential inhibition of secretion providing additional evidence for N- to C- terminal zippering model (Sorensen et al., 2006). Sequential N- to C-terminal SNARE complex assembly exerts a mechanical force on membranes which may mediate membrane fusion. In this case, the linker region between the SNARE motif and the transmembrane domain appears to be critical as a force transducer to translate the energy released by SNARE complex assembly into the catalytic force for membrane fusion (Sudhof and Rothman, 2009). Insertion of extra amino acids between the SNARE motif and the transmembrane domain of synaptobrevin inhibits Ca^{2+} evoked exocytosis, consistent with this force model (Kesavan et al., 2007).

In summary, SNARE proteins are the key elements in membrane fusion of all eukaryotic organisms. Investigations of how SNARE proteins act and how they

cooperate with other molecules will provide new insights into the molecular mechanism of exocytosis.

1.3.2 Munc13

Munc13s are mammalian homologs of unc-13, a gene identified by mutation screening in *C. elegans*, as a gene whose mutation leads to an uncoordinated (*unc*) phenotype. Munc13s are priming factors in neuron and neuroendocrine cells. They contain one diacylglycerol (DAG) binding and phobol-ester binding C_1 domain, two Munc13 homologue domains (MHD) and three C_2 domains (the structure shown in Fig. 4). The Munc13 homology domains are crucial for the priming role of Munc13 in synaptic transmission.
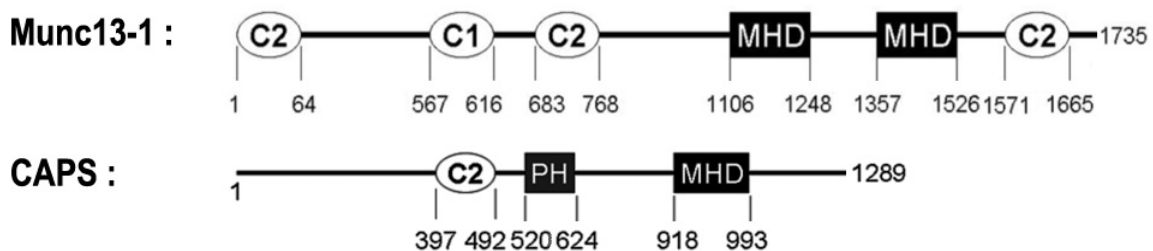
Figure 4. Domain structure of Munc13-1 and CAPS. MHD, Munc13 homology domain. PH, pleckstrin homology domain.

Glutamatergic hippocampal neurons from mice lacking Munc13-1 form ultrastructurally normal synapses whose neurotransmitter release is strongly inhibited, indicating that Munc13-1 is essential for synaptic transmission (Augustin et al., 1999). However, synaptic transmission is not completely blocked in Munc13-1 deletion mutants, due to the presence of Munc13-2 in these cells. Deletion of both Munc13-1 and Munc13-2 totally abolished the spontaneous and evoked synaptic transmission (Varoqueaux et al., 2002). Studies from Munc13-1 knockout mutants, Munc13-2 knockout mutants and double knockout mutants indicate that both Munc13-1 and Munc13-2 are priming factors and differentially control short-term plasticity in synaptic transmission (Rosenmund et al., 2002). Although the expression level of Munc13-1 in chromaffin cells is very low, overexpression of Munc13-1 in bovine chromaffin cells

leads to three-fold increase of Ca^{2+} evoked secretion but does not change the distribution of vesicles. Thus it is likely that Munc13-1 acts as a priming factor (Ashery et al., 2000).

Biochemical studies show C-terminal structures of Munc13-1 interact with the N-terminus of syntaxin (Betz et al., 1997). Overexpression of an open form of syntaxin partially rescues neurotransmitter release in unc-13 null mutants in *C. elegans*, indicating that Munc13´s displacement of Munc18 from syntaxin facilitates the assembly of SNARE complex (Richmond et al., 2001). The minimal domains required for Munc13 function include the two Munc13 homologue domains followed by a C_2 domain (Basu et al., 2005; Stevens et al., 2005). Point mutations deficient in binding with syntaxin block the priming activity of Munc13, supporting the conclusion that the interaction between Munc13 and syntaxin is crucial for Munc13´s function (Madison et al., 2005; Stevens et al., 2005).

Munc13s also bind to other factors modulating the synaptic transmission. It has been found that Munc13 interacts with RIM and Rab3A to form tripartite complex mediating vesicle targeting to the presynaptic active zone (Dulubova et al., 2005; Schoch et al., 2002). Mutation studies show that DAG/ß phorbol ester binding to the C_1 domain of Munc13-1 induces augmentation of neurotransmitter release (Rhee et al., 2002). Munc13 and Calmodulin form Ca^{2+} sensor/effector complex which controls the short term synaptic plasticity in neuron (Junge et al., 2004).

1.3.3 CAPS

CAPS (Ca^{2+}-dependent activator protein for secretion) was identified as a 145-kDa soluble protein which reconstitutes Ca^{2+}-dependent secretion in permeabilized PC12 neuroendocrine cells. A CAPS-specific antibody inhibits the reconstitution of Ca^{2+}-activated secretion by cytosol containing CAPS, indicating an essential role of CAPS for neurotransmitter release (Walent et al., 1992). Later it was found that CAPS is the mammalian homologue of unc-31 in *C. elegans* (Ann et al., 1997). Unc-31 mutant worms exhibit uncoordinated movements and diverse defects in behaviour suggesting unc-31 is an important nervous system protein (Avery et al., 1993). The CAPS homologue in *Drosophila* is also involved in neurotransmitter

release. Null dCAPS mutants display a reduction of glutamatergic transmission and locomotor deficits (Renden et al., 2001). CAPS binds to Ca^{2+} with low affinity (K_d = 270 µM), indicating that CAPS function may be Ca^{2+}-dependent.

Mammals express two CAPS isoforms that are highly homologous to unc-31 and dCAPS (Speidel et al., 2003). Both isoforms contain one C_2 domain proximal to the N-terminus, a Pleckstrin homology (PH) domain located centrally, a Munc13 homology domain (MHD) and a C-terminal membrane-association domain (structure shown in Fig. 4; (Grishanin et al., 2002)). Recent studies show that there is also an N-terminal dynactin 1 binding domain (DBD) that may be required for protein sorting (Sadakata et al., 2007). The C_2 domain is known to bind with Ca^{2+} thus likely acts as a Ca^{2+} sensor. The PH domain associates with acidic phospholipids and could mediate an interaction between CAPS and plasma membranes. The Munc13 homology domain is required for priming activity of unc-13 homologs in Mouse and *C. elegans*, consistent with the results indicating that CAPS may also be a priming factor. The C-terminal membrane-association domain is required to mediate the binding to large dense core vesicles (LDCVs). Both CAPS isoforms are present in brain and adrenal gland but exhibit different developmental expression patterns. CAPS-1 protein expression is first detectable late in embryo-genesis (E14) and increases to reach a plateau 20 days after birth. In contrast, CAPS-2 protein expression is more stable during development and even higher in the embryonic brain than in later phases of development (Speidel et al., 2005). CAPS-1 protein is also found in mouse pancreas, whereas CAPS-2 is present in liver, testis, lung, kidney and pancreas (Sadakata et al., 2006; Speidel et al., 2003). The different tissue distribution indicates a CAPS-1 function in neuronal and neuroendocrine tissues. Since CAPS-2 is also found in other tissues, it may be involved in secretion in non-neuronal cells.

The function of CAPS in Ca^{2+}-triggered vesicle release has been intensively investigated. In synaptosomes, CAPS is associated with LDCVs but not with SVs suggesting CAPS selectively regulates the LDCVs exocytosis (Berwin et al., 1998; Tandon et al., 1998). Studies from Drosophila show that the dCAPS null mutants reveal a reduction of neurotransmission and an accumulation of LDCVs and SVs in presynaptic terminals at the NMJ (Renden et al., 2001). Reintroduction of dCAPS into

identified motoneurons on the dCAPS null background failed to rescue glutamatergic synaptic transmission suggesting that dCAPS is required but not directly responsible for SV release. Studies from *C. elegans* using a prepro-atrial natriuretic factor-green fluorescent protein fusion protein (ANF-GFP) as an index of release of dense-core vesicle exocytosis also indicate that UNC-31 is specifically required for LDCVs but not SVs exocytosis (Speese et al., 2007). However the groups of Brose and Rhee have examined synaptic transmission in autaptic cultures of neurons from mouse hippocampus and concluded that CAPS is required for synaptic vesicle priming (Jockusch et al., 2007). They found that deletion of CAPS-1 and CAPS-2 results in a strong reduction in EPSC amplitude which is caused by a reduction of readily releasable pool size of vesicles. The ultrastructure of synapses, the synapse numbers and the distribution of LDCVs and SVs are normal in the absence of CAPS. High-frequency stimulation in CAPS deficient neurons caused an augmentation of secretion. Increasing the extracellular calcium concentration could transiently bypass the priming defect caused by deletion of CAPS. The results indicate that CAPS is directly involved in the priming of SVs. It has been reported that CAPS acts via LDCV exocytosis to activate the neuronal $G\alpha_s$ pathway, thus modulating synaptic transmission in motor neurons from *C. elegans* (Charlie et al., 2006).

The role of CAPS in LDCV exocytosis has been studied by a number of different approaches. Antibody studies in bovine chromaffin cells show that catecholamine release induced by sequential trains of action potentials is inhibited when a CAPS specific antibody is applied via patch pipette, consistent with a role of CAPS in LDCVs secretion. The kinetic characteristics of amperometric spikes were also changed in these experiments indicating that CAPS is involved in the LDCVs exocytosis, modulating fusion pore formation and dilation (Elhamdani et al., 1999). Application of CAPS antibody in rat melanotroph cells showed that CAPS is required for the rapid secretory response but not for the slow component upon flash photolysis of caged Ca^{2+} (Rupnik et al., 2000). Knockdown of CAPS-1 in PC12 cells (CAPS-2 was not expressed at a detectable level in these cells) resulted in a reduction of release of NE and of a transfected neuropeptide Y (NPY) secretion, indicating that CAPS is required for the priming of LDCVs (Fujita et al., 2007). CAPS-1 deficient

mice have been generated and investigated. New-born CAPS-1 knockout mice die immediately after birth. Capacitance measurements show that exocytosis is not affected in chromaffin cells of CAPS-1 deletion mutants. However, amperometric records indicate a deficit in catecholamine release in CAPS-1 knockout mice, with no change of event charge, amplitude, rise time, half-width or foot duration. Studies combined with TIRF microscopy and amperometry show that in CAPS-1 deficient chromaffin cells many vesicles fuse with the plasma membrane without catecholamine release implying the exocytosis of empty vesicles. The results indicate that CAPS-1 regulates the catecholamine loading of LDCVs (Speidel et al., 2005), which is supported by the recent reports that overexpression of either CAPS-1 or CAPS-2 in CHO cells enhances vesicular monoamine uptake via the vesicular monoamine transporters VMAT1 and VMAT2 (Brunk et al., 2009). Studies from primary cultured *C. elegans* neurons using capacitance recordings and TIRF microscopy indicate that CAPS is required for the docking of LDCVs at the plasma membrane (Zhou et al., 2007). Electron microscopy studies also support a docking role of CAPS in *C. elegans*. An open form of syntaxin can reverse the docking deficit in the absence of CAPS (Hammarlund et al., 2008). In summary, capacitance experiments indicate a role for CAPS in priming, while imaging and electron microscopy studies support a role for CAPS in docking. Examination of catecholamine release indicates an additional role for CAPS in vesicle filling. It is still unclear where in the secretory pathway CAPS acts.

At which steps of LDCVs exocytosis CAPS acts is still not clear. It has been found that the full length of CAPS binds to acidic phospholipids, the plasma membrane and phosphatidyl inositol 4,5 bisphosphate (PI (4, 5) P_2) through PH domain, and the presence of PI (4, 5) P_2 and PI (3, 5) P_2 enhances the binding of CAPS with the plasma membrane (Grishanin et al., 2002). Using a SNARE-dependent liposome fusion assay, it has been shown that CAPS accelerate liposome fusion in a calcium- and PIP_2-dependent manner. CAPS with mutations in PH domain impairing the binding with PIP_2 failed to promote the liposome fusion, thus indicating that PIP_2 binding is required for CAPS-mediated acceleration of secretion (James et al., 2008). Recently Nojiri et al showed that the phosphorylation of CAPS by protein kinase CK2

is required for CAPS activity (Nojiri et al., 2009). They identified Ser-5, -6 and -7 as phosphorylation sites using mass spectrometry. Nonphosphorylatable CAPS mutants did not support secretion *in vitro* and *in vivo* indicating phosphorylation is necessary for CAPS activity. The presence of an MHD domain in CAPS leads to a hypothesis that CAPS interacts with syntaxin, as Munc13-1 does. James et al. tested this hypothesis by using liposome fusion assay and suggested that CAPS binding with syntaxin-1 promotes the trans-SNARE complex formation to accelerate fusion (James et al., 2009).

1.4 Aim of my work

The aim of this work is to investigate the function of CAPS in Ca^{2+} evoked exocytosis in chromaffin cells. As introduced above, mammals express two CAPS isoforms which share a similar domain structure. A variety of studies designed to perturb CAPS function indicate that CAPS is involved in the secretion of large dense core vesicles, but where in the secretory pathway CAPS acts is still under debate. CAPS-1 knockout mice have been generated and investigated. We have used CAPS-2 knockout (KO) mice and CAPS-1/CAPS-2 double knockout (DKO) mice to further study how CAPS functions in regulated exocytosis.

Using high time resolution recording of secretion via membrane capacitance measurements, combined with photolysis of Ca^{2+}-caged compound, we have examined the role of CAPS-1 and CAPS-2 on a genetically clean, CAPS-free background. We have examined docking, priming and catecholamine release in cells lacking CAPS and we examined the effects of expression of CAPS-1 and CAPS-2 in these cells. We have tested whether CAPS can be replaced in the system. The results of these experiments will add to our understanding of how CAPS functions.

2. Materials and Methods

2.1 Materials

2.1.1 Reagents

Agarose	Roth
Albumin	Sigma
Aprotinin	Sigma
BAPTA	Molecular Probes
Bovine serum albumin (BSA)	Sigma
$CaCl_2$ (1M standard solution)	BDH
Caesium hydroxide (CsOH)	Sigma
DMEM	Invitrogen
DPTA	Aldrich
EDTA	Sigma
Ethanol	Roth
Fetal calf serum (FCS)	Invitrogen
Fura-4F	Molecular Probes
Furaptra	Molecular Probes
Glucose	Merck
ITS-X	Invitrogen
L-cysteine	Sigma
L-glutamate acid	Sigma
Normal goat serum (NGS)	Invitrogen
HEPES	Sigma
HPLC-H_2O	Merck
NP- EGTA	Hannover
OptiMEM	Invitrogen
Pen / Strep	Invitrogen
Triton X-100	Serva
Tris	Roth
Trpsin inhibitor	Sigma
Tryptosephosphat	Invitrogen

The reagents used in electron microscopy are from Electron Microscopy Science.

2.1.2 Enzymes

Chymotrypsin	Sigma

---------- Materials ----------

Papain	Roche
	Worthington
Proteinase K	Qiagen
RedTaq-Polymerase	Sigma
Trypsin	Invitrogen

2.1.3 Antibodies

anti CAPS-1 monoclonal (from mouse)	BD Biosciences
anti CAPS-2 polyclonal (from rabbit)	MPI for experimental Med., Göttingen
Alexa 568 nm goat anti-rabbit	Molecular Probes
Alexa 488 nm goat anti-mouse	Molecular Probes

2.1.4 Virus

pSFV1- CAPS1-IRES-GFP

pSFV1- CAPS2-IRES-GFP

pSFV1- Munc13-1-GFP

pSFV1- Syntaxin LE 165/166A-PV-IRES-GFP

pSFV1- CAPS1-200-1289-PV-IRES-GFP

2.1.5 Solutions

2.1.5.1 General solutions

<u>HBS</u>

140 mM	NaCl
10 mM	HEPES
5 mM	KCL
10 mM	$MgCl_2 \times 6\ H_2O$
20 mM	$CaCl_2 \times 2\ H_2O$
pH 7.2, ~ 359 mOsm	

<u>PBS</u>

140 mM	NaCl
7 mM	KCl
10 mM	Na_2HPO_4
1.8 mM	KH_2PO_4
sterile filtered pH 7.4	

<u>TAE</u>

| 40 mM | Tris |
| 0.11 % (v/v) | Acetic acid |

1 mM	EDTA
pH 8.0	

<u>TBS 10×</u>

100 mM	Tris-HCl
1.5 M	NaCl
pH 7.8	

2.1.5.2 Solutions for chromaffin cell preparation

<u>Locke´s</u>

154 mM	NaCl
5.6 mM	KCl
0.85 mM	Na_2HPO_4
2.15 mM	KH_2PO_4
10 mM	Glucose
pH 7.4, ~ 312 mOsm	

<u>Papain solution</u>

50 ml	DMEM
10 mg	L-Cysteine (activates the papain)
0.5 ml	100 mM $CaCl_2$
0.5 ml	50 mM EDTA (activates the papain)
frozen in aliquots (3ml or 2 ml aliquots, freezer)	
after thawing	20 units papain per 1 ml enzyme solution
	bubble 20 minutes with carbogen
	sterile filtered

<u>Inactivation solution</u>

50 ml	DMEM
5 ml	FCS
125 mg	albumin
125 mg	trypsin inhibitor
sterile filtered	
frozen in aliquots (3ml or 2 ml aliquots, freezer)	
after thawing incubate at 37°C , 9% CO_2 incubator	

<u>Medium</u>

40 ml	DMEM
400 µl	ITS-X

---------- Materials ----------

160 µl   Pen / Strep (1 ml aliquots, freezer)
after thawing incubate at 37°C , 9% CO_2 incubator

2.1.5.3 Solutions for BHK cells and virus generation

OptiMEM + 2.5% FCS

100 ml   Tryptose phosphate
20 ml   1 M HEPES
25 ml   FCS
1 ml   Pen / Strep
fill up to 1000 ml with OptiMEM
sterile filtered, store at 4°C

OptiMEM + 5% FCS

15 ml   Tryptose phosphate
3 ml   1 M HEPES
7.5 ml   FCS
150 µl   Pen / Strep
fill up to 150 ml with OptiMEM
sterile filtered, store at 4°C

OptiMEM without FCS + 0.2% BSA

44 ml   OptiMEM
5 ml   Tryptose phosphate
1 ml   1 M HEPES
50 µl   Pen / Strep
0.1 g   BSA
sterile filtered, store at 4°C

Aprotinin
6 mg / ml in HBS
110 µl aliquots store at -20 °C

Chymotypsin
2 mg / ml in HBS
100 µl aliquots store at -20 °C

Virus is activated as following:

450 µl Virus aliquot

450 µl OptiMEM without FCS + 0.2% BSA

---------- Materials ----------

100 µl Chymotrypsin

Mixed and incubated 40 minutes at room temperature

Add 110 µl Aprotinin

2.1.5.4 Solutions for Immunocytochemistry

<u>Fixation solution</u>

3.7 % (v/v)	Formaldehyde
0.1 % (v/v)	Glutaraldehyde
in PBS	
sterile filtered	

<u>Blocking solution</u>

10 % (v/v)	NGS
0.25 % (v/v)	Triton-x-100
in PBS	
sterile filtered, store at 4°C	

<u>1 × PBS</u>

58 mM	Na_2HPO_4
17 mM	NaH_2PO_4
83 mM	NaCl
pH 7.4 adjusted by NaOH, 322 mOsm	
Sterile filtered, store at 4°C	

<u>Mounting Medium</u>

Mowiol 4-88	2.4 g
Glycerol	6 g
H_2O	6 ml
0.2 M Tris-buffer pH 8.5	12 ml

2.1.5.5 Solutions for Electron Microscopy

<u>Paraformaldehyde</u>

15% dissolved in double distilled water at 70°C
filtered after cooling, freshly made
pH 7.1-7.4

---------- Materials ----------

Cacodylate buffer

0.1 M and 0.2 M in double distilled water, freshly made
pH 7.4 adjusted by HCl

Fixation solution

3 ml	Glutaraldehyde (10%)
1.66 ml	Paraformaldehyde (15%)
5 ml	Cacodylate buffer (0.2 M)
0.34 ml	H_2O

pH 7.2

Osmium

2% in 0.1 M Cacodylate buffer, freshly made

Uranyl acetate

20 mg / ml in double distilled water, freshly made

Lead citrate

0.4 mg / ml
pH 12.0

Embedding resin

Epon	5 g
DDSA	3.3 g
NMA	2.1 g
BDMA	0.3 g

2.1.5.6 Solutions for Electrophysiology

2 × Buffer

0.1906 g	HEPES 80 mM	
0.3678 g	L-Glutamate acid	250 mM
300 µl	CsOH (50%)	
8 ml	HPLC-H_2O	

pH 7.6 adjusted by CsOH, ~ 600 mOsm
sterile filtered, 50 µl aliquots at -20°C

BAPTA

100 mM in HPLC-H_2O

---------- Materials ----------

pH 7.2 adjusted by HCl, 304 mOsm

sterile filtered, 500 µl aliquots at -20°C

DPTA

100 mM in HPLC-H_2O

pH 7.2 adjusted by KOH, 316 mOsm

sterile filtered, 1 ml aliquots at -20°C

NP-EGTA

100 mM NP-EGTA stock in 100 mM HEPES, pH 7.2, 917 mOsm, 400 µl aliquots at -80°C

after thawing, add 600 µl HPLC-H_2O to get 40 mM NP-EGTA stock, 12.5 µl aliquots at
-20°C

Nucleotides

0.0507 g	Mg-ATP	20 mM
0.0050 g	Na$_2$-GTP	2 mM
0.0119 g	HEPES	10 mM
4 ml	HPLC-H_2O	

pH 7.2 adjusted by CsOH, 55 mOsm

sterile filtered, 20 µl aliquots at -20°C

$CaCl_2$

Serial dilution from 1 M standard $CaCl_2$ solution with HPLC-H_2O or HEPES buffer

Fura-4F + Furaptra

Same volume of 10 mM Fura-4F in 20 mM HEPES (HPLC-H_2O) and 10 mM Furaptra in 20 mM HEPES (HPLC-H_2O) mix together to get final concentration as 5 mM.

Intracellular solution for amperometry

4.9 µl 10 mM $CaCl_2$ in 2 × Buffer mixed with 5.1 µl 10 mM EGTA to get 4.2 µM free calcium

Extracellular solution for flash & ramp experiment

145 mM	NaCl
2.4 mM	KCl
10 mM	HEPES
4 mM	$MgCl_2$
1 mM	$CaCl_2$

---------- Materials ----------

10 mM $\quad\quad\quad\quad\quad$ Glucose

pH 7.2, ~310 mOsm

Intracellular solution for flash & ramp experiment

12.5 µl	NP-EGTA (40 mM)
8 µl	Nucleotides
6.4 µl	Fura-4F + Furaptra (5 mM)
3.4 µl	$CaCl_2$ (100 mM)
30.5 µl	2 × Buffer
19.2 µl	HPLC-H_2O

pH 7.2, ~300 mOsm

Calibration Solutions

	Sol_1	Sol_2	Sol_3	Sol_4	Sol_5	Sol_6	Sol_7	Sol_8	Sol_9a	Sol_9	Sol_10	Sol_12	Sol_11
Cs/Glu/Hepes (2x)	25.6 µl (pH=7.2, 582 mOsm)	22 µl (pH=7.3, 590 mOsm)	19.4 µl (pH=7.3, 590 mOsm)	17.8 µl (pH=7.3, 590 mOsm)	17.6 µl (pH=7.4, 592 mOsm)	21.8 µl (pH=7.4, 592 mOsm)	21.1 µl (pH=7.52, 598 mOsm)	20 µl (pH=7.7, 608 mOsm)	18.2 µl (pH=8.26, 631 mOsm)	18.6 µl (pH=7.8, 618 mOsm)	15.2 µl (pH=9, 674 mOsm)	14.3 µl (pH=9.43, 706 mOsm)	36.5 µl (pH=7.3, 590 mOsm)
Nucleotides (10x ATP, 20 mM; GTP, 2 mM, 55 mOsm)	8 µl [2 mM]	8 µl [2mM]	8 µl [2mM]	8 µl [2 mM]	8 µl [2 mM]	8 µl [2 mM]	8 µl [2 mM]	8 µl [2 mM]	8 µl [2 mM]	8 µl [2 mM]	8 µl [2 mM]	8 µl [2 mM]	8 µl [2 mM]
Dye-Mixture (12.5X, Fura-4F, 5 mM; Furaptra, 5 mM	6.4 µl [0.4 mM]	6.4 µl [0.4 mM]	6.4 µl [0.4 mM]	6.4 µl [0.4 mM]	6.4 µl [0.4 mM]	6.4 µl [0.4 mM]	6.4 µl [0.4 mM]	6.4 µl [0.4 mM]	6.4 µl [0.4 mM]	6.4 µl [0.4 mM]	6.4 µl [0.4 mM]	6.4 µl [0.4 mM]	6.4 µl [0.4 mM]
BAPTA 0.1 M (304 mOsm) purity 80%	28 µl [28 mM]	28 µl [28 mM]	28 µl [28 mM]	28 µl [28 mM]	26 µl [26 mM]	-	-	-	-	-	-	-	-
DPTA 0.1M (316 mOsm) purity 98%	-	-	-	-	-	32 µl [39.2 mM]	32 µl [39.2 mM]	32 µl [39.2 mM]	32 µl [39.2 mM]	32 µl [39.2 mM]	32 µl [39.2 mM]	28 µl [34.3 mM]	-
$CaCl_2$ 0.1M (255 mOsm)	-	8.1 µl [10 mM]	13.6 µl [17 mM]	17.2 µl [21.5 mM]	17.6 µl [22 mM]	1.6 µl [2 mM]	2.8 µl [3.5 mM]	4.4 µl [5.5 mM]	7.2 µl [9 mM]	7.2 µl [9 mM]	12 µl [15 mM]	17.6 µl [22 mM]	8 µl [10 mM]
HPLC-H_2O	12 µl	7.5 µl	4.6 µl	2.6 µl	4.4 µl	10.2 µl	9.7 µl	9.2 µl	8.2 µl	7.8 µl	6.4 µl	5.7 µl	21.1 µl
Total	80 µl	80 µl	80 µl	80 µl	80 µl	80 µl	80 µl	80 µl	80 µl	80 µl	80 µl	80 µl	80 µl
mOsm calculated	300	300	300	300	300	300	300	300	300	300	300	300	300
$[Ca^{2+}]_{free}$	0	124 nM	343 nM	721 nM	1.16 µM	3.64 µM	7 µM	12.1 µM	22.6 µM	22.6 µM	47.5 µM	132 µM	7.63 mM
pH	7.15	7.19	7.24	7.15	7.22	7.16	7.17	7.23	7.24	7.05	7.16	7.2	7.17
$[Ca^{2+}]_{free}$ recalculated from pH	0	127 nM	338 nM	735 nM	1.16 µM	4.07 µM	7.68 µM	11.1 µM	20.2 µM	35.32 µM	53.4 µM	132 µM	7.63 mM

2.2 Methods

2.2.1 Knockout mice

Mice with a deletion of the mouse CAPS-1 protein (CAPS-1 knock-out) were generated by homologous recombination in embryonic stem cells as described previously (Speidel et al., 2005). The mouse CAPS-2 gene was deleted using same strategy (Jockusch et al., 2007). CAPS-1/-2 double knock-out (DKO) mice were generated by breeding the CAPS-1 mutation into the CAPS-2 mutant background. CAPS-1 knock-out mice and CAPS-1/-2 double knock-out mice died shortly after birth, so their embryos [embryonic day 18 (E18) and E19] were prepared after cesarean section and cervical dislocation. Appearance of CAPS-1/-2 double knock-out mouse embryos was different from that of wild type (WT) mice (Fig. 1). CAPS-2 knock-out mice were viable and fertile. New born CAPS-2 knock-out mice [postnatal1-2 day] were used for experiments. They resembled wild type mice.

Figure 1. CAPS-1/-2 double knock-out mouse embryo (left) shows different appearance as compared with wild type mouse (right).

2.2.2 Genotyping of mice

2.2.2.1 Preparation of mice genomic DNA

Tails of mice were digested by 180 µl lysis-Reagent 2 and 20 µl proteinase K for 5 hours or overnight at 1400 rpm, 55°C. After a short centrifuge step, the products were mixed for 45 minutes ~ 1 hour at 1400 rpm, 85°C. Purified DNA gotten from above processes can be used for next Polymerase chain reaction (PCR).

---------- Methods ----------

2.2.2.2 Polymerase chain reaction

18.5 µl mastermix and 1 µl Red Taq polymerase were added into 0.5 µl purified DNA template then mixed by pipette. It is important to put all solutions always on ice, especially for Red Taq polymerase.

2.2.2.2.1 CAPS-1 PCR protocol

Primer #1502   TGC GGT GGG CTC TAT GGC TTC T

Primer #1503   CTC GAG TGG CCT GAT CTT TGT CA

Primer #1504   TAT GAG GAG TTT ATG TGC GTG GAT

Primer Pair #1502/ Primer #1504   detects CAPS-1 KO 465 bp

Primer Pair #1503/ Primer #1504   detects CAPS-1 WT 382 bp

Reaction mix for 1 reaction

1 µl	dNTPs	2.5 mM
1 µl	Primer #1502	5 pM/µl
1 µl	Primer #1503	5 pM/µl
1 µl	Primer #1504	5 pM/µl
2 µl	PCR buffer	10 ×
12.5 µl	Sigma-H_2O	
0.5 µl	DNA sample	
1 µl	Red Taq DNA Polymerase	

Number of cycles: 40

1 = 94.0 °C for 5 minutes

2 = 94.0 °C for 30 seconds

3 = 60.0 °C for 30 seconds

4 = 72.0 °C for 30 seconds

5 = GO TO 2 repeat 39

6 = 72.0 °C for 7 minutes

7 = HOLD 4.0 °C

---------- Methods ----------

2.2.2.2.2 CAPS-2 PCR protocol

Primer #5471 sensePrimer   5' GTA CCA TAG TTC TGT GCC GTG TAA TC 3'

Primer #5472 antisensePrimer   5' GGA GGC TCG CAG CTC TTC AAT G 3'

Primer #4174 antisensePrimer   5' CGC ATC GCC TTC TAT CGC CTT CTT 3'

Primer Pair #5471/ Primer #5472   detects CAPS-2 KO 225 bp

Primer Pair #5471/ Primer #4174   detects CAPS-2 WT 153 bp

<u>Reaction mix for 1 reaction</u>

1 µl	dNTPs	2.5 mM
2 µl	Primer #5471	5 pM/µl
1 µl	Primer #5472	5 pM/µl
1 µl	Primer #4174	5 pM/µl
2 µl	PCR buffer	10 ×
11.5 µl	Sigma-H_2O	
0.5 µl	DNA sample	
1 µl	Red Taq DNA Polymerase	

<u>Number of cycles: 30</u>

1 = 94.0 °C for 3 minutes

2 = 94.0 °C for 30 seconds

3 = 60.0 °C for 30 seconds

4 = 72.0 °C for 30 seconds

5 = GO TO 2 repeat 29

6 = 72.0 °C for 7 minutes

7 = HOLD 4.0 °C

2.2.2.3 Agarose gel electrophoresis for DNA separation

After PCR, a 380 bp amplicon was generated for the CAPS-1 wild type allele, a 465 bp amplicon was generated for the CAPS-1 knock-out allele, and a 153 bp amplicon was generated for CAPS-2 wild type allele and a 225 bp amplicon for CAPS-2 knock-out allele. These DNA fragments with different lengths can be distinguished by agarose gel electrophoresis. 0.6 g agarose was added into 30 ml TAE solution then boiled using a

microwave. After the agarose dissolved totally and the solution cooled to 37°C, 3 µl ethidium bromide was added. The agarose solution was carefully mixed and poured into a gel tray to avoid air bubbles. The gel which was solidified at room temperature in 20 minutes was put into the electrophoresis chamber contained 1×TAE buffer. DNA products generated using PCR were then added to gel pockets. λ –DNA marker was used as standard control. Electrophoresis was performed at 80 Volts for 1 hour. The results were visualized under UV- light illumination.
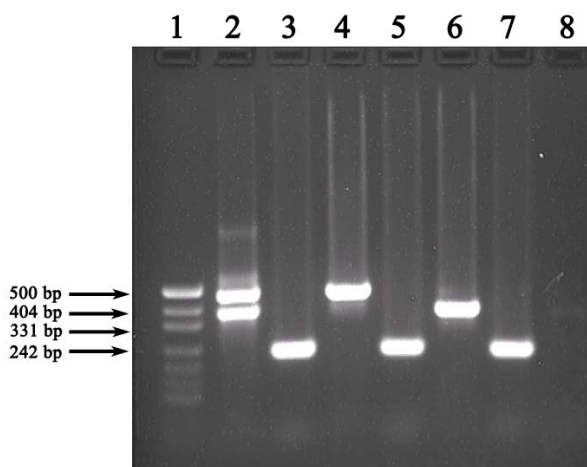
Figure 2. An example of genotyping results.
The first lane is the standard control from λ–DNA marker. The second, fourth and sixth lanes are the results of DNA products from CAPS-1 PCR; the third, fifth and seventh are the results of DNA products from CAPS-2 PCR. Thus the genotyping results from left to right are CAPS1+-/CAPS2--, CAPS1--/CAPS2-- and CAPS1++/CAPS2-- respectively.

2.2.3 Mouse chromaffin cell culture

Adult female and male CAPS-1+-/CAPS-2-- mice were paired in breeding cages for 2 days and separated. Embryonic age was calculated from the first day of pairing. Pregnant female mice at stage E18 or E19 were asphyxiated by carbon dioxide then decapitated. Embryos were taken by caesarean section. Mice having unusual appearance as shown in Fig. 1 were highly likely to be DKOs, and were picked. Embryos were decapitated and placed on ice. Both adrenal glands were rapidly removed by forceps and scissors and then placed into a drop of cold Locke´s solution and carefully cleaned with fine forceps under microscopic control. It was important to remove fat, blood and other tissues connected with adrenal glands and avoid damage glands at the same time. Cleaned glands were put into another clean drop of Locke´s solution and then transferred into a 15 ml Falcon tube containing 400 µl of the enzyme

solution and digested for 20 ~ 21 minutes in a shaking water bath at 37°C. The enzyme solution was then removed, and 400 µl of inactivating solution was added and incubated 4 minutes in the shaking water bath at 37°C. The inactivating solution was replaced by 600 µl culture medium and the glands were carefully triturated with a 200 µl pipette tip until the tissue was dissociated. 100 µl cell-suspensions were plated on sterilized 25 nm coverslips (No.1001/0025, Assistant, Germany) in six-well plates and were kept in the incubator (37°C, 9% CO_2) for 30 minutes before adding 3 ml of culture medium to each well. The cells could be cultured for up to 4 days in the incubator. Wild type and CAPS-2 knock-out mouse chromaffin cells were prepared following similar steps. The enzyme digestion time was adjusted for the age of the mice.

2.2.4 Morphological Methods

2.2.4.1 Immunocytochemistry

Mouse chromaffin cells were cultured for 2 days before immunostaining. The culture medium was removed and the cells were washed twice with 2ml PBS. Next cells were fixed with 3.7% Formaldehyde and 0.1% Glutaraldehyde in PBS for 20 minutes in darkness. Fixation solutions were prepared fresh, filtered and kept cold (4°C). During fixation process, shaking of the tissue was avoided.

After washing 3 times with PBS, cells were blocked 30 minutes with blocking solution under gentle shaking. During this time primary antibodies were diluted in blocking solution and kept on ice. 100 µl diluted primary antibody solution were added per coverslip on a piece of parafilm. Coverslips with the cell on the underside were carefully put onto these drops of solution and incubated in a wet chamber (self-made) overnight at 4°C or 1 hour at room temperature. Then cells were washed with PBS twice and incubated with the second antibody diluted in blocking solution 45-60 minutes in the dark at the room temperature under gentle shaking. After washing 3 times with PBS, the coverslips were mounted upside down on microscope slides with 30 µl mounting medium per coverslip and incubated for 30 minutes at 37°C. One coverslip without cells was used as control for the drying process of the mounting medium. Finally the edges of coverslips were sealed with nail polish to avoid further drying. All washing steps were done quickly to avoid contact of cells with air and were

done carefully to avoid washing cells away. CAPS-1 monoclonal antibody (from mouse, 1:100 v/v, BD Biosciences), CAPS-2 polyclonal antibody (from rabbit, 1:100 v/v, N. Brose MPI for Experimental Medicine, Göttingen), secondary antibody Alexa 488 nm goat anti-mouse (1:2000 v/v, molecular probes) and Alexa 568 nm goat anti-rabbit (1:2000 v/v, molecular probes) were used.

2.2.4.2 Electron Microscopy

Acutely dissociated chromaffin cells from wild type and CAPS-1/-2 double knock-out mice were plated on Petriperm dishes (Sigma-Aldrich). The cells were cultured 2 days before embedding. The solutions for cell embedding were freshly prepared. Paraformaldehyde was dissolved at 70°C, and was filtered after cooling. Cacodylate buffers with two different concentrations, 0.1M and 0.2 M, were made and the pH was adjusted to 7.4 using HCL. The fixation solution was prepared by mixing 15% paraformaldehyde, 10% glutaraldehyde (cat # 16120, Electron Microscopy Sciences), 0.2 M cacodylate buffer and double distilled water to get a final concentration as 2.5% paraformaldehyde, 3% glutaraldehyde and 0.1M cacodylate. The cells were washed twice with TBS. Then they were fixed for 1 hour at room temperature using the fixation solution described above, under gentle shaking. After washing 3 times with 0.1 M Cacodylate buffer, the cells were treated with 2% Osmium in 0.1 M cacodylate buffer for 1 hour under gentle shaking. 2% uranyl acetate solution and embedding resin (Embed-512, Electron Microscopy Sciences) were prepared during this step. Uranyl acetate was light-sensitive and toxic. It was weighed in a Falcon tube and dissolved by double distilled water. Embedding resin was prepared by mixing 4 solutions of EMBed-812 Embedding Kit (cat # 14120, Electron Microscopy Sciences). After osmication, cells were washed twice for 5 minutes, with double distilled water under gentle shaking; 2% uranyl acetate was added and gently shaken for 1 hour in darkness; washed twice by double distilled water again. Serial dehydration in ethanol and infiltration with embedding resin were carried out as follows:

　　1. 30% ethanol, 10 minutes, gentle shaking
　　2. 50% ethanol, 10 minutes, gentle shaking
　　3. 70% ethanol, 15 minutes, gentle shaking

4. 80% ethanol, 15 minutes, gentle shaking

5. 90% ethanol, 15 minutes, gentle shaking

6. 96% ethanol, 15 minutes, gentle shaking

7. 99% ethanol, 15 minutes, gentle shaking

8. Aceton, 15 minutes, gentle shaking

9. Aceton: Embedding resin (3:1), 30 minutes, gentle shaking

10. Aceton: Embedding resin (1:1), 30 minutes, gentle shaking

11. Aceton: Embedding resin (1:3), 30 minutes, gentle shaking

Finally, embedding resin was added and polymerized for 48 hours at 60°C. Extra embedding resin was poured into embedding capsules and polymerized.

Embedded cells were observed under the microscope. The regions having many cells were marked and cut out. The sample side of embedding resin was glued to embedding capsules. The other side with cells was trimmed into trapezoidal shape and sliced by diamond knife (Elementsix, Holland). Ultrathin sections (70 nm) were collected on single-slot, pioloform-coated grids; poststained with 2% uranyl acetate for 10 minutes and lead citrate for 5 minutes; analyzed with a Philips Tecnai12 Biotwin electron microscope. Cells with large nuclei and a clear plasma membrane were chosen. The number and spatial distribution of vesicles were analyzed using a self-written labview program (National Instruments, München, Germany). An outline of both the plasma membrane and the nucleus was generated manually. Each vesicle was marked, and the shortest distance of its centre to the plasma membrane was determined.

2.2.5 Electrophysiology

2.2.5.1 Whole-cell capacitance measurement

The patch clamp technique provides the possibility to investigate electrical properties of single cells. Originally it was designed to measure the current in a small patch of cell membrane. Since then many applications have been developed including the measurement of membrane capacitance with high resolution. Capacitance of cell membrane is proportional to the cell plasma membrane area as near $1 \mu F / Cm^2$ (Cole, 1968). Under the whole-cell mode, an electrical connection was established between

the pipette and the entire cell surface, which allows recording of cell membrane capacitance (Fig. 3). Upon exocytosis or endocytosis, fusion or retrieval of vesicles will increase or decrease the cell surface area which can be evaluated by measuring membrane capacitance change.
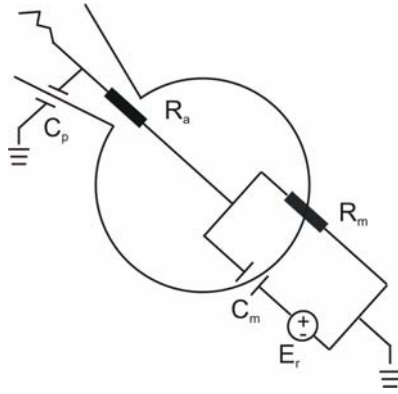
Figure 3. Whole-cell patch clamp configuration.
C_m is the cell capacitance; R_m is the cell resistance which is determined by ion channels and pores in the membrane; R_a is the access resistance; E_r is the resting membrane potential which is clamped to -70 mV normally. (Modified from Gillis, 1995)

In my experiments, conventional whole-cell recordings were performed with 4-6 MΩ pipettes (GB150F-8P, Science products, Germany) using an EPC-9 patch-clamp amplifier controlled with Pulse software (HEKA). Pipettes were coated with wax and polished. Capacitance measurements were performed using the Lindau-Neher technique implemented as the "sine+dc" mode of the "software lock-in" extension of Pulse software. A 1 kHz, 70 mV peak-to-peak sinusoid stimuli was applied at a DC holding potential of -70 mV. All experiments were performed at room temperature. Only cells with a whole cell capacitance between 4-10 pF, a series resistance lower than 20 MΩ and leak current less than 50 pA were analyzed. Data analyses were done using IGOR Pro (Wavemetrics).

2.2.5.2 Photolysis of caged calcium and $[Ca^{2+}]_i$ measurement

Calcium is an important second messenger in neurosecretory cells. Intracellular calcium not only acts on vesicle exocytosis triggering but also regulates the earlier steps of secretory pathway before vesicle fusion (Voets et al., 2001). Photolysis of caged calcium combined with dual-wavelength ratiometric of $[Ca^{2+}]_i$ fluorimetry allows accurate measurement and control of the intracellular calcium concentration spatially and temporally.

2.2.5.2.1 Purity trituration of NP-EGTA

We used the NP-EGTA as a calcium caging compound which was developed by Ellis-Davies and Kaplan. It exhibits a high selectivity for Ca^{2+}. Upon UV-illumination, its K_d increases from 80 nM to 1mM. Because of its low affinity for Mg^{2+}, photolysis of caged NP-EGTA does not perturb the physiological Mg^{2+} level. Its structure is shown in Fig. 4.
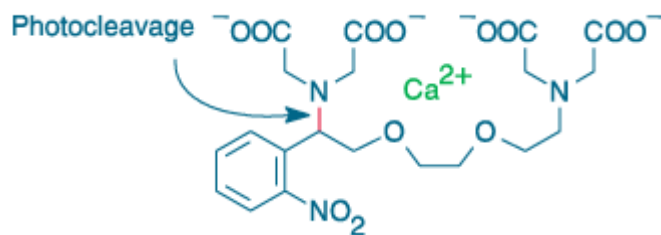
Figure 4. NP-EGTA complexed Ca^{2+}. Upon illumination, this complex is cleaved to yield free Ca^{2+} and two iminodiacetic acid photoproducts (Invitrogen, molecular probes).

Purity of NP-EGTA is determined by titrating with Ca^{2+} in the presence of the photosensitive calcium dye furaptra. 100 µl NP-EGTA (10 mM) in 80 mM HEPES and 250 mM Cs-glutamate buffer was adjusted to pH 7.6 using CsOH and put into a cuvette. The fluorescence intensity of the testing solution excited at 350 nm (F_{350}) and 380 nm (F_{380}) was measured and used as the background. Then 1 µl Furaptra (10 mM, in 20 mM HEPES pH=7.2) was added into the cuvette and mixed. The fluorescence ratio (R) was calculated as following equation: $R = (F_{350} - F_{350\ background}) / (F_{380} - F_{380\ background})$. Next a defined amount of the calcium solution (10 mM in 100 mM HEPES, serially diluted from 1 M standard calcium solution) was added and mixed, and the fluorescence ratio was recorded. This step was repeated and more calcium solution was added. Because the K_d of furaptra (40 µM) is much larger than the K_d of NP-EGTA (80 nM), Ca^{2+} will bind with NP-EGTA first. Only when NP-EGTA in the cuvette is saturated, Ca^{2+} will bind with furaptra and cause a change of the fluorescence ratio from low to high levels. As shown in Fig. 5, when 77.5 µl calcium solutions were added, the ratio did not change. After addition of 2.5 µl calcium solution more, the ratio increased obviously. The calculated purity of NP-EGTA used in this study was 80%.
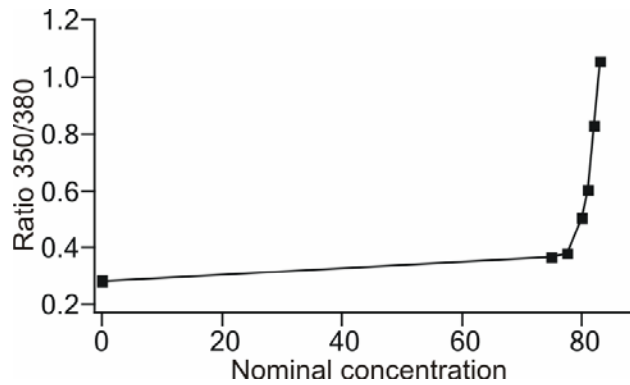
Figure 5. Purity trituration of NP-EGTA.

The purities of other calcium chelators used in this study, BAPTA and DPTA, were also calibrated. BAPTA with a K_d of 220 nM, can be triturated in a similar way as NP-EGTA. The purity of BAPTA used in this work was determined as 80%. The K_d of DPTA is 80 µM which is in the same range of the K_d of Furaptra; Furaptra will bind with Ca^{2+} more efficiently than DPTA. The purity of DPTA was determined as 98% as experienced value. Since both K_d of NP-EGTA and DPTA are pH sensitive, strict control of pH is important.

2.2.5.2.2 In vivo Calibration curve

Fura-2 calcium indicator, was used to measure the intracellular calcium concentration. This method is based on the principle that Fura-2 binding with Ca^{2+} displays an absorption shift when excitation light wavelength range from 300 nm to 400 nm. As shown in Fig. 6, the fluorescence intensity of Fura-2 increase with the increasing Ca^{2+} concentration at excitation light wavelength 350 nm, no change at 360 nm, decrease at 380 nm.

---------- Methods ----------
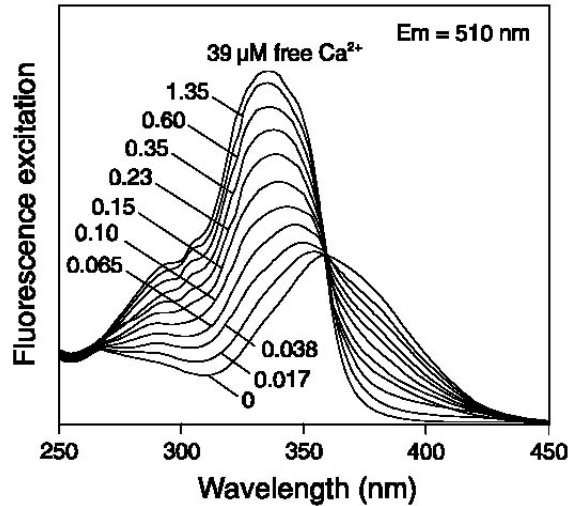
Figure 6. Spectral response of Fura-2 in 0-39 µM Ca^{2+} solution. (from Molecular Probes handbook)

The ratio of fluorescence intensity at excitation light wavelength 350 nm and 380 nm can be used to calculate the Ca^{2+} concentration by the following equation:

$$[Ca^{2+}]_i = K_{eff} * (R - R_{min}) / (R_{max} - R)$$

$$R = F_{350}/F_{380}$$

R_{min} fluorescence ratio of free Ca^{2+} solution

R_{max} fluorescence ratio of high Ca^{2+} concentration (10 mM) solution

K_{eff} effective binding constant

With the K$_d$ of 220 nM, Fura-2 is a good candidate to measure calcium concentrations below 1µM. However the range of Ca^{2+} concentration in this study was from hundreds of nM to tens of µM. To get adequate resolution of higher Ca^{2+} concentrations, a combination of Fura-4F (K$_d$ = 770 nM) and Furaptra (K$_d$ = 40 µM) was used. In this case, an *in vivo* calibration curve was needed for the calculation of Ca^{2+} concentrations. Cells were patched in the whole cell configuration with different solutions of known Ca^{2+} concentration, buffered by BAPTA or DPTA. The mixture of two dyes was allowed to diffuse into cells and after the ratio become stable, it was recorded and the ratios were plotted vs Ca^{2+} concentration as shown in Fig. 7.
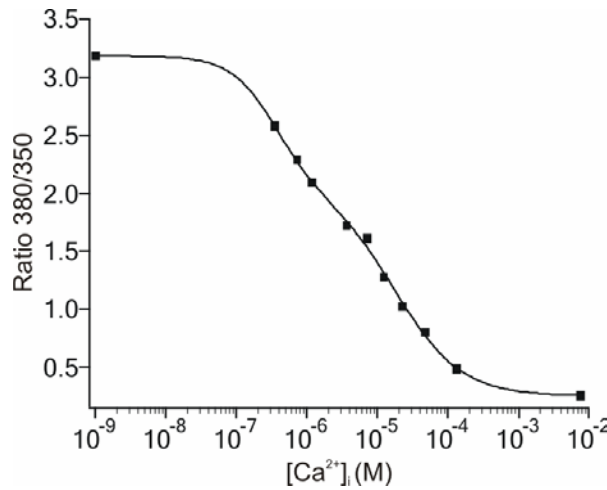
Figure 7. In vivo calibration curve.
Every point is the average of several experiments.

The relationship between fluorescence ratio and Ca^{2+} concentration can be described as the following equation:

$$R = R_{min} - R_1 * [Ca^{2+}]_i /([Ca^{2+}]_i + K_{Fura-4f}) - R_2 * [Ca^{2+}]_i /([Ca^{2+}]_i + K_{Furaptra})$$

$$R = F_{350}/F_{380}$$

R_{min} fluorescence ratio of free Ca^{2+} solution

$R_{min} - R_1 - R_2$ fluorescence ratio of high Ca^{2+} concentration (7.6 mM) solution

Using this equation to fit the data points gotten from above experiments, a calibration curve was created to convert the fluorescence ratio to Ca^{2+} concentration.

2.2.5.2.3 Photolysis efficiency at the setup

To reach appropriate Ca^{2+} concentrations after the UV flash, the photolysis efficiency of the flash lamp was determined. A solution containing 0.5 mM NP-EGTA, 0.56 mM $CaCl_2$, 0.5 mM Fura-2 was perfused into cells in the whole cell configuration and the fluorescence ratio was measured before and after UV flash. The recorded fluorescence ratio was converted to Ca^{2+} concentration based on the Fura-2 calibration curve. The basal Ca^{2+} concentration of the calibration solution was calculated to be 175 nM. Post-flash Ca^{2+} concentrations are variable depending on different photolysis efficiencies. Ca^{2+} concentrations measured experimentally and those calculated with the program should be in agreement. The flash lamp photolysis efficiency was adjusted to near 30% by using a neutral density filter if it is too high, and increasing the flash strength if it is too low.

In the whole-cell patch clamp mode, caged-calcium compound (NP-EGTA) and calcium indicators (Fura-4F and Furaptra) were perfused into the cell. Upon UV-illumination (Rapp Opto Electronics, Hamburg, Germany), calcium was cleaved from NP-EGTA compound and released, producing a step-like increase of intracellular calcium concentration. The mixture of two fluorescence dyes was excited with UV-illumination alternated between 350 nm and 380 nm with the monochromator (Polychrome, TILL Photonics, Planegg, Germany), emission was monitored at 510 nm.

2.2.6 Amperometry

Amperometry provides an additional method to investigate exocytosis. A small-sized carbon fibre electrode was fabricated to detect the transmitter release from single cells. The carbon fibre electrode is held at a constant electrical potential greater than the redox potential of the catecholamine we want to measure and positioned very close to the cell to minimize the transmitter diffusion effect. When the released transmitters contact the surface of the carbon fibre, they are oxidized immediately generating an electrical signal which is recorded as current at the carbon fibre surface.

2.2.6.1 Fabrication of carbon fibre electrodes

Carbon fibre electrodes used for amperometry were produced as following. Copper cannulas were cleaned; the carbon fibres (5 µm diameter) were glued to the copper cannulas using a conducting carbon paste (Electrodag 5513, Bavaria Elektronik, Germany). When the glue was dry, the copper cannula with a carbon fibre was glued inside a glass pipette using a drop of 2-component epoxy glue. After hardening overnight, the pipettes were then pulled with a conventional puller. The carbon fibre extending beyond the pulled pipette tip was put into a drop of cathodal paint (Electrocoating ZQ 84-3255, BASF, Germany) on a U-shaped platinum foil and coated by electrolysis. The assembly was then baked for 4 min at 190°C. The junction between the fibre and the glass was sealed with Sylgard and baked again for 4 min at 190°C (Fig. 8). Before use, the carbon fibres were cut to expose the tip for recording and tested on stimulated chromaffin cells. The electrode was connected to the head stage of an EPC7 patch-clamp amplifier (HEKA), and a holding potential of -800 mV

was applied in the voltage-clamp mode. When the carbon fibre was immersed into the extracellular solution, the appearance of a large spike of current indicates the electrode sensitivity. The carbon fibre then was positioned lightly touching the surface of a chromaffin cell. The chromaffin cell was mechanically stimulated by a glass pipette. Released catecholamines from chromaffin cell contacting with the carbon fibre were immediately oxidized, producing a spike-like current indicating catecholamine sensitivity.
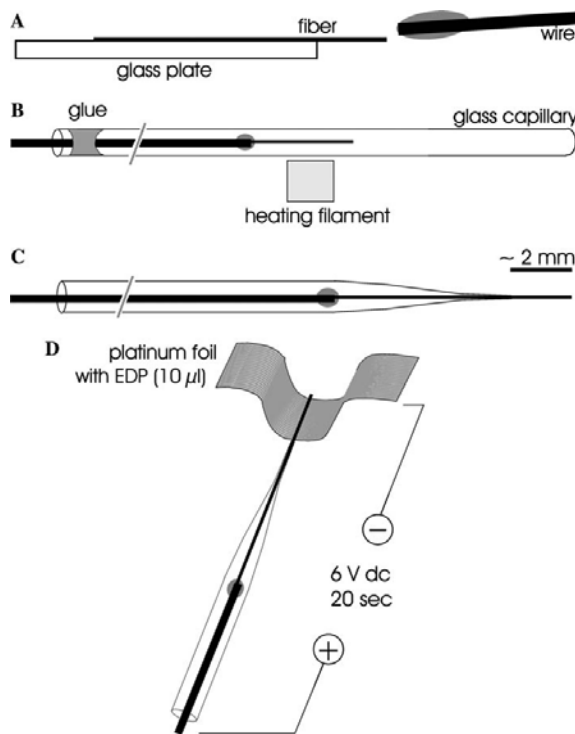
Figure 8. Schematic steps of carbon fiber electrodes fabrication.
A. The carbon fibre is glued to the copper wire.
B. The copper wire with a carbon fibre is glued to a glass pipette.
C. The pipette is pulled by a puller. The carbon fibre extending beyond the pulled pipette tip is trimmed to around 2 mm.
D. The trimmed carbon fibre tip is coated with EDP. (Modified from (Bruns, 2004)).

2.2.6.2 Single spike analysis

The highly sensitive amperometric method allows detection of single vesicles exocytosis. As shown in Fig. 9, a spike represents the secretion from an individual vesicle. Analysis of single spike characteristics of amplitude, charge, half-width, 50% to 90% rise time provides information about the vesicle fusion event. Vesicle release probability can also be examined by measuring the frequency of spikes. Sometimes the spike is preceded with a small "foot" like signal which reflects the diffusion of transmitters through an opening fusion pore. Kinetic analysis of this foot signal was used to investigate the formation and dilating of fusion pore.
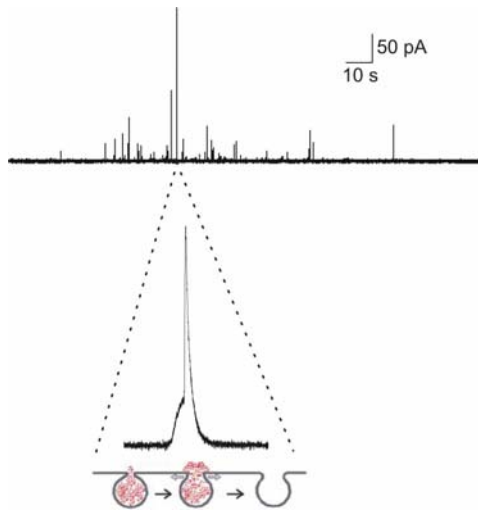
Figure 9. Example of amperometric spikes.
Inset is the enlarged single spike with preceded foot. Below the single spike is the schematic graph of dilating of fusion pore. (Modified from (Borisovska et al., 2005))

To get separate individual spikes, the stimulation to trigger exocytosis should be moderate. In this study an intracellular solution containing 4 µM free calcium was perfused into the cell. Before the formation of whole-cell configuration, the carbon fibre electrode was placed lightly on the patched cell. After sealing and subsequently break in, the calcium solution diffused into cells causing secretion, which was monitored by the carbon fibre electrode. The amperometric signals were filtered at 3 kHz. Spikes with amplitude larger than the averaged noise level were collected. Pre-spike foot (PSF) signals were determined and analyzed as previously described (Mosharov and Sulzer, 2005).

2.2.6.3 Combined amperometry and capacitance measurement

Capacitance measurements indicate the change of cell plasma membrane surface area. Fusion of vesicles with the plasma membrane increases the plasma membrane area. Retrieval of vesicles decreases the plasma membrane area. Both exocytosis and endocytosis can be detected by capacitance measurement. Amperometry directly detects the released transmitter thereby avoiding errors caused by endocytosis. However amperometric measurement is affected by the diffusion of the transmitter from cell to carbon fibre and not all vesicles are released adjacent to the carbon fibre. Thus there are variabilities in the response. Combined amperometry and capacitance measurement provide two independent and complementary methods to investigate

exocytosis.
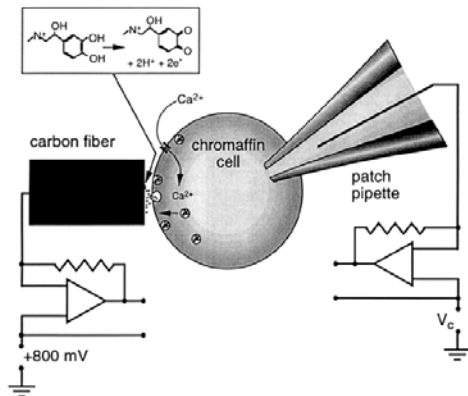
Figure 10. Combined amperometry and capacitance measurement.
The flux of Ca^{2+} through Ca^{2+} channel trigger exocytosis detected by amperometry and capacitance measurement simultaneously.

2.2.7 Data analysis

Data obtained were analyzed with IGOR Pro (Wavemetrics, Lake Oswego, OR). Capacitance curves of flash experiments were fit with the following equation: $f(t) = A_0 + A_F*(1 - exp(-(t-T_0)/T_F)) + A_S*(1 - exp(-(t-T_0)/T_S)) + SL*(t-T_0)$. A_0 is the cell capacitance before flash. T_0 is the fitting starting time point. A_F, A_S, T_F, T_S are the amplitude and time constant of RRP and SRP respectively. SL represents the sustained release rate (fF/s). Capacitance curves of ramp experiments were fit with the following equation: $f(x) = Base + Max\_1/ (1+exp ((xhalf\_1-x)/rate\_1)) + Max\_2/ (1+exp ((xhalf\_2-x)/rate\_2))$. Base is the cell capacitance before ramp. Max_1, Max_2, xhalf_1, xhalf_2, rate_1, rate_2 are maximum amplitude, x value of half maximum amplitude and rate of first and second component respectively. Data are shown as Mean ± SEM.

3 Results

3.1 Secretion from CAPS-2 deficient mice

3.1.1 Deletion of CAPS-2 does not change the secretion

We have examined the release of catecholamines from CAPS-2 KO mice. In contrast to CAPS-1 KO mice, CAPS-2 KO mice did not show a perinatal lethal phenotype. To make the results comparable with the data from CAPS-1 KO cells published previously, chromaffin cells from new born (p1) CAPS-2 KO and wild-type mice were used. The caged calcium compound and fluorescence dye are loaded into cells through the glass pipettes in the whole-cell mode. Upon a UV flash, the intracellular calcium concentration is elevated triggering secretion which is detected as a capacitance change and amperometric responses simultaneously. By combining flash photolysis, which allows immediate, global increases in calcium, with ratiometric calcium monitoring, we bypassed problems of microdomains while confirming that intracellular calcium levels in controls and CAPS-2 KO mice were comparable. The results are shown in Fig. 1. The pre-flash $[Ca^{2+}]_i$ (337.8 ± 18.6 nM in CAPS-2 KO; 350.3 ± 17.6 nM in WT) and post-flash $[Ca^{2+}]_i$ (22.2 ± 2.0 µM in CAPS-2 KO; 24.2 ± 2.5 µM in WT) are comparable in CAPS-2 KO and wild-type cells. Both capacitance measurement and integration of amperometric response indicate that the secretion from CAPS-2 KO chromaffin cells was unchanged compared to wild-type cells. The capacitance increase was fitted as the sum of two exponentials and a linear phase estimating the size of two releasable pools and the sustained release rate. The amplitude of RRP (88.5 ± 9.2 fF in CAPS-2 KO; 99.5 ± 17.5 fF in WT) and SRP (95.8 ± 19.6 fF in CAPS-2 KO; 123.9 ± 19.6 fF in WT) as well as the sustained release rate (17.4 ± 2.0 fF/s in CAPS-2 KO; 19.8 ± 3.1 fF/s in WT) were not significantly different between the CAPS-2 KO and wild-type cells. The time constants of RRP (28.8 ± 4.0 ms in CAPS-2 KO; 30.1 ± 4.7 ms in WT) and SRP (590.4 ± 125.3 ms in CAPS-2 KO; 612.7 ± 186.7 ms in WT) were also not different.
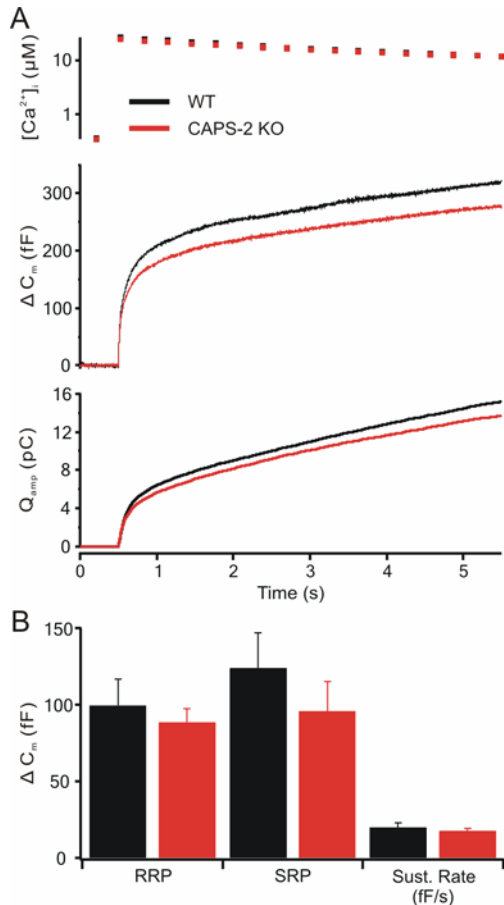
Figure 1. Secretion of chromaffin cells from CAPS-2 deficient mice is not altered.

A. Averaged calcium concentration ($[Ca^{2+}]_i$; top), capacitance (ΔC_m; middle) and cumulative amperometric charge (Q_{amp}; bottom) in response to flash-photolysis of NP-EGTA in wild-type cells (black; n=21, N=2) and CAPS-2 KO cells (red; n=23, N=2). Both capacitance and amperometric traces of CAPS-2 KO cells show a similar secretion as WT cells.

B. Kinetic analysis of experiment shown in (**A**). The amplitude of RRP and SRP as well as the rate of sustained component are not significantly different between the two groups (mean ± SEM).

3.1.2 The calcium-sensing is not changed when CAPS-2 is absent

To test whether the absence of CAPS-2 causes a change of the calcium-sensing, ramp experiments are performed with CAPS-2 KO and wild-type cells. In contrast to the stepwise increase of $[Ca^{2+}]_i$ in flash experiments, a slowly increasing calcium concentration in a ramp-like manner is generated by a sequence of UV illuminations. The secretion is measured as the change of capacitance. The results are shown in Fig. 2. In CAPS-2 KO and wild-type cells the $[Ca^{2+}]_i$ is continuously elevated from several hundreds of nM to tens of micromolar in a similar pattern. The $[Ca^{2+}]_i$ in CAPS-2 KO cells is comparable with that of wild-type cells and the capacitance response in CAPS-2 KO cells is quite similar to that of wild-type cells, the calcium-sensitivities appear to be unchanged in CAPS-2 KO chromaffin cells. The averaged total secretion in CAPS-2 KO cells is 246.4 ± 45.1 fF which is also comparable to the secretion of wild-type cells (267.0 ± 50.2 fF), consistent with the oberservations in flash experiments.
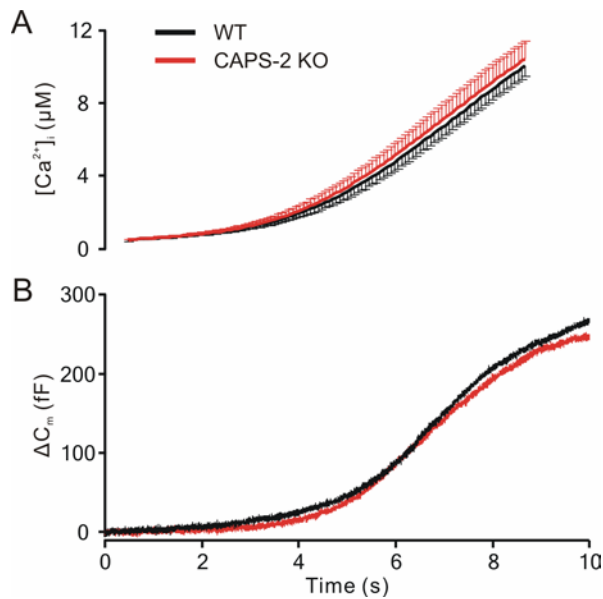
Figure 2. Calcium-sensing is not altered in CAPS-2 KO mouse chromaffin cells.
A. The calcium concentration ($[Ca^{2+}]_i$) is raised slowly and continuously by alternative weak UV illumination of 350 and 380 nm. There is no significant difference of calcium concentration between CAPS-2 KO (red; n=23, N=2) and wild-type (black; n=21, N=2) cells (mean ± SEM). **B**. The capacitance trace (ΔC_m) from CAPS-2 KO cells is similar as WT cells.

3.1.3 CAPS-2 deficiency has no effect on vesicle fusion

Next amperometric measurements were performed to quantify the single vesicle secretory events. Wild-type and CAPS-2 KO Cells were perfused by 4 µM calcium solution through glass pipettes to stimulate the secretion. A carbon fibre electrode was placed close to the cell detecting the released catecholamines. In Fig. 3A, representative amperometric traces from wild-type and CAPS-2 KO cells are shown. Every single spike represents the fusion of a single secretory granule. The kinetic parameters of single spikes are shown in Fig. 3B-G. There was no difference in amplitude, charge, 50%-90% rise time, half-width and foot-duration between the WT and CAPS-2 KO cells (Fig. 3B-F). The event frequency of CAPS-2 KO cells (1.6 ± 0.2 events/s) was also comparable with that of wild-type cells (1.8 ± 0.2 events/s) which is consistent with the observation from flash and ramp experiments.
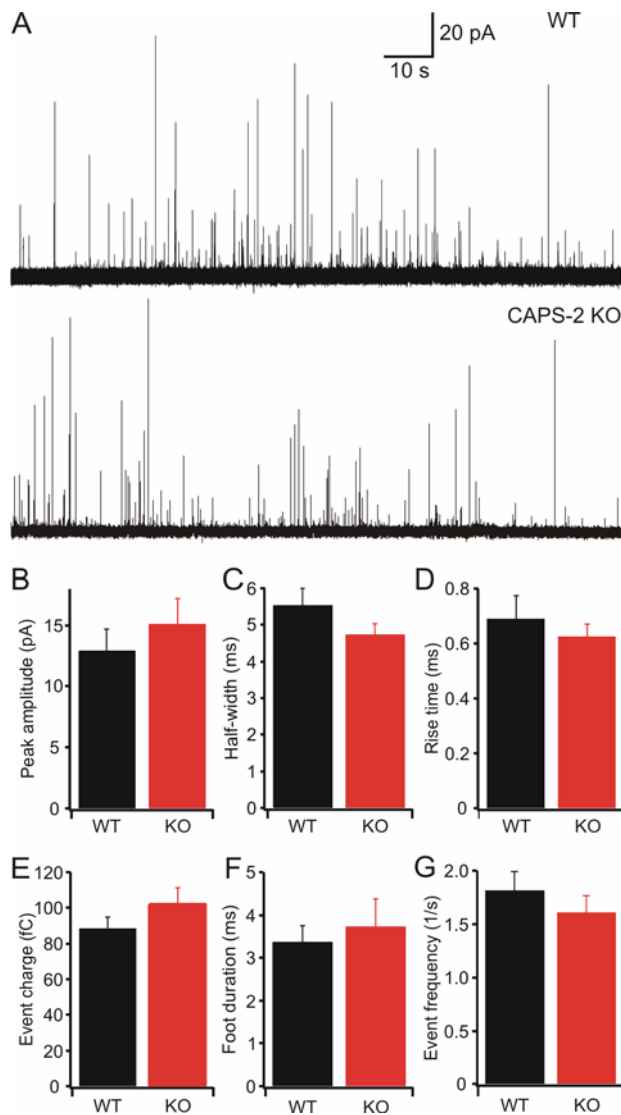
Figure 3. The characteristics of fusion are unchanged in CAPS-2 KO mouse chromaffin cells.
A. Representative amperometric trace from wild-type (upper) and CAPS-2 KO (lower) chromaffin cells perfused by 4 µM calcium solution.
B–G. Average of cell medians of amperometric event parameters. Amplitude (**B**), half-width (**C**), 50%-90% rise time (**D**), charge (**E**), foot duration (**F**) and event frequency (**G**) are statistically identical between two groups (mean ± SEM). Data are collected from 1533 events of 16 wild-type cells and 1304 events of 14 CAPS-2 KO cells.

3.2 Secretion from CAPS-1/CAPS-2 DKO mice

3.2.1 CAPS DKO cells exhibit a large deficit in exocytosis

We then compared secretion in CAPS DKO mice with that observed in wild-type cells. After flash photolysis, the intracellular free calcium was raised instantly from the resting level of ~450 nM to ~20 µM. This increase in calcium caused fusion of catecholamine-containing vesicles, leading to an increase in cell capacitance (Fig. 4A, ΔCm). The cumulative charge (Qamp) measured by the carbon fiber is shown in the third trace. Secretion as measured either by capacitance change or amperometric charge was less in the CAPS DKO cells than that observed in the wild-type cells (46 and 38% of WT values, respectively). The relatively larger reduction in amperometric

current can be attributed to the influence of CAPS on vesicle filling (presence of empty vesicles) as reported previously (Speidel et al., 2005).

Exocytosis of LDCVs in chromaffin cells is a highly regulated event consisting of a burst phase and a sustained phase. The burst phase consists of release of an RRP and a slowly releasing pool (SRP) of vesicles. The sustained release phase is attributable to maturation (priming) of LDCVs that were not primed at the time of the initial calcium increase, followed by their fusion (Burgoyne and Morgan, 2003; Rettig and Neher, 2002; Sorensen, 2004). The responses were fit as the sum of two exponentials, one each for the RRP and SRP, and a linear component of sustained release. Summarized results are shown in Fig. 4B. The burst phase of vesicle fusion in wild-type chromaffin cells was measured as a capacitance change of 153.4 fF, with 65.4 ± 8.3 fF contributed by the RRP and 88 ± 17.3 fF contributed by the SRP. The sustained release in the wild-type cells was 19.5 ± 2.2 fF/s. In CAPS DKO chromaffin cells, the burst phase of fusion amounted to 101.8 fF, with 31.3 ± 9.8 fF attributable to the RRP and 70.5 ± 14.5 fF attributable to the SRP. The reduction in the RRP in CAPS DKO cells was highly significant, whereas the reduction in the SRP was not, possibly indicating a selective action of CAPS on the RRP. Sustained secretion was virtually absent (0.5 ± 2.1 fF/s) in the DKO cells. The release time constants for the RRPs (29 ± 9 vs 56 ± 15 ms) and SRPs (400 ± 56 vs 500 ± 51 ms), in wild-type and CAPS DKO chromaffin cells, respectively, were not significantly different ($p > 0.05$).
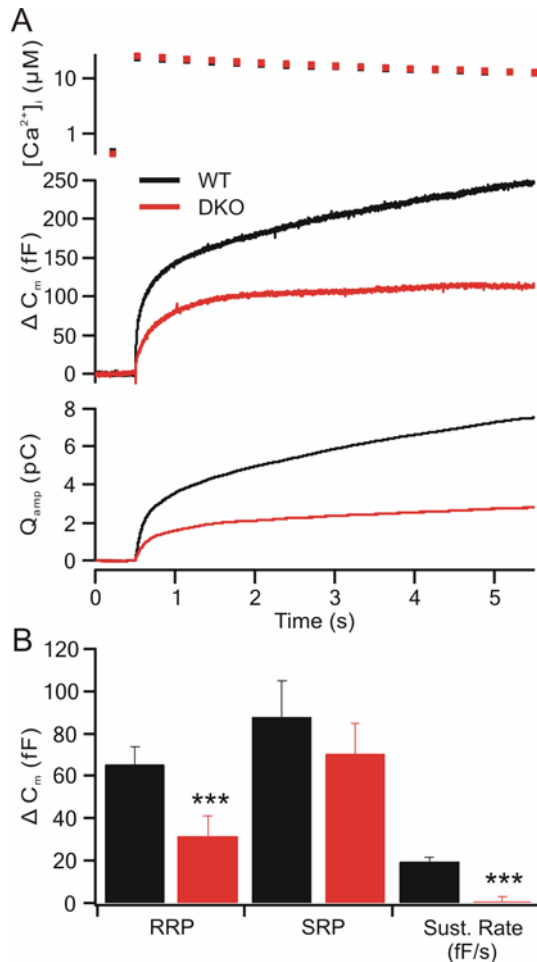
Figure 4. Catecholamine secretion is suppressed in CAPS DKO chromaffin cells compared with wild-type cells.

A. The intracellular calcium after flash photolysis of NP-EGTA (top trace) is shown along with capacitance changes (ΔC_m) and cumulative charge (Qamp) released from chromaffin cells as determined by amperometric measurements using carbon fiber electrodes in wild-type (WT; black traces; n=30) and CAPS DKO (red traces; n=29) chromaffin cells. Both the capacitance response and the amperometric response indicate a strong reduction in secretion in the CAPS DKO cells.

B. Kinetic analysis of the capacitance responses indicates that the CAPS DKO cells exhibit a significantly reduced RRP and a strong reduction in the sustained component (Sust. Rate; ***p<0.001). The SRP was not significantly reduced, although the average SRP was also smaller. Error bars indicate SEM.

3.2.2 CAPS deficiency does not change morphological docking

The reductions in the burst amplitude and in the sustained component of release observed in CAPS DKO chromaffin cells are consistent with a deficit in available vesicles at the plasma membrane or a defect in vesicle priming. To distinguish between these two alternatives, we quantified LDCVs in chromaffin cells using electron microscopy. We examined the density and location of LDCVs (wild type, 3281 from 28 cells; DKO, 4090 from 28 cells) with respect to the plasma membrane. Wild-type cells and CAPS DKO cells exhibited a similar distribution of vesicles (Fig. 5). The mean numbers of "morphologically docked" vesicles, those with centres within a vesicle radius (~80 nm) of the plasma membrane, were not different in the two populations. Thus, the observed reduction in secretion is most likely attributable to a defect in priming rather than in docking of LDCVs.
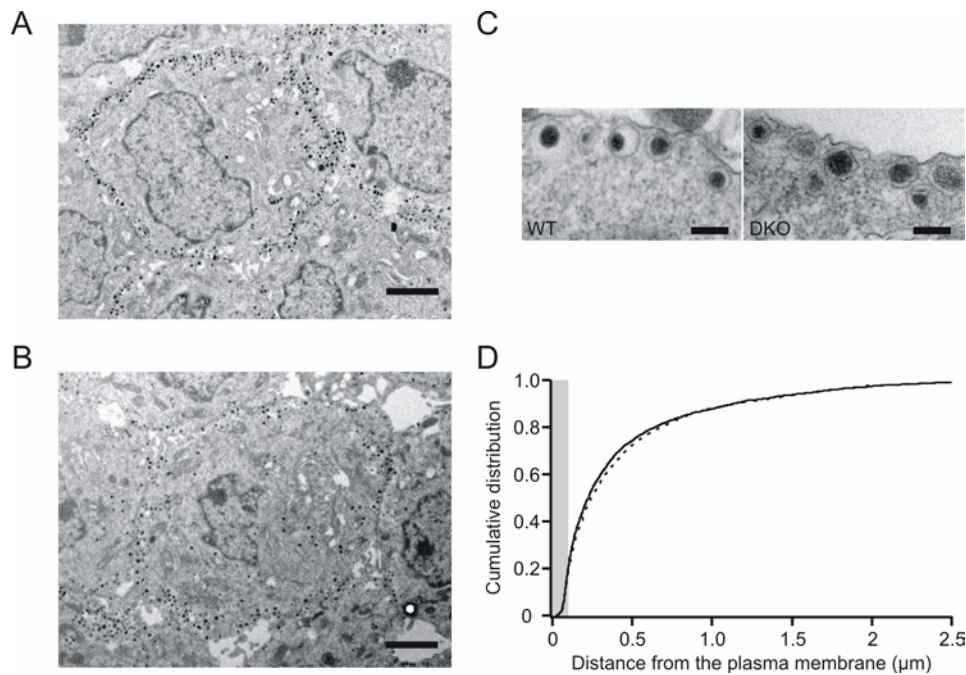
Figure 5. The distribution of LDCVs in CAPS DKO chromaffin cells is similar to that observed in wild-type chromaffin cells.

A. and **B**. Electron micrographs showing wild-type (**A**) and CAPS DKO (**B**) chromaffin cells. Scale bars, 2 μm. **C**. Higher-magnification micrographs showing details of individual vesicles in chromaffin cells. Scale bars, 200 nm. **D**. The cumulative distribution of distance of the midpoint of the vesicle from the plasma membrane. Although the wild-type (solid line) and DKO (dashed line) distributions were significantly different with p < 0.05 (Kolmogorov–Smirnov test), the greatest difference was 3.3% and occurred at a distance of 177 nm, outside of the morphologically docked zone (radius, 100 nm; gray). There was no significant difference in the density of vesicles with centres within a vesicle radius (80 nm) of the plasma membrane. WT, Wild type.

3.2.3 Refilling of the RRP is reduced in CAPS DKO chromaffin cells

A defect in priming efficacy would be expected to decrease not only the size of the releasable vesicle pools and sustained release, but also to reduce the degree or rate of pool recovery after stimulation. We examined the recovery of the releasable vesicle pools using paired flash stimulations (Fig. 6). In these experiments, we did not maintain calcium at high levels after the flash, but rather allowed free calcium levels to decrease after the flash to allow more rapid recovery of releasable vesicle pools. An interstimulus interval (ISI) of 2 min between flashes allows for the recovery of releasable vesicle pools, and the second of a pair of responses is typically quite similar to the first.

We first examined an ISI of 45 s (Fig. 6A). In wild-type cells, the burst amplitude after the second flash was similar to that in the first flash (Fig. 6A, left) with an RRP and

SRP of similar amplitude (Fig. 6A, middle). In CAPS DKO cells, the RRP was reduced and the SRP was moderately increased after the second flash, with a net decrease in the burst phase of release. With an ISI of 25 s (Fig. 6B), the secretion from wild-type cells was similar to that observed at a 45 s ISI, whereas the CAPS DKO cells exhibited a marked reduction in the RRP and an overfilling of the SRP (Fig. 6B, middle), resulting in a net increase in the burst phase of release (Fig. 6B, right). With an ISI of 15 s (Fig. 6C), the wild-type cells exhibited burst responses with reduced RRP and increased SRP amplitudes in the second response, whereas the CAPS DKO cells had virtually no RRP and a more strongly enhanced SRP (Fig. 6C, middle), resulting in an even larger burst (Fig. 6C, right). There was no evidence of a sustained component in the CAPS DKO cells, with some endocytosis occurring during the second response. Notably, the burst amplitudes (Fig. 6C, right) of the wild-type responses remained constant, whereas the burst in the second flash in DKO mice increased at shorter ISIs. Thus, although the RRP refilled quite slowly in DKO mice, relative to that in the wild-type cells (Fig. 6C, middle), priming into the SRP approached wild-type levels at the 15 s ISI (Fig. 6C, middle). This may indicate that the SRP primes quickly but decays again at longer ISIs. There were no changes in the release kinetics of the RRP and SRP ($p > 0.2$).

The enlarged SRP at short intervals could be attributable to the increased intracellular calcium levels present between the two flashes. This is reminiscent of the temporary reversal of the deficit in transmitter release in hippocampal neurons in CAPS DKO mice when extracellular calcium was raised (Jockusch et al., 2007).
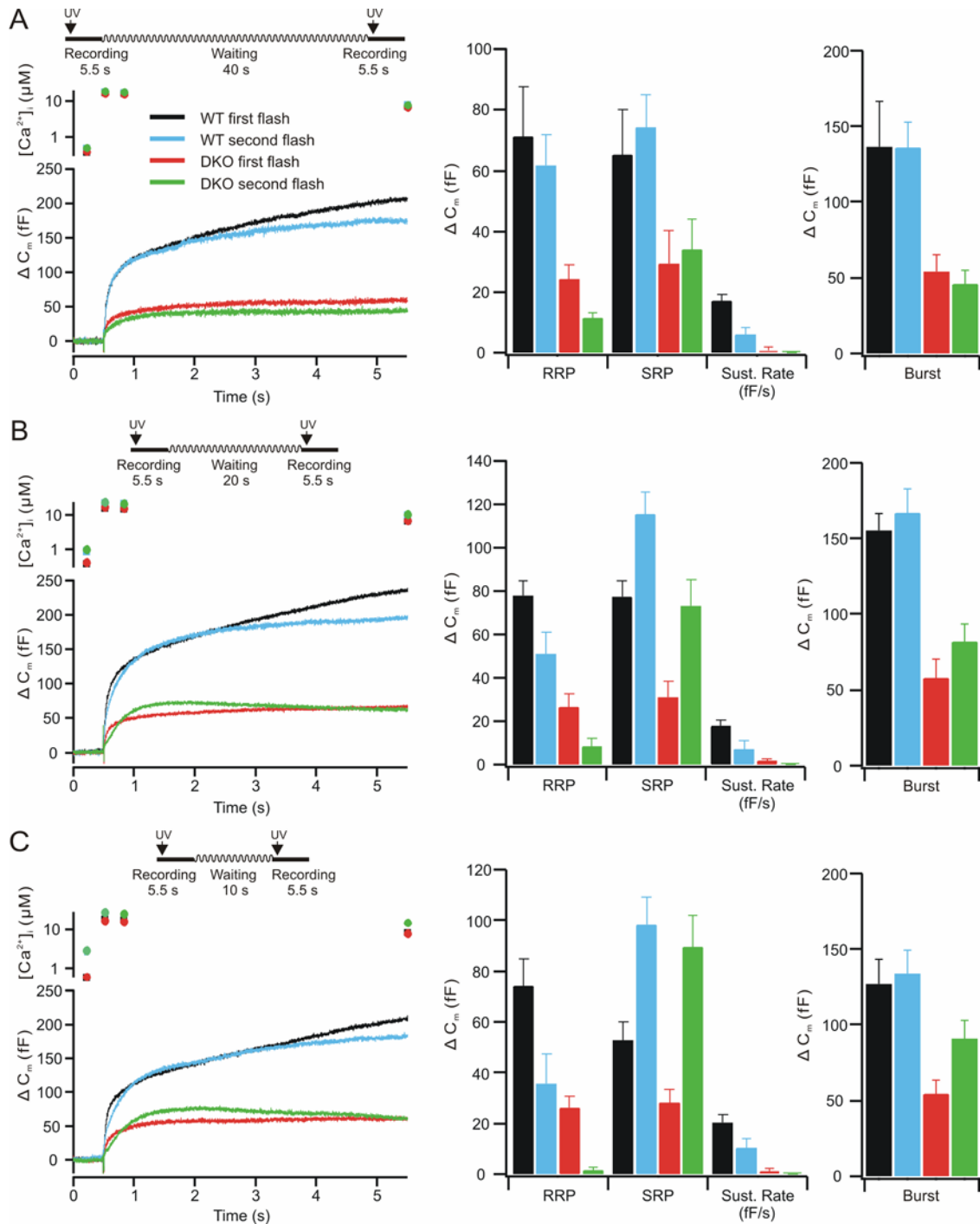
Figure 6. Responses to flash stimulation with decreasing ISIs.
A. At an ISI of 45 s, the burst phase is fully recovered in both wild-type (n=13) and DKO (n=14) cells. **B**. When the ISI was shortened to 25 s, the RRP was reduced although the SRP was enhanced in wild-type (n=25) and in DKO (n=25) cells, but this trend was much stronger in the CAPS DKO cells. **C**. At an ISI of 15 s, the trend to smaller RRP and greater SRP was again apparent in both wild-type (n=20) and DKO (n=22) cells. The RRP in the CAPS DKO mice was almost nonexistent. The SRP was, in contrast, overfilled. There was no sustained component in the DKO cells, although one was present in the wild-type cells. The averages of pool sizes (mean ± SEM) for the double-flash experiments are shown in the middle traces. Wild-type (black, first flash; blue, second flash) and DKO (red, first flash; green, second flash) cells RRPs, SRPs, and

sustained release rates (Sust. Rate) are shown for the 45 s interval (**A**), for the 25 s interval (**B**), and for the 15 s interval (**C**). The DKO cells exhibited less secretion in all phases of the response. In addition to significantly lower secretion in the DKO cells, the sustained release was strongly reduced. At 45 s, ISI secretion was similar to that observed at a 2 min ISI. At shorter ISIs, refilling of the RRP was strongly reduced in the CAPS DKO cells, whereas the SRP was refilled. The averaged burst responses (sum of RRP and SRP) are shown on the right and indicate that although the burst remained constant for wild-type cells, they actually were greater at short intervals in the DKO cells. Error bars indicate SEM.

3.2.4 Calcium-sensing does not change in CAPS DKO chromaffin cells

We tested whether secretion in CAPS DKO cells has a different calcium requirement than that of wild-type cells. To this end, we applied a calcium "ramp" stimulus (Sorensen et al., 2002), a slowly rising calcium concentration generated by photolysis of calcium from NP-EGTA in small increments over a longer time (10 s), as opposed to the stepwise increase achieved using a flash lamp. This was done using short pulses of UV light of 350 and 380 nm at short intervals. The calcium ramp stimulus led to robust secretion (Fig. 7A). The response to the ramp stimulus was sigmoid in both the wild-type and CAPS DKO cells (Fig. 7A). Scaling the release response of CAPS DKO mice to that of wild-type cells indicated a slightly steeper early rising phase in the DKO cells (data not shown). The total secretion in the wild-type cells (334.4 ± 32.3 fF; n =16) was approximately four times that in the DKO cells (76.3 ± 10.8 fF; n = 15). The secretion response in wild-type cells, although sigmoid, was best fit with the sum of two sigmoids, whereas the secretion in the CAPS DKO cells could be well fit with a single sigmoid curve (Fig. 7A). In the case of the wild-type cells, the first component had a midpoint near 5 s and consisted of 198 fF. This component likely represents the burst response. The additional secretion is likely attributable to sustained release. The sigmoid fit for the CAPS DKO cells had a midpoint near 5.6 s and likely consists of only a burst response of ~80 fF. The thresholds for calcium induced secretion during the ramp stimulation were similar (~800 nM) in wild-type and CAPS DKO cells. We estimated the rate constants for secretion (Sorensen et al., 2002), and these are plotted versus the calcium concentration in Fig. 7B. For both wild-type and CAPS DKO responses, estimated rate constants rose with the calcium concentration and were similar over the entire

range tested. Thus, CAPS does not alter calcium sensing during secretion.
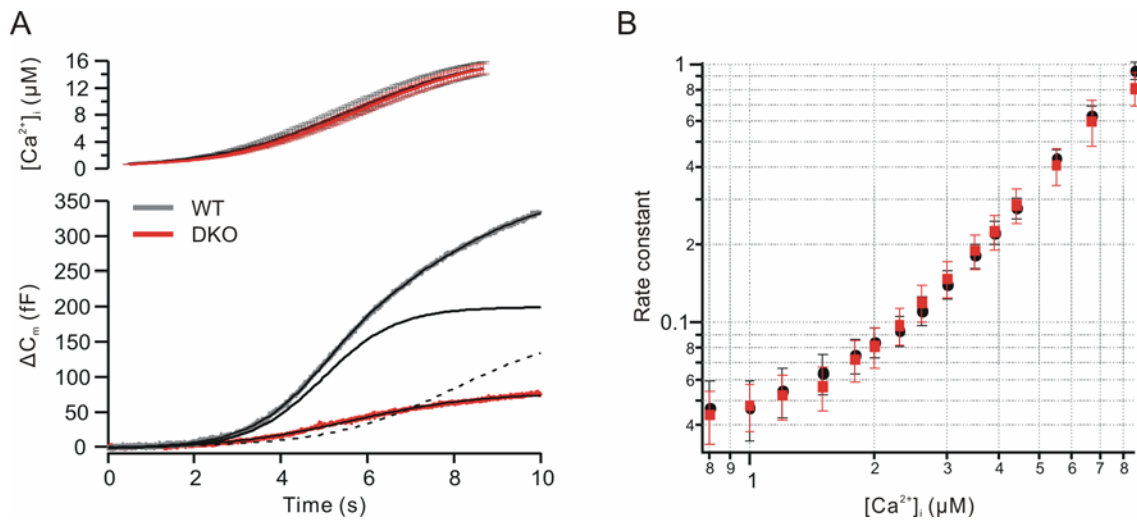
Figure 7. The calcium dependence of secretion is unchanged in CAPS DKO chromaffin cells.

A. Ramp-like calcium increases (mean ± SEM; top trace) lead to robust secretion in wild-type chromaffin cells (WT;ΔCm). The total mean secretion during the ramp stimulus was 334 fF in wild-type cells (n=15) and 76 fF in CAPS DKO cells (n=16). The capacitance trace of wild-type cells (gray) was fit with a dual sigmoid curve (overlaid black line), with an early phase (solid line) and a later phase (dashed line). The capacitance response of the DKO cells (red trace) was well fit with a single sigmoid (overlaid). **B**. The rate constant of stimulated release (based on the capacitance change) was similar in wild-type (black) and CAPS DKO (red) cells. The threshold for calcium-dependent secretion was not different. The results show that the calcium dependence of secretion is similar in wild-type and CAPS DKO cells and indicate that CAPS does not alter calcium sensing in the secretion phase.

3.2.5 Deletion of CAPS-1 and CAPS-2 does not change the fusion kinetics

To determine whether there were qualitative changes in vesicle fusion, we examined the properties of single amperometric events. An example of such an experiment is shown in Fig. 8A. There was no significant difference between wild-type and CAPS DKO cells in the amplitude, half width, rise time, single spike charge, or "foot" parameters of the amperometric events (Fig. 8B–F). The only difference we observed between wild-type and CAPS DKO cells in amperometric events was in the frequency of events in calcium-perfused chromaffin cells (Fig. 8G), consistent with the observations in CAPS-1 knock-out cells, which we have reported previously (Speidel et al., 2005), and with reports in PC12 cells after CAPS knockdown (Fujita et al., 2007). Thus deletion of CAPS-1 and CAPS-2 does not change the fusion kinetics.
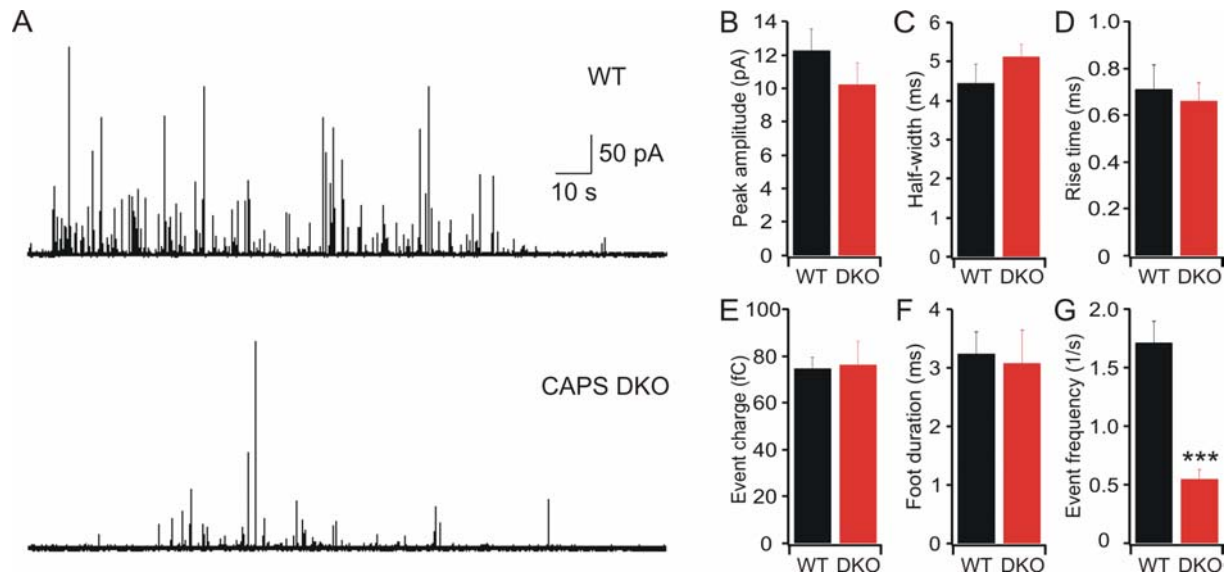
Figure 8. **Amperometric spike parameters are normal in CAPS DKO chromaffin cells.**
A. Example of amperometric activity during calcium perfusion (~4 µM) in wild-type (top trace) and DKO (bottom trace) cells. **B–F**. There was no difference in the following: the amplitude of amperometric responses between wild-type (n=12, 2151 events) and DKO cells (n=10, 479 events) (**B**); the half-width of amperometric spikes for DKO cells compared with wild type cells (**C**); the rise time of amperometric responses was similar in wild type and CAPS DKO chromaffin cells (**D**); the catecholamine content of the vesicles was also similar in wild-type and CAPS DKO cells (**E**); the duration of so-called foot events in the CAPS DKO cells compared with those events observed in wild-type cells (**F**). **G**. There was a strongly significant difference in the frequency of amperometric events compared with those observed in wild-type chromaffin cells during calcium perfusion (4 µM; ***$p<0.001$). The mean median values ± SEM are shown. WT, Wild type.

3.3 Restoration of secretion in CAPS DKO cells

3.3.1 CAPS-1 restores secretion in CAPS DKO chromaffin cells

To rule out the possibility that our results are an artifact because of secondary consequences of the CAPS deletion, we reintroduced CAPS-1 into chromaffin cells from CAPS DKO mice, using the Semliki Forest virus expression system. In flash experiments, the characteristics of CAPS DKO cells were similar to those described above, exhibiting a small burst response of ~47 fF (Fig. 9A) (n=15), with an RRP of 22.1 ± 5.7 fF, an SRP of 25.2 ± 8.4 fF, and little sustained release (2.4 ± 1.5 fF/s) (Fig. 9B). Recordings from CAPS DKO cells expressing CAPS-1 showed significantly stronger secretion, with a burst that was approximately five times larger than that observed in CAPS DKO cells (226 fF; n = 17) (Fig. 9A). The RRP of the DKO cells expressing CAPS-1 was 155.6 ± 23 fF, greater than that of the wild-type cells (Fig. 4),

whereas the SRP (69.1 ± 8.3 fF) and sustained release (20.9 ± 3.3 fF/s) were similar to that observed in wild-type cells (Figs. 4, 9B). The capacitance changes were associated with comparable amperometric responses as well (Fig. 10A). This result emphasizes the selective effect of CAPS on the filling of the RRP described in Fig. 4 and 6. The difference in release time constants of the RRP approached significance (CAPS DKO, 40 ms; CAPS-1 rescue, 27 ms; p > 0.05), but not in the SRP (CAPS DKO, 630 ms; CAPS-1 rescue, 461 ms; p > 0.2).
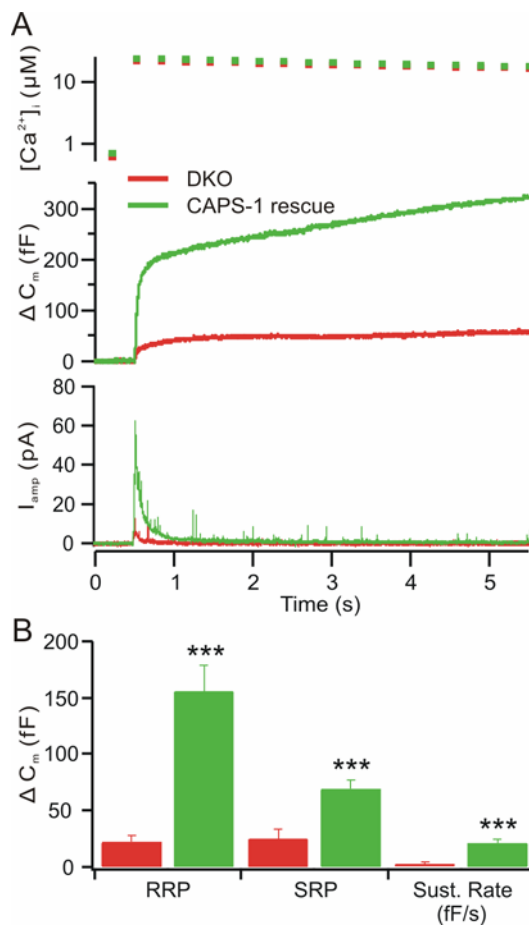
Figure 9. CAPS-1 reintroduction rescues the RRP and sustained release in CAPS DKO chromaffin cells.

A. Flash photolysis of NP-EGTA was performed in DKO chromaffin cells. These cells were used as controls for cells from littermates in which CAPS-1 was expressed using the Semliki Forest virus as vector. DKO cells exhibited low levels of secretion (Δ Cm) with no sustained component, whereas CAPS-1-expressing cells exhibited approximately fivefold secretion and a robust sustained component. The calcium levels reached in both groups were similar (top trace). The amperometric responses (catecholamine release; I_{amp}) observed during the capacitance change was also greatly enhanced after CAPS-1 expression.

B. The mean values ± SEM of the RRP, SRP (***p<0.001) and sustained phases in the above described rescue experiments. Sust. Rate, sustained rate.

We also tested whether overexpression of CAPS-1 in wild-type mice enhanced secretion. The results of this experiment are shown in Fig. 10. CAPS-1 overexpression in wild-type chromaffin cells led to a modest enhancement of the secretory burst and sustained release following photolysis of caged calcium. The RRP following CAPS-1 overexpression in wild type cells was 105 ± 16.1 fF compared to 79 ± 13.8 fF in control cells (no significant difference). The SRP sizes were 60.8 ±

10.7 and 60.7 ± 9.4 fF in CAPS-1 expressing wild-type cells and control cells, respectively. The sustained rate was also greater in CAPS-1 expressing cells (26.1 ± 5.2 fF and 19.1 ± 2.4 fF, CAPS-1 expression, and control, respectively, no significant difference). Although the overexpression of CAPS-1 in wild-type cells did not cause a significant difference of secretion, it selectively enhanced the RPP size and the sustained rate compared to control cells.
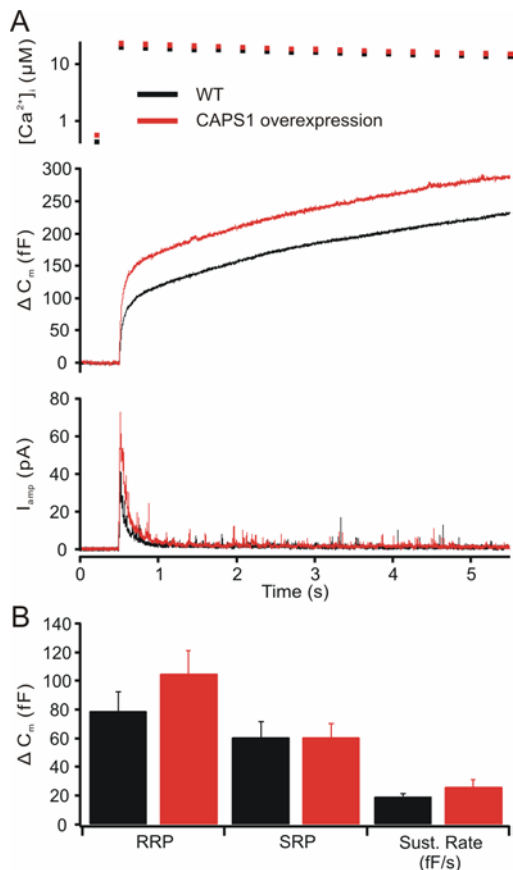
Figure 10. CAPS-1 enhances secretion in wild-type cells.
A. Overexpression of CAPS-1 in wild-type chromaffin cells results in a modest enhancement of secretion.
B. A modest strengthening of the readily releasable pool of vesicles and sustained rate did not reach statistical significance.

3.3.2 CAPS-2 also can rescue the CAPS DKO phenotype

To test whether CAPS-2 can also rescue the CAPS DKO phenotype, we performed CAPS-2 rescue experiments with CAPS DKO chromaffin cells. Expression of CAPS-2 in chromaffin cells from CAPS DKO mice resulted in a strong enhancement of the secretory burst and of sustained release (Fig. 11). By fitting the capacitance increase as the sum of two exponentials and a linear phase, we have estimated the size of the readily releasable pool and the slowly releasable pool, their time constants, and the rate of the linear sustained phase. The results of this analysis are shown in

Fig. 11B. There was a significant increase in the RRP (42.8 ± 18.6 fF, DKO; 125.3 ± 25.8 fF, CAPS-2 overexpressing DKO cells, p<0.001, Mann-Whitney U test) with no change in its time constant (23.5 ± 5.2 vs. 23.2 ± 1.4 ms), no change in the SRP (51.7 ± 12.8 fF, DKO; 51.8 ± 7.5 fF, CAPS2 overexpressing DKO cells), and an increase in sustained release which was not measurable in the DKO and 19.2 ± 3.7 fF/s in the CAPS-2 expressing DKO cells. Thus, as is the case for CAPS-1, expression of CAPS-2 in the CAPS DKO cells restores secretion with a selective effect on the RRP and the sustained phase.
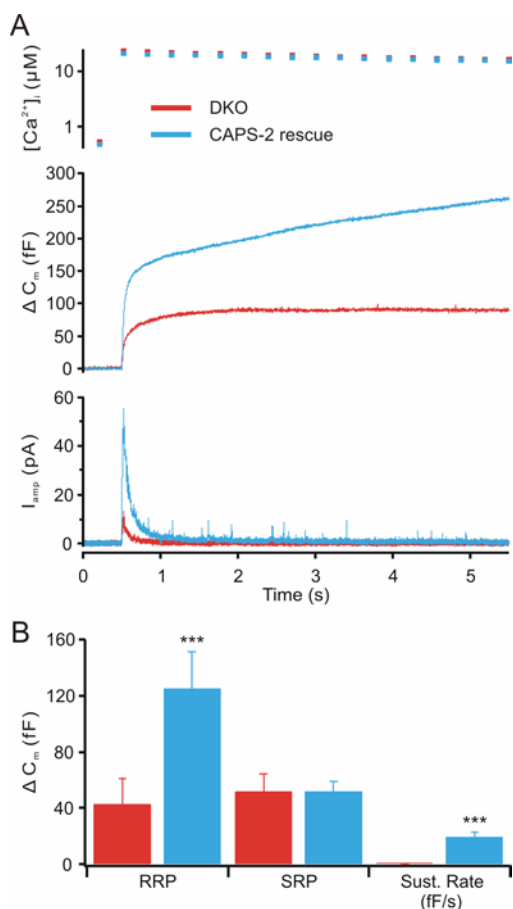
Figure 11. CAPS-2 restores secretion to wild type levels in CAPS DKO cells.
A. Responses to flash photolysis of caged calcium in CAPS DKO cells (red; n=19, N=3) and in CAPS DKO cells expressing CAPS-2 protein (blue; n=24, N=3). The calcium concentration (upper traces), the resulting change in membrane capacitance (middle traces) show a clear enhancement in those cells expressing CAPS-2. Carbon fibre responses to released catecholamines (lower traces) to show catecholamine release.
B. Analysis of the kinetics of the capacitance traces yield estimates of the releasable pools and the sustained release rate. The RRP was strongly enhanced by CAPS-2 expression, while there was no clear effect on the slowly releasable pool. The rate of sustained release in the period in which calcium remained elevated was also enhanced following CAPS-2 expression. ***p<0.001.

3.3.3 Open syntaxin rescues the RRP but not sustained release in CAPS DKO cells

As CAPS-1 and CAPS-2 both containing a MHD domain facilitate the priming and the MHD domain is critical for priming function of Munc13-1, an attractive hypothesis is that CAPS carries out its priming function in a fashion similar to that of the Munc-13's,

which bind to the Munc18-syntaxin complex (Betz et al., 1997; Richmond et al., 2001) promoting a conformational change in syntaxin, allowing it to engage into the SNARE complex (Dulubova et al., 1999). So we tested whether expression of an open form of syntaxin (Syntaxin1A - L165A/E166A; (Dulubova et al., 1999)) can reverse the CAPS DKO chromaffin cell secretion deficit (Fig. 12A). Expression of open-syntaxin in chromaffin cells from CAPS DKO mice led to strongly enhanced secretion (~3 fold increase). The enhancement was accounted for by a ~ 3 fold increase in the RRP (43.5 ± 8.9 fF, DKO; 129.2 ± 21.8 fF, open-syntaxin expressing DKO cells) (Fig. 12B). There was a modest increase in the SRP (52.3 ± 8.9 fF, DKO versus 79.5 ± 11.3 fF open-syntaxin expressing DKO cells) but there was virtually no sustained component in either group of cells. The lack of a sustained component may be due to exhaustion of the UPP since application of a second flash after a two minute recovery period resulted in a reduced open-syntaxin response, with a small RRP and no sustained component, while in the CAPS DKO cells the response to the second flash was equivalent to the first response (Fig. 12C and 12D). The secretory burst in the open-syntaxin expressing DKO cells was smaller than that in the DKO cells following the second flash application.
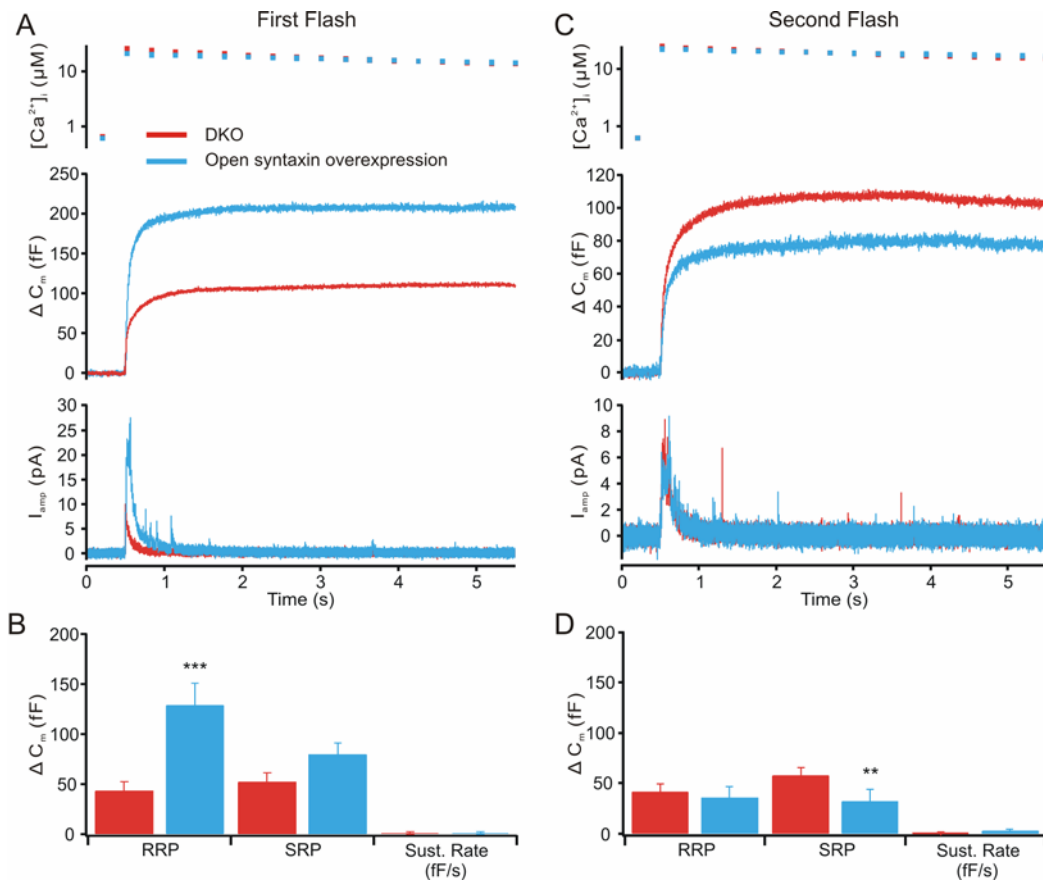
Figure 12. Open-syntaxin restores secretion in CAPS DKO cells.
A. The results of flash photolysis of caged which increases calcium (upper trace) in DKO cells (red; n=23, N=5) and DKO cells expressing open-syntaxin (blue; n=24, N=5) show that open-syntaxin restores secretion. The burst of secretion is much greater (middle traces) in the open syntaxin expressing cells, and the catecholamine release, as integral of the carbon fibre response (lower traces) is also strongly enhanced. **B**. Estimates of the releasable pools and the sustained rate indicate that open syntaxin enhances selectively the RRP. Note that there is little sustained release following the burst. **C**. Examination of a second flash stimulation to the same cells after a two minute recovery period shows that open syntaxin treated DKO cells recover poorly after flash stimulation. **D**. Pool analysis shows that open-syntaxin expressing DKO cells recover more poorly and do not exhibit a greater RRP after a second flash. **p<0.01;***p<0.001.

We next examined the effects of ramp stimulation in DKO cells in which open-syntaxin was expressed (Fig. 13). In agreement with the data obtained by flash stimulation (Fig. 12) these cells showed strongly enhanced secretion (295.5 ± 38.9 fF), as compared to that of untreated DKO cells (72.2 ± 13.2 fF, Fig. 13A). There was no difference between the calcium concentration threshold for secretion in DKO cells and open-syntaxin expressing cells. At the end of the ramp stimulus, a flash is applied to test the residual secretory capacity. The response is shown in Fig. 13B. The DKO cells secreted slightly more in response to the post-ramp flash, than did the open-syntaxin expressing DKO cells. The fraction of the total secretion released in

the post-ramp flash was ~64% in the DKO cells and ~25% in the open-syntaxin expressing DKO cells. Thus, in the open-syntaxin expressing DKO cells ~ 75% of the secretory capacity was released during the ramp stimulation. Only about 36% of the secretory capacity was released by the ramp stimulation in the DKO cells. The release following the flash stimulation was slow, and similar in both groups, indicating that residual release came from a slowly releasable pool of vesicles. The total secretion was much greater in the open-syntaxin expressing DKO cells, as was the case in the original flash experiments. Thus, though open-syntaxin bypasses the requirement for CAPS and generates a pool of vesicles that can be released by ramp or flash stimulation, it does not appear to support sustained release.
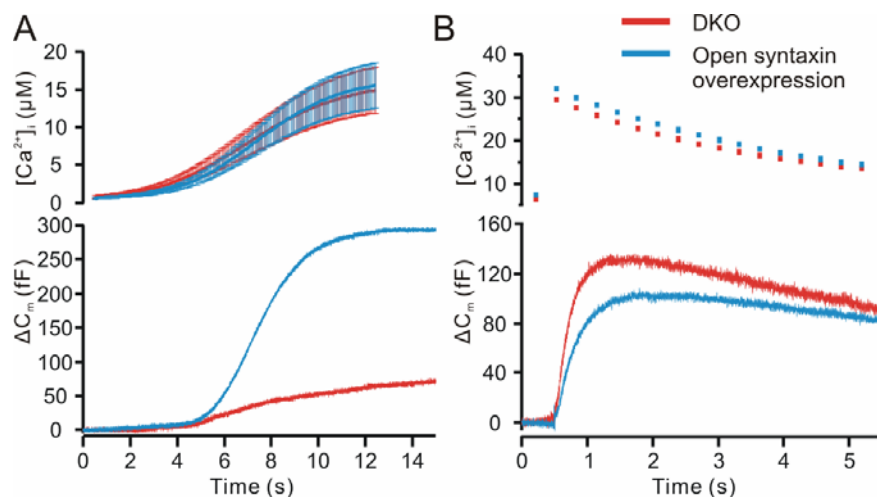
Figure 13.   The response of CAPS DKO cells and those expressing open-syntaxin to stimulation of secretion using slowly rising calcium signal.
A. The free calcium concentration is shown in the upper trace and the capacitance change is shown in the lower trace. Those cells expressing open-syntaxin (blue; n=27, N=5) exhibit very strong secretion compared to DKO cells not expressing open-syntaxin (red; n=29, N=5). **B**. In order to determine the amount of secretion remaining after the ramp stimulation, a flash was applied to increase calcium to high levels. The residual secretion in the CAPS DKOs was larger than that of the DKOs expressing open-syntaxin, and accounted for 64% of the total secretion, while the flash response in the open-syntaxin expressing DKO cells accounted for about 25% of the total secretion.

To test whether the lack of sustained release in open-syntaxin expressing CAPS DKO cells is related to CAPS or not, we expressed open-syntaxin in wild-type chromaffin cells and compared secretion in these two groups (Fig. 14A). In these cells we also observed an increase in the RRP 95.8 ± 9.4 fF versus 209.3 ± 26.0 fF, 2

fold increase, wild-type versus open-syntaxin expressing wild-type cells, no significant increase in the SRP (101.7 ± 14 fF versus 146.6 ± 25.3 fF, wild type versus open-syntaxin expressing wild type, respectively), and a reduction in the sustained phase (22.5 ± 3.8 and 4.6 ± 2.1 fF/s, wild type versus open-syntaxin expressing wild type, Fig. 14B). These experiments indicate that open-syntaxin promotes secretion by selectively enhancing the readily releasable pool, but simultaneously reduces sustained release. As in CAPS DKO cells, wild-type cells expressing open-syntaxin exhibited only modest pool refilling with a reduction in the second flash response (Fig. 14C) and a strong reduction in secretion (RRP, 136.8 ± 21.5 and 104.6 ± 18.9 fF; SRP 99.8 ± 13.0 and 56.3 ± 10.5 fF; sustained 11.4 ± 2.5 and 1.6 ± 1.0 fF (Fig. 14D). Thus it appears that open-syntaxin exhausts the secretory response and that the effects on sustained release are independent of CAPS.
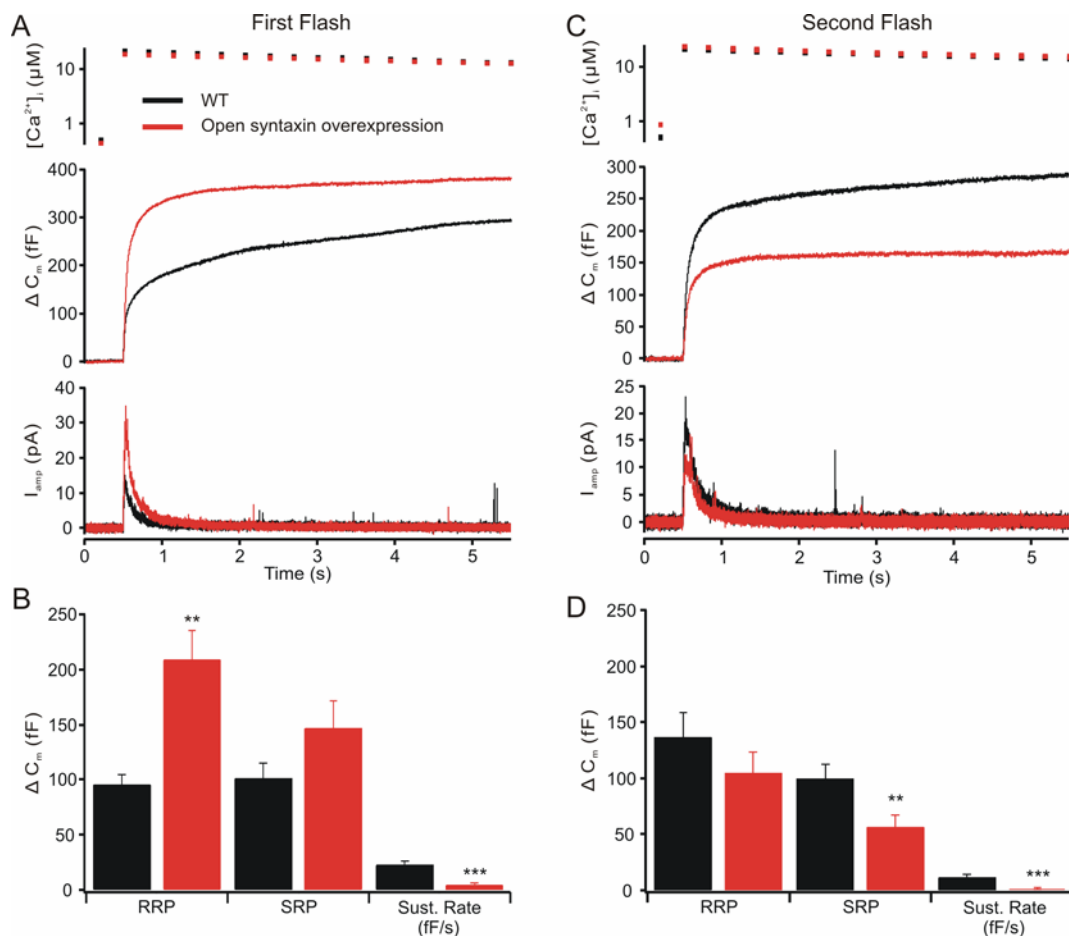
Figure 14. Expression of open syntaxin in wild type cells enhances the RRP selectively.
A. Flash photolysis release of calcium produces a larger burst of secretion in open-syntaxin

expressing wild type cells (red; n=24, N=4), when compared to cells not expressing open-syntaxin (black; n=22, N=4). This is mirrored in an increase in catecholamine release. **B**. Analysis of the kinetics of the releasable pools and the rate of sustained release show that the RRP is strongly enhanced while the SRP is unaltered. The sustained release is reduced. **C**. Examination of a second flash response after a two minute recovery period shows a deficit in refilling pools emptied by a flash stimulation in open-syntaxin expressing wild type cells. **D**. Pool analysis for the second stimulation. **p<0.01;***p<0.001.

3.3.4 Rescue of Munc13-1

3.3.4.1 Munc13-1 expression does not rescue the CAPS DKO phenotype

The above results indicate that CAPS exerts its function in LDCV priming through the opening of syntaxin, thus enabling syntaxin to engage in SNARE complex formation. The MHD domain of CAPS may be involved in the conformational change of syntaxin required for priming, as is believed to be the case for the MHD domains of Munc13 in synaptic vesicle release (Basu et al., 2005; Madison et al., 2005; Stevens et al., 2005). If this is indeed the case, rapid secretion in chromaffin cells from CAPS DKO mice should also be restored by expression of Munc13-1. Surprisingly, expression of a full-length Munc13-1-GFP construct in CAPS DKO cells failed to restore normal secretion (Fig. 15A). Actually, there was a decrease in all phases of flash-induced secretion in DKO cells expressing Munc13-1 (RRP, 48.4 ± 12.8 and 31.1 ± 8.5, DKO and Munc13-1 expression in DKO respectively; SRP, 58.1 ± 10.0, 24.7 ± 5.6, DKO and Munc13-1 expression, respectively; sustained, 2.9 ± 1.6, 1.9 ± 1.0, DKO and Munc13-1 expression, respectively; Fig. 15B).
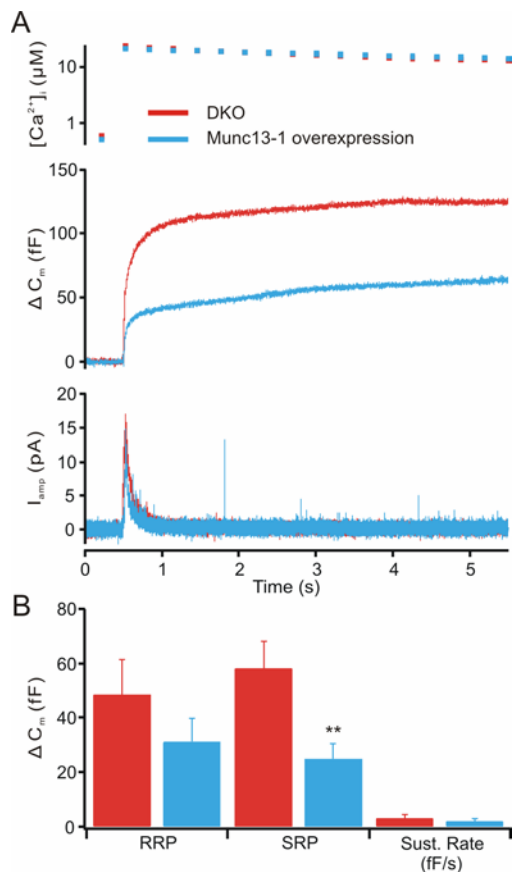
Figure 15. Expression of Munc13-1 does not enhance secretion in CAPS DKO chromaffin cells.
A. The free calcium (upper trace), the capacitance changes (middle traces) and the amperometric recordings (lower traces) show that Munc13-1 expression (blue; n=23, N=5) did not restore release to wild type levels in CAPS DKO cells (red; n=22, N=4).
B. Estimates of the kinetic parameters show that all phases were suppressed in cells expressing Munc13-1. **p<0.01.

3.3.4.2 Munc13-1 enhances exocytosis in CAPS1+-/CAPS2-- cells

Since expression of Munc13-1 strongly enhance secretion in wild type chromaffin cells, we considered whether the lack of enhanced secretion in CAPS DKO cells following Munc13-1 expression may be directly related to the lack of CAPS. We therefore examined the ability of full length Munc13-1 to enhance secretion in cells from CAPS1 +/- CAPS2 -/- mice (Fig. 16A). In these cells Munc13-1 expression enhanced all phases of secretion significantly (RRP, 145.8 ± 19 fF and 281.5 ± 39.9 fF; SRP, 82.5 ± 10.0 fF and 278.3 ± 44.0 fF; sustained, 20.0 ± 3.3 fF/s and 50.7 ± 7.2 fF/s; CAPS1+/- CAPS2-/- and CAPS1+/- CAPS2-/- expressing Munc13-1, respectively, Fig. 16B).
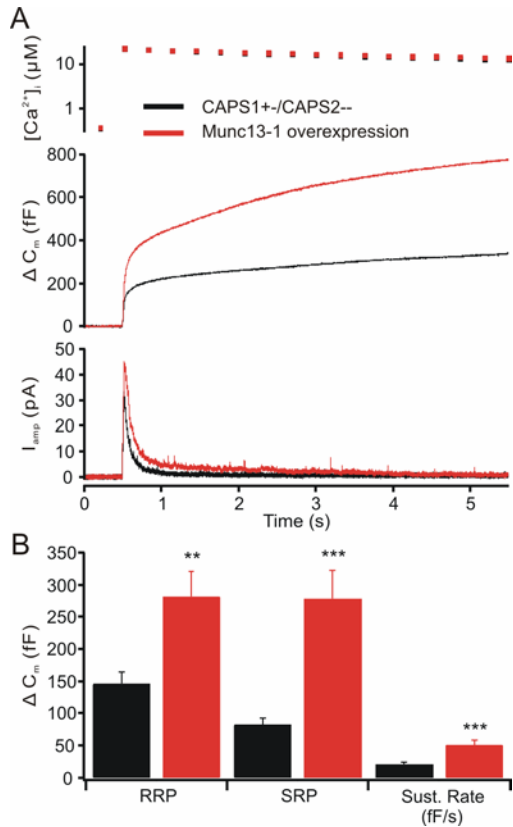
Figure 16. Munc13-1 enhances the secretion in CAPS1+-/CAPS2-- cells.

A. Munc13-1 overexpression in CAPS heterozygotes has the expected effect on secretion. Secretion was enhanced in CAPS-1 heterozygotes expressing Munc13-1 (red; n=25, N=5), when compared to CAPS-1 heterozygotes not expressing Munc13-1 (black; n=23, N=5).

B. Analysis of the kinetics of capacitance responses show that Munc13-1 enhances all phases of the response in CAPS-1 expressing chromaffin cells. **p<0.01;***p<0.001.

3.3.4.3 Munc13-1 does not enhance the exocytosis when CAPS-1 is missing

We then examined the effect of expression of Munc13-1 in cells in which CAPS1 was deleted but which had one intact allele of CAPS-2. In these cells, Munc13-1 failed to enhance secretion, and, as in the DKO cells, there was a depression of release (Fig. 17A), associated with no clear change in the relationship in releasable pools (RRP, 98.8 ± 12.4 fF and 72.8 ± 16.6 fF; SRP, 50.3 ± 7.5 fF and 33.8 ± 5.7 fF; sustained, 9.2 ± 2.4 fF/s and 6.3 ± 2.2 fF/s; CAPS1-/- CAPS2+/- and CAPS1-/- CAPS2+/- expressing Munc13-1, respectively, Fig. 17B). Expression of Munc13-1 in wild type cells resulted in the expected robust enhancement of all phases of secretion. Thus it appears that in the absence of CAPS-1, Munc13-1 does not enhance secretion while in cells expressing CAPS-1, expression of Munc13-1 causes an enhancement of all secretory phases. Fig. 17C shows a summary of the effects of Munc13-1 expression on the secretory burst in these experiments. This indicates an interaction between CAPS-1 and Munc13-1 in the priming process of chromaffin cells.
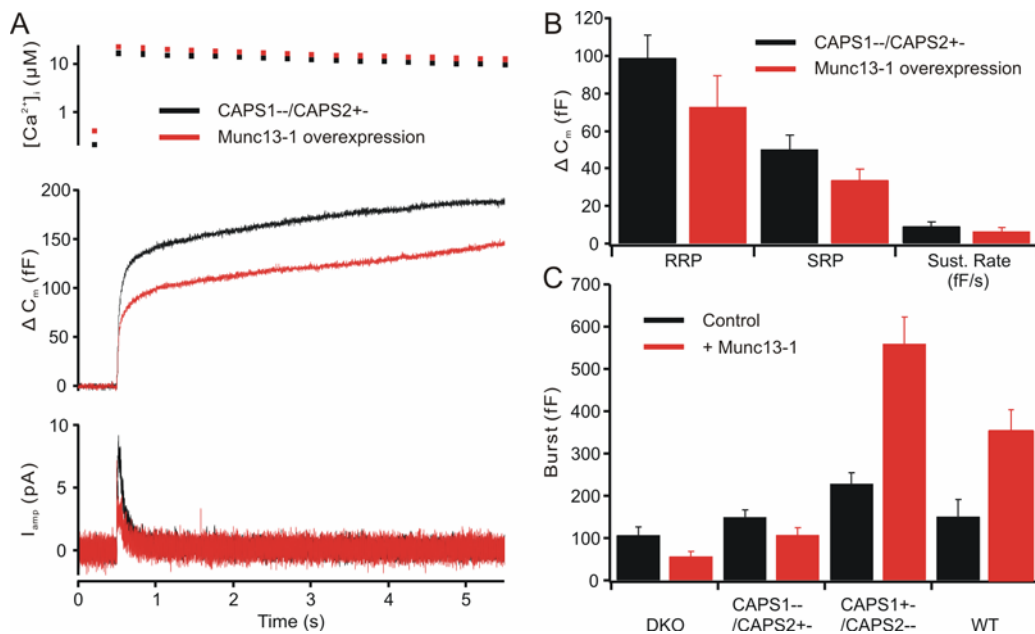
Figure 17. Munc13-1 does not enhance secretion in cells which do not express CAPS-1, even when the gene for CAPS-2 is functional.
A. Responses to flash photolysis in CAPS-1 deletion cells having one functional CAPS-2 allele. Munc13-1 expressing cells (red; n=23, N=5), in spite of slightly higher resting calcium concentrations (upper trace) secreted less than did cells from CAPS1--/CAPS2+- (black; n=22, N=5) littermates (middle trace). The catecholamine release results are consistent with the capacitance data (lower trace). **B**. The kinetic analysis of flash responses demonstrates that Munc13-1 did not enhance any component of the responses. **C**. Summary of the results of expressing Munc13-1 in chromaffin cells. In the DKO and in the CAPS1--/CAPS2+- cells, Munc13-1 expression failed to enhance responses while in CAPS1+-/CAPS2-- cells and in wild type cells, expression of munc13-1 produced a robust enhancement of secretion.

3.3.5 Treatment with PMA but not Forskolin enhances the secretion in CAPS DKO chromaffin cells

PMA induces the augmentation of neurotransmitter release through Munc13-1 and via a PKC-dependent pathway (Gillis et al., 1996; Rhee et al., 2002). Forskolin activates the PKA pathway to regulate the neurosecretion (Nagy et al., 2004). Previous reports show that application of phorbol esters rescues the neurotransmitter release from CAPS deficient hippocampal neurons to wild-type level (Jockusch et al., 2007). However in *C.elegans* Forskolin, but not phobol esters can bypass the requirement of UNC-31 for LDCVs exocytosis (Zhou et al., 2007). We tested whether the application of PMA(a phobor ester) and Forskolin enhance the secretion from chromaffin cells when CAPS is missing. PMA (500 nM) was added into the extracellular solution. Forskolin (50 µM) was perfused into the CAPS DKO cell

through the glass pipette. A train of depolarizations from -70 mV to 20 mV at 3 HZ is applied to stimulate the catecholamine release. The results are shown in Fig. 18. PMA treatment causes an increase of the secretion while Forskolin induces a modest reduction of secretion compared to CAPS DKO cells (113.6 fF from CAPS DKO cells; 164.3 fF from PMA treated DKO cells; 102.4 fF from Forskolin treated DKO cells). The calcium inward currents are comparable in all three groups suggesting that the difference of secretion is not due to the different calcium influx. PMA, but not Forskolin, enhanced the secretion from CAPS DKO cells indicates that the deficit of secretion in CAPS DKO cells can be reversed through Munc13-1 or PKC-dependent pathway but not PKA-dependent pathway.
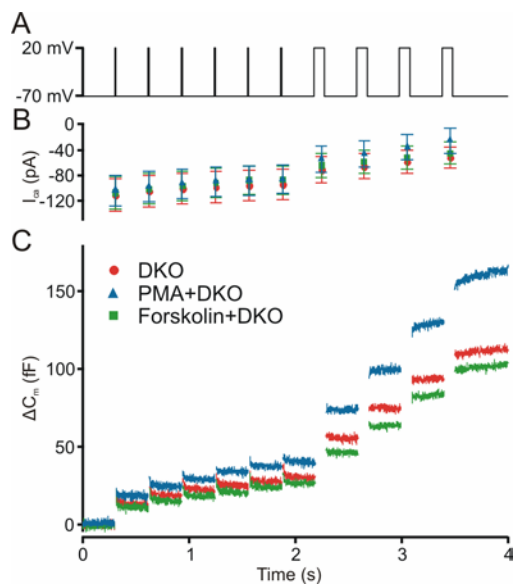
Figure 18. PMA treatment enhances the secretory response of chromaffin cells from CAPS DKO mice.
A. The schematic graph of the stimulation protocol consisting of six 10 ms depolarizations followed by four 100 ms depolarizations with 300 ms interval.
B. Averaged peak values of Ca^{2+} current (I_{ca}) are shown (mean ± SEM).
C. Averaged capacitance trace (ΔC_m) in response to the depolarization protocol. PMA (500 nM) treated CAPS DKO cells (blue; n=21, N=3) exhibit larger secretion than that of DKO cells (red; n=22, N=3), while Forskolin (50 µM) treatment (green; n=19, N=3) does not enhance the secretion of CAPS DKO cells.

3.3.6 CAPS-1 deletion mutant does not rescue the CAPS DKO phenotype

The above results suggest a priming function for CAPS which is mechanistically similar to that of Munc13's. Therefore, we tested whether the putative MUN domain of CAPS is sufficient to prime LDCVs in chromaffin cells by expressing deletion constructs of CAPS in which the proposed MUN domain remains intact. An N-terminal deletion of the first 200 amino-acids of CAPS-1 failed to enhance secretion in CAPS DKO chromaffin cells (Fig. 19A). The expression of this construct in CAPS DKOs led to a modest reduction in secretion associated with a slight

decrease in the SRP size (RRP, 45.0 ± 7.2 fF and 41.6 ± 5.4 fF; SRP, 51.9 ± 6.0 fF and 34.1 ± 5.1 fF; sustained, 2.3 ± 1.2 fF/s and 3.8 ± 1.3 fF/s; CAPS DKO and CAPS DKO expressing deletion construct, respectively, Fig. 19B). So N-terminal of CAPS may contain the information for CAPS sorting and localization thus is important for CAPS function.
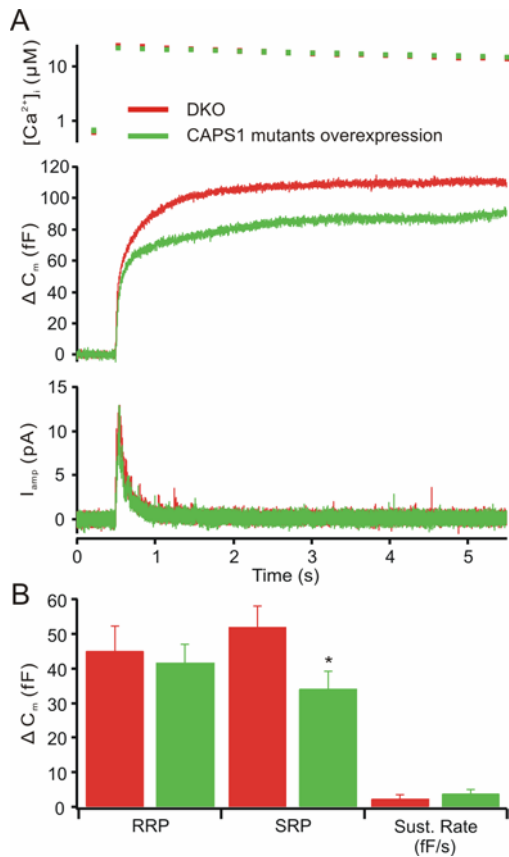
Figure 19. N-terminal 200 amino-acids deletion mutant of CAPS-1 does not retain the function.
A. Averaged $[Ca^{2+}]_i$ (upper trace), capacitance change (ΔC_m, middle trace) and amperometric response (I_{amp}, lower trace) from flash photolysis experiments are shown. The secretion of CAPS DKO cells expressing deletion mutant (green; n=23, N=5) is slightly smaller than that of DKO cells (red; n=23, N=5).
B. The SRP size is significantly reduced (*, $p<0.05$) in deletion mutant expressing DKO cells compared to DKO cells. The RRP size and sustained rate are comparable in two groups.

Table 1. Detailed parameters of flash photolysis experiments

Flash experiments	n	Pre-flash $[Ca^{2+}]_i$ (nM)	Post-flash $[Ca^{2+}]_i$ (µM)	RRP (fF)	SRP (fF)	Sustained rate (fF/s)	τ_{RRP} (ms)	τ_{SRP} (ms)
WT	23	350.3 ± 17.6	24.2 ± 2.5	99.5 ± 17.5	123.9 ± 19.6	19.8 ± 3.1	30.1 ± 4.7	612.7 ± 186.7
CAPS-2 KO	23	337.8 ± 18.6	22.2 ± 2.0	88.5 ± 9.2	95.8 ± 19.6	17.4 ± 2.0	28.8 ± 4.0	590.4 ± 125.3
WT	30	454.0 ± 28.4	23.9 ± 1.5	65.4 ± 8.3	88.0 ± 17.3	19.5 ± 2.2	28.7 ± 8.6	400.5 ± 54.7
CAPS DKO	29	435.2 ± 20.6	25.9 ± 1.8	31.3 ± 9.8	70.5 ± 14.5	0.5 ± 2.1	55.8 ± 15.3	500.4 ± 51.2
CAPS DKO 10s ISI first flash	20	593.4 ± 69.8	17.4 ± 1.2	26.0 ± 4.5	28.2 ± 5.5	1.2 ± 1.1	44.7 ± 12.8	609.3 ± 157.1
WT 10s ISI first flash	19	577.8 ± 52.5	18.5 ± 0.7	74.1 ± 10.6	52.8 ± 7.0	20.3 ± 3.2	35.6 ± 9.0	734.1 ± 261.4
CAPS DKO 10s ISI second flash	19	2.8 ± 0.3(µM)	28.1 ± 0.7	1.6 ± 4.5	89.5 ± 12.5	0 ± 0	23.4 ± 2.3	430.5 ± 51.3
WT 10s ISI second flash	19	2.4 ± 0.2(µM)	28.6 ± 0.6	35.5 ± 11.7	98.3 ± 11.0	20.3 ± 3.2	47.6 ± 20.8	529.2 ± 135.4
CAPS DKO 20s ISI first flash	25	428.8 ± 28.4	17.3 ± 0.7	26.5 ± 6.1	31.2 ± 7.4	1.8 ± 0.6	29.4 ± 4.7	619.3 ± 152.0
WT 20s ISI first flash	25	398.7 ± 16.1	16.7 ± 0.5	77.7 ± 7.2	77.4 ± 7.4	18.0 ± 2.7	30.0 ± 3.0	702.5 ± 127.3
CAPS DKO 20s ISI second flash	24	1.1 ± 0.1(µM)	24.0 ± 0.7	8.5 ± 3.6	73.2 ± 12.3	0 ± 0	41.2 ± 16.0	411.7 ± 69.5
WT 20s ISI second flash	25	0.9 ± 0.1(µM)	23.2 ± 0.5	51.0 ± 10.3	115.7 ± 10.2	7.1 ± 4.1	30.0 ± 4.9	562.8 ± 82.5
CAPS DKO 40s ISI first flash	15	407.2 ± 33.6	16.8 ± 1.0	24.2 ± 4.6	29.3 ± 11.0	0.8 ± 1.2	30.6 ± 4.9	578.5 ± 117.6

WT40s ISI first flash	12	382.6 ± 24.7	17.3 ± 0.8	71.2 ± 16.3	65.2 ± 15.0	17.0 ± 2.2	32.5 ± 6.4	502.8 ± 144.7
CAPS DKO 40s ISI second flash	13	524.3 ± 52.8	19.5 ± 0.9	11.5 ± 1.8	34.1 ± 10.1	0 ± 0	29.3 ± 5.0	663.4 ± 186.7
WT 40s ISI second flash	13	479.9 ± 28.5	18.7 ± 0.7	61.6 ± 10.1	74.2 ± 10.8	6.1 ± 2.4	37.7 ± 5.9	634.6 ± 161.0
CAPS DKO	15	597.1 ± 58.5	21.9 ± 1.4	22.1 ± 5.7	25.2 ± 8.4	2.4 ± 1.5	40.0 ± 2.0	630.0 ± 27.6
CAPS-1 rescue	17	694.5 ± 71.1	24.0 ± 1.5	155.6 ± 23.0	69.1 ± 8.3	20.9 ± 3.3	26.7 ± 3.0	461.0 ± 13.0
CAPS DKO	19	541.3 ± 43.5	23.2 ± 1.1	42.8 ± 18.6	51.7 ± 12.2	0 ± 0	23.5 ± 5.2	532.9 ± 14.4
CAPS-2 rescue	24	479.6 ± 36.1	21.1 ± 1.0	125.3 ± 25.8	51.8 ± 7.5	19.2 ± 3.7	23.2 ± 1.4	401.9 ± 10.8
WT	26	428.9 ± 26.1	20.0 ± 0.7	79.0 ± 13.8	60.8 ± 10.7	19.1 ± 2.4	30.6 ± 2.7	505.2 ± 41.5
CAPS-1 in WT	24	565.0 ± 47.1	23.1 ± 0.9	105.0 ± 16.1	60.7 ± 9.4	26.1 ± 5.2	23.5 ± 2.7	579.2 ± 140.0
CAPS DKO first flash	23	647.4 ± 90.9	26.3 ± 1.3	48.5 ± 11.9	53.9 ± 8.9	1.4 ± 1.0	24.3 ± 12.0	258.6 ± 37.2
Open syntaxin in CAPS DKO first flash	24	604.2 ± 69.1	21.0 ± 1.0	129.2 ± 21.8	79.5 ± 11.3	1.1 ± 1.5	34.4 ± 9.0	300.0 ± 41.9
CAPS DKO second flash	20	641.0 ± 106.0	25.6 ± 1.6	42.0 ± 7.5	58.0 ± 7.6	0.2 ± 1.9	28.9 ± 4.1	330.2 ± 54.0
Open syntaxin in CAPS DKO second flash	17	553.9 ± 49.5	20.7 ± 1.0	35.9 ± 11.2	32.6 ± 11.7	3.1 ± 1.2	22.6 ± 4.0	259.5 ± 59.6
WT first flash	24	501.2 ± 34.3	22.0 ± 0.9	95.8 ± 9.4	101.7 ± 14.0	22.5 ± 3.8	19.7 ± 1.6	459.1 ± 68.7
Open syntaxin in WT first flash	22	434.3 ± 34.2	19.2 ± 1.0	209.3 ± 26.0	146.6 ± 25.3	4.6 ± 2.1	35.1 ± 5.5	338.4 ± 42.4
WT second flash	18	510.5 ± 41.5	22.2 ± 1.1	136.8 ± 21.5	99.8 ± 13.0	11.4 ± 2.5	33.7 ± 4.6	293.2 ± 47.9
Open syntaxin in WT second Flash	20	578.2 ± 122.4	20.9 ± 1.7	104.6 ± 18.9	56.3 ± 10.5	1.6 ± 1.0	34.9 ± 5.6	389.2 ± 54.5
CAPS DKO	22	575.8 ± 45.6	23.9 ± 1.2	48.4 ± 12.8	58.1 ± 10.0	2.9 ± 1.6	19.7 ± 4.0	324.7 ± 51.3
Munc13-1 in CAPS DKO	23	499.2 ± 48.2	21.5 ± 1.4	31.1 ± 8.5	24.7 ± 5.6	1.9 ± 1.0	22.9 ± 5.2	792.7 ± 193.8

CAPS1+-/CAPS2--	23	359.7 ± 45.7	21.0 ± 1.0	145.8 ± 19.0	82.5 ± 10.0	20.0 ± 3.3	22.9 ± 3.1	519.2 ± 8.2
Munc13-1 in CAPS1+-/CAPS2--	25	360.7 ± 47.2	20.6 ± 1.0	281.5 ± 39.9	278.3 ± 44.0	50.7 ± 7.2	22.5 ± 2.5	1038.7 ± 214.4
CAPS1--/CAPS2+-	22	210.8 ± 36.7	17.0 ± 0.9	98.8 ± 12.4	50.3 ± 7.5	9.2 ± 2.4	27.4 ± 3.3	376.0 ± 42.0
Munc13-1 in CAPS1--/CAPS2+-	23	399.3 ± 46.5	23.2 ± 0.9	72.8 ± 16.6	33.8 ± 5.7	6.3 ± 2.2	21.9 ± 3.4	474.7 ± 37.6
CAPS DKO	23	619.3 ± 90.4	24.4 ± 1.2	45.0 ± 7.2	51.9 ± 6.0	2.3 ± 1.2	31.6 ± 5.5	435.4 ± 43.9
200-1256 Deletion construct in CAPS DKO	23	674.8 ± 96.6	22.1 ± 1.4	41.6 ± 5.4	34.1 ± 5.1	3.8 ± 1.3	30.8 ± 6.6	476.1 ± 104.1

Table 2. Properties of individual fusion events measured by amperometry

	n	Events frequency (1/s)	Charge (fC)	Amplitude (pA)	Rise time (ms)	Half-width (ms)	Foot amplitude (pA)	Foot duration (ms)	Foot charge (fC)
WT	16	1.8 ± 0.2	88.5 ± 6.3	12.9 ± 1.8	0.69 ± 0.08	5.5 ± 0.5	1.4 ± 0.2	3.3 ± 0.4	3.1 ± 0.7
CAPS-2 KO	14	1.6 ± 0.2	102.2 ± 9.2	15.2 ± 2.0	0.63 ± 0.05	4.7 ± 0.3	1.6 ± 0.2	3.7 ± 0.6	3.4 ± 0.7
WT	12	1.7 ± 0.19	74.7 ± 4.6	12.3 ± 1.3	0.71 ± 0.10	4.5 ± 0.5	1.4 ± 0.2	3.2 ± 0.4	2.7 ± 0.5
CAPS DKO	10	0.54 ± 0.08	76.3 ± 10.0	10.2 ± 1.3	0.66 ± 0.08	5.1 ± 0.3	1.1 ± 0.2	3.1 ± 0.6	2.0 ± 0.5

4 Discussion

Studies in last twenty years provide detailed insight into the regulation of neurotransmitter release. It has been widely accepted that the SNARE complex is the core machinery of membrane fusion. Many proteins are involved to control the assembly of the SNARE complex and regulate the membrane fusion. CAPS (Ca^{2+}-dependent activator protein for secretion) is found as a soluble factor that reconstitutes calcium-dependent secretion in permeabilized PC 12 cells. Disturbance of CAPS leads to motor and nervous system defects indicating an important role of CAPS in LDCVs and SVs exocytosis. However at which step in the secretory pathway CAPS functions is still unknown. In the present work, we take the advantage of CAPS knockout mice, investigated the role of CAPS in mouse adrenal medulla chromaffin cells using morphological and electrophysiological assays.

4.1 Deletion of CAPS-2 does not change the secretion

Mammals express two CAPS isoforms which are highly homologous to UNC-31 and contain a coiled-coil domain (Munc13 homology domain, MHD) with similarity to UNC-13/Munc-13. As UNC-13/Munc-13 functions in priming of synaptic vesicles and secretory granules and the presence of a region containing two MHDs is critical for its priming action, CAPS has a conserved MHD, raising the possibility that CAPS functions similarly to UNC-13/Munc-13. Previous studies in permeabilized PC12 cells show that CAPS is required for ATP dependent priming in LDCV secretion (Berwin et al., 1998; Grishanin et al., 2004). Deletion of CAPS-1 causes a deficit in catecholamine secretion from mouse chromaffin cells and leads to fusion of LDCVs containing no catecholamines indicating a role of CAPS-1 in catecholamine loading as well as in secretion (Speidel et al., 2005). We have now examined the secretion from CAPS-2 knockout mice chromaffin cells using flash photolysis and amperometric techniques. Results from flash photolysis experiments show that the absence of CAPS-2 does not cause a change of the secretion. Ramp experiments also show that the secretion of CAPS-2 knockout chromaffin cells is comparable with that of wild-type cells, and indicate that Ca^{2+}-sensitivity of secretion is unchanged

when CAPS-2 is missing. We examined the kinetics of single vesicle fusion using carbon-fibre electrode. No significant difference of properties of single amperometric spikes was found. Since CAPS-1 and CAPS-2 are highly homologous and both are present in mouse chromaffin cells, the phenotype observed from CAPS-1 or CAPS-2 single knockout mouse chromaffin cells was probably mitigated by the presence of another CAPS isoform. To get a better understanding of CAPS function, CAPS DKO mice were required.

4.2 CAPS facilitates the filling of the rapidly releasable pool

We have examined catecholamine secretion in mouse chromaffin cells deficient in both CAPS-1 and CAPS-2. Mouse chromaffin cells from which both CAPS-1 and CAPS-2 are deleted exhibit a large deficit in exocytosis, with a pronounced deficit in the RRP, whereas the deficit in the SRP is not statistically significant. The sustained rate of release, which reflects the refilling of the readily releasable pool under elevated Ca^{2+}, is dramatically depressed in CAPS DKO cells. The reduction of the readily releasable pool and the sustained release rate in CAPS DKO cells could be due to either a deficit in vesicle docking or priming. Because we observed no difference in vesicle density or distribution, or in the number of morphologically docked vesicles, we conclude that there is a specific deficit in priming in CAPS DKO cells.

Our dual flash experiments indicate that while refilling occurs, recovery of the RRP following strong secretory activity was greatly reduced in CAPS DKO cell as compared to wild type cells. Surprisingly, SRP filling approaches wild type levels at short intervals, indicating that priming into the SRP proceeds normally in CAPS DKO cells. In spite of filling of the SRP, the RRP does not adequately refill. Since the burst size at interstimulus intervals (ISIs) of two minutes or 45 s is smaller than that at an ISI of 15 s in CAPS DKO cells, and the RRP is not refilled at 45 s. This may result from unpriming in mutant cells.

A defect in priming from the SRP to the RRP, or a lack of stability of the RRP could explain this result and the lack of RRP refilling, as well as the decrease in secretory burst size in CAPS DKO cells. Thus, in wild type cells the secretory burst (i.e. the

sum of SRP and RRP) remains relatively constant while in CAPS DKO cells the burst at an ISI of 15 s is larger than that after a 25 s or 45 s ISI. A similar increase in SRP in wild type cells is translated into a filled RRP, as the decrease in SRP over time is similar to the gain in the RRP, while only about 50 % of the decrease in SRP in CAPS DKO cells is translated into a gain in RRP. Thus, in the absence of CAPS, vesicles primed to the SRP are lost without being secreted. Although pool refilling occurs in CAPS DKO cells, there is little sustained release at intracellular calcium levels which normally would release primed vesicles. This is underscored by the lack of sustained secretion in spite of overfilling of the SRP, which can be explained if sustained release comes from the RRP rather than from the SRP. We cannot rule out that sustained release is masked to a degree by endocytosis.

Our data indicate that CAPS is a priming factor favouring the filling of RRP, consistent with the recent reports that CAPS is critical for vesicle priming in hippocampal neurons, pancreatic β-cells and PC12 cells (Fujita et al., 2007; Jockusch et al., 2007; Speidel et al., 2008). However the lack of a change in morphologically docked vesicles and the efficient filling of the SRP in CAPS DKO cells are not consistent with a deficit in docking observed in *C. elegans* neurons (Hammarlund et al., 2008; Zhou et al., 2007). The distinct conclusions about CAPS function may arise from the different definitions of docking and priming. Docked vesicles are defined by the close apposition to the plasma membrane and a fraction of docked vesicles have undergone the priming process to be release competent. Hammarlund et al. counted the vesicles without a measureable distance between vesicles and plasma membrane as docked vesicles. This criterion of docking is so strict that the number of docked vesicles maybe underestimated. It is also possible that the requirement for visible contact with the membrane selects a subset of docked vesicles which are also primed. We have examined the cumulative distribution of distance between vesicles and plasma membrane in CAPS DKO and wild-type cells. The comparable distance distributions in both groups indicate that the deficit of exocytosis in CAPS DKO cells can not be due to a defect of docking, indicating that CAPS is a priming factor.

4.3 Calcium sensitivity and fusion kinetics in CAPS DKO cells

The calcium-dependence of release, as determined by calcium ramp stimulation, is the same in DKO cells and wild type cells. As in the flash experiments, the ramp stimulation caused robust secretion in wild type chromaffin cells. Secretion in the CAPS DKO cells during the ramp stimulation was ~20 % of that observed in wild type cells, a greater deficit than that observed in the flash experiments (~46 %). In ramp experiments, the total burst in the CAPS DKO cells was ~80 fF, while the burst in the wild type cells was about 200 fF, similar to those observed in flash experiments. The ratio of wild type burst size to that of the DKO was ~ 2.5, also similar to that observed in the flash experiment (~2). As the calcium concentration reached in the ramp protocol is similar to that achieved after the flash, the greater decrease in net secretion observed in CAPS DKO cells after ramp stimulation is likely due to a lack of sustained release in the DKO.

The chromaffin granule priming process is calcium-dependent, with an estimated Kd for calcium of 2.3 µM (Moser and Neher, 1997). Thus, priming is promoted at increased intracellular calcium levels. In hippocampal neurons lacking CAPS, deficits in glutamatergic neurotransmission can be partially reversed by increasing extracellular calcium (Jockusch et al., 2007). However it is not clear whether this enhancement of secretion under high calcium is due to the change of calcium dependence for release or for priming. In our experiments we show that the calcium sensing for release does not change in CAPS DKO cells. The lack of sustained release and the greater deficit in ramp experiments may indicate that the calcium-dependence of priming is impaired in the absence of CAPS. CAPS is thought to function in a calcium-dependent manner, and thus is likely more effective at higher calcium concentrations. If CAPS favours RRP priming and is involved in the calcium-dependent enhancement of priming, both enhancement of the RRP and sustained release could be explained.

We have examined the fusion parameters in CAPS DKO cells using carbon fibre electrodes. No significant difference in the kinetic properties of single granule fusion events were found after the detailed analysis of spike charge, amplitude, half-width,

50-90% rising time and foot duration. This fits with the previous reports in CAPS-1 knockout cells and in CAPS knockdown PC12 cells (Fujita et al., 2007; Speidel et al., 2005) but is not consistent with the previous report from (Elhamdani et al., 1999). They perfused CAPS antibody into calf adrenal chromaffin cells via a patch pipette and tested the kinetics of catecholamine secretion using amperometric technique. Their results suggest that CAPS regulates the fusion pore dilation of LDCVs to the plasma membrane. The discrepancy is likely because they used antibody which may bind with CAPS localized to the vesicle membrane causing the fusion pore effect. In our experiments, genetic deletion was used to inactivate CAPS. Our results indicate absence of CAPS does not change the fusion kinetics.

4.4 Either CAPS-1 or CAPS-2 expression rescue CAPS DKO phenotype

Expression of either CAPS-1 or CAPS-2 in the CAPS-DKO cells rescued the RRP, the SRP and sustained release, with a more pronounced effect on the RRP. This finding indicates that the observed deficits are due to the lack of CAPS, and not to indirect effects of the CAPS loss, e.g. on cell differentiation and development, and that CAPS in chromaffin cells facilitates the filling of the RRP and supports sustained release. It also indicates that both CAPS isoforms have similar activity and both can replace deleted CAPS proteins. The preferential effect on the RRP is consistent with a post docking effect, since, in the currently accepted linear priming pathway, increased docking will not selectively enhance the RRP.

CAPS-1 and CAPS-2 are highly homologous, sharing very similar domain structures. Overexpression of CAPS-1 or CAPS-2 in permeabilized PC12 cells reconstituted the Ca^{2+}-triggered LDCV exocytosis to similar levels indicating that CAPS-1 and CAPS-2 are functionally equivalent in Ca^{2+}-dependent LDCV exocytosis (Speidel et al., 2003). This fits with our observations that CAPS-1 and CAPS-2 have similar activity. However CAPS-1 and CAPS-2 exhibit distinct spatial and developmental expression patterns. The expression level of CAPS-2 is more constant than CAPS-1 during development. CAPS-1 is exclusively expressed in brain and neuroendocrine tissues

and CAPS-2 is also found in other tissues. Immunostaining studies in mouse chromaffin cells show that CAPS-1 and CAPS-2 are localized to different populations of LDCVs (Speidel et al., 2003). Deletion of CAPS-1 but not CAPS-2 induces the perinatally lethal phenotype. Expression of CAPS-1 in CAPS DKO cells enhances the size of the SRP, while expression of CAPS-2 does not. All above results indicate that there is subtle functional difference between CAPS-1 and CAPS-2. Experiments form mouse pancreatic β-cells show that the size of the RRP is similarly affected whereas the morphologically docked pool is differentially reduced in CAPS-2 KO and CAPS-1+-/CAPS-2-- β-cells. It was suggested that CAPS-1 regulates the movements of secretory granules towards the plasma membrane and CAPS-2 is involved in the maintenance of the RRP (Speidel et al., 2008). The differential regulation of exocytosis by CAPS-1 and CAPS-2 may be caused by either distinct Ca^{2+} affinities or compartmentalization within cells. These results suggest distinct roles of CAPS-1 and CAPS-2 in β-cells but are not consistent with our oberservations that deletion of CAPS does not change the morphological docking of LDCVs in chromaffin cells. Our data suggest that only when CAPS-1 is present overexpression of Munc13-1 cause an enhancement of secretion in mouse chromaffin cells. This leads to the possibility that Munc13-1 selectively interacts with CAPS-1 but not CAPS-2. The reason for this is still not clear. Further investigation in neuronal development and molecular mechanism of CAPS function might provide new insight into this issue.

An N-terminal deletion mutant of CAPS-1 failed to rescue the secretion in CAPS DKO cells. This is consistent with the previous findings that there is a N-terminal dynactin 1 binding domain (DBD) which is required for CAPS protein sorting (Sadakata et al., 2007) and phosphorylation of N-terminal Ser-5, -6 and -7 is necessary for CAPS activity (Nojiri et al., 2009). Deletion of N-terminal 200 amino-acids might cause improper sorting of CAPS protein or the lack of phosphorylation sites and block the activity of CAPS. James et al. examined whether the PH domain or the MHD domain of CAPS is sufficient to stimulate liposome fusion as the full length CAPS did. Both fragments failed to stimulate the liposome fusion even at high concentration, indicating that full length CAPS is required for the function of CAPS (James et al., 2008, 2009). This could also explain why the deletion mutant of CAPS-1 does not

rescue the CAPS DKO phenotype.

4.5 Interaction between CAPS, syntaxin and Munc13-1

Expression of a constitutively open syntaxin mutant (open-syntaxin, (Dulubova et al., 1999)) reversed the RRP deficit in CAPS DKO cells in flash photolysis experiments, although sustained release remained suppressed. The lack of sustained release in the open-syntaxin expressing cells may be due to the reported docking deficit (Gerber et al., 2008). It is unrelated to the absence of CAPS, since it also occurs in wild type chromaffin cells.

When secretion in open-syntaxin expressing cells was stimulated using a calcium ramp, there was a ~4-fold increase in secretion during the stimulus compared to that in the CAPS DKO cells. A flash application following the ramp showed that residual secretion was slightly greater in the CAPS DKO cells than in open-syntaxin expressing cells. Though the apparent reluctance of the pools to empty in DKO cells may indicate a higher calcium requirement for the SRP, it is more likely due to more rapid exhaustion of the pools in open-syntaxin expressing cells, with secretion in response to the post-ramp flash consisting of slowly releasable vesicles.

Since CAPS shares an RRP-enhancing effect with open-syntaxin, it may well function to open syntaxin (Richmond et al., 2001). Open-syntaxin rescues the locomotion defects in *C. elegans* unc-31 mutants and the vesicle docking defect that is detectable in high-pressure frozen EM samples of these mutants (Hammarlund et al., 2008; Zhou et al., 2007) but rescue of transmitter release defects was not tested in these studies. The highly restricted definition of morphological docking used in this study may be a structural correlate of functional priming.

In light of the effects of open-syntaxin, we expected that Munc13-1 expression would also reverse the priming deficits in the CAPS DKO. Introduction of Munc13-1 failed to enhance pool size in CAPS DKO cells and actually led to reduced secretion. Since Munc13-1 strongly enhanced secretion in CAPS-1 heterozygotes and CAPS-2 KOs, it appears that exogenous Munc13-1 cannot prime in the absence of CAPS-1. This may indicate a functional interaction between CAPSs and Munc13s. Such an interaction has been suggested to occur in mouse hippocampal neurons (Jockusch et

al., 2007), where overexpression of Munc13-1 also failed to reverse deficits in synaptic transmission in CAPS DKO neurons, although in these cells Munc13 apparently still functioned in priming, based on the ability of phorbol esters and calcium to enhance the remaining priming and transmitter release in CAPS DKO cells. Interestingly, also in *C. elegans* neurons, dense-core vesicle secretion, which is strongly CAPS dependent, is enhanced by phorbol esters, but only when CAPS is present (Zhou et al., 2007). Open syntaxin expression enhanced the RRP selectively, as does CAPS, while expression of Munc13-1 (in the presence of CAPS1) led to a non-selective enhancement of secretion from both the SRP and the RRP. This indicates that Munc13-1 acts upstream of CAPS and that opening of syntaxin may also involve CAPS. The effects on sustained release indicate a role for CAPS in Ca^{2+}-dependent priming. An interaction of CAPS with syntaxin has recently been reported (James et al., 2009) in a study showing that the fusogenic effect of CAPS in a SNARE complex-dependent liposome fusion assay is inhibited by a soluble syntaxin fragment and that CAPS binds to syntaxin containing SNAREs as well as to syntaxin alone. This function of CAPS appears to result in enhanced SNARE complex formation, which would be congruent with our results indicating a combined Munc13/CAPS function.

4.6 Outlook

CAPS is found on LDCVs of chromaffin cells (Speidel et al., 2005). Its attachment is mediated by a C-terminal DCV-binding sequence (Grishanin et al., 2002). A central pleckstrin homology domain allows CAPS to associate at PIP-4,5- inositol bisphosphate-rich patches of membrane (Grishanin et al., 2004), leading to the suggestion that CAPS may bridge the gap between DCV and presynaptic membrane, tethering the vesicle at the membrane (James et al., 2008), consistent with the role of PIP-4,5- inositol bisphosphate in secretion (Aoyagi et al., 2005; Milosevic et al., 2005); The presence of a MUN domain and the binding of CAPS to syntaxin (James et al., 2009) support a role of CAPS in SNARE complex formation. The latter is consistent with our results showing that CAPS facilitates priming and increases the RRP (Liu et al., 2008). Here we show that open-syntaxin can replace CAPS in its

priming function, but that Munc13-1 cannot, indicating an interdependence of these two proteins. These results suggest that though CAPS may seed SNARE complex formation, its influence on the RRP indicates that it remains associated with the complex to final maturation and its presence encourages maturation to the readily releasable state. The calcium-dependence of CAPS function can be due to intrinsic calcium binding, its dependence on Ca^{2+}-dependent processes such as phosphoinositol-4, 5 bisphosphate formation or due to its association with Ca^{2+}-modulated proteins such as Munc13. This scenario is consistent with the requirement for CAPS in multiple steps of the maturation of LDCVs, i.e. in morphological docking (Hammarlund et al., 2008), its association with syntaxin (Hammarlund et al., 2008; James et al., 2009) and its role in priming the RRP (Liu et al., 2008).

5. Summary

The regulated exocytosis of neurotransmitters and many hormones occurs at specialized secretory complexes via Ca^{2+} - triggered fusion of secretory vesicles with the plasma membrane. The molecular machinery of neurotransmitter or hormone release has been the focus of intensive research. Many proteins have been isolated that may play a role in this highly regulated form of exocytosis. CAPS (calcium-activator protein for secretion) is a cytosolic protein that associates with large dense core vesicles and is involved in their secretion. Mammals express two CAPS isoforms which share a similar domain structure including a Munc13-homology domain (MHD) that is believed to be involved in the priming of secretory vesicles. Where in the secretory pathway CAPS acts is still under debate. We examined the secretion from CAPS-2 KO chromaffin cells which exhibit similar secretion as wild-type cells. We then examined secretion from chromaffin cells in which both CAPS genes were deleted in an attempt to discover how CAPS functions in regulated exocytosis.

Deletion of both CAPS isoforms causes a strong reduction of the pool of rapidly releasable chromaffin granules and of sustained release during ongoing stimulation. The similar distribution of LDCVs in CAPS DKO and wild type cells excludes the possibility that suppressed secretion in CAPS DKO cells is caused by a defect in docking of LDCVs. Dual flash experiments indicate the recovery of RRP is greatly reduced but the refilling of SRP remains normal following strong secretory activity in CAPS DKO cells as compared to wild type cells. The calcium sensitivity of exocytosis and the fusion kinetics were examined by "calcium ramp" experiments and single spike analysis experiments respectively. Deletion of CAPS does not alter calcium sensing or the kinetics of single vesicle fusion during secretion.

Either CAPS-1 or CAPS-2 can rescue secretion in cells lacking both CAPS isoforms. Furthermore, the deficit in the readily releasable LDCV pool upon CAPS loss is rescued by a constitutively open form of syntaxin, but not by Munc13-1, a priming protein that facilitates the conversion of syntaxin to the open conformation. We conclude that CAPS is required for the refilling and/or maintenance of the rapidly

---------- Summary ----------

releasable granule pool and appears to function downstream of Munc13s, a functional interaction between these two proteins seems to be required throughout the entire LDCV priming process, including the opening of syntaxin.

6. Reference:

Albillos, A., Dernick, G., Horstmann, H., Almers, W., Alvarez de Toledo, G., and Lindau, M. (1997). The exocytotic event in chromaffin cells revealed by patch amperometry. Nature *389*, 509-512.

Alvarez de Toledo, G., Fernandez-Chacon, R., and Fernandez, J.M. (1993). Release of secretory products during transient vesicle fusion. Nature *363*, 554-558.

Ann, K., Kowalchyk, J.A., Loyet, K.M., and Martin, T.F. (1997). Novel Ca2+-binding protein (CAPS) related to UNC-31 required for Ca2+-activated exocytosis. J Biol Chem *272*, 19637-19640.

Aoyagi, K., Sugaya, T., Umeda, M., Yamamoto, S., Terakawa, S., and Takahashi, M. (2005). The activation of exocytotic sites by the formation of phosphatidylinositol 4,5-bisphosphate microdomains at syntaxin clusters. J Biol Chem *280*, 17346-17352.

Ashery, U., Varoqueaux, F., Voets, T., Betz, A., Thakur, P., Koch, H., Neher, E., Brose, N., and Rettig, J. (2000). Munc13-1 acts as a priming factor for large dense-core vesicles in bovine chromaffin cells. EMBO J *19*, 3586-3596.

Augustin, I., Rosenmund, C., Sudhof, T.C., and Brose, N. (1999). Munc13-1 is essential for fusion competence of glutamatergic synaptic vesicles. Nature *400*, 457-461.

Avery, L., Bargmann, C.I., and Horvitz, H.R. (1993). The Caenorhabditis elegans unc-31 gene affects multiple nervous system-controlled functions. Genetics *134*, 455-464.

Axelrod, D. (2001). Total internal reflection fluorescence microscopy in cell biology. Traffic *2*, 764-774.

Basu, J., Shen, N., Dulubova, I., Lu, J., Guan, R., Guryev, O., Grishin, N.V., Rosenmund, C., and Rizo, J. (2005). A minimal domain responsible for Munc13 activity. Nat Struct Mol Biol *12*, 1017-1018.

Berwin, B., Floor, E., and Martin, T.F. (1998). CAPS (mammalian UNC-31) protein localizes to membranes involved in dense-core vesicle exocytosis. Neuron *21*, 137-145.

Betz, A., Okamoto, M., Benseler, F., and Brose, N. (1997). Direct interaction of the rat unc-13 homologue Munc13-1 with the N terminus of syntaxin. J Biol Chem *272*, 2520-2526.

Blasi, J., Chapman, E.R., Link, E., Binz, T., Yamasaki, S., De Camilli, P., Sudhof, T.C., Niemann, H., and Jahn, R. (1993). Botulinum neurotoxin A selectively cleaves the synaptic protein SNAP-25. Nature *365*, 160-163.

---------- Literature----------

Bollmann, J.H., Sakmann, B., and Borst, J.G. (2000). Calcium sensitivity of glutamate release in a calyx-type terminal. Science *289*, 953-957.

Bonifacino, J.S., and Glick, B.S. (2004). The mechanisms of vesicle budding and fusion. Cell *116*, 153-166.

Borisovska, M., Zhao, Y., Tsytsyura, Y., Glyvuk, N., Takamori, S., Matti, U., Rettig, J., Sudhof, T., and Bruns, D. (2005). v-SNAREs control exocytosis of vesicles from priming to fusion. EMBO J *24*, 2114-2126.

Borst, J.G., and Sakmann, B. (1996). Calcium influx and transmitter release in a fast CNS synapse. Nature *383*, 431-434.

Breckenridge, L.J., and Almers, W. (1987). Currents through the fusion pore that forms during exocytosis of a secretory vesicle. Nature *328*, 814-817.

Brose, N., Rosenmund, C., and Rettig, J. (2000). Regulation of transmitter release by Unc-13 and its homologues. Curr Opin Neurobiol *10*, 303-311.

Brunk, I., Blex, C., Speidel, D., Brose, N., and Ahnert-Hilger, G. (2009). Ca2+-dependent activator proteins of secretion promote vesicular monoamine uptake. J Biol Chem *284*, 1050-1056.

Bruns, D. (2004). Detection of transmitter release with carbon fiber electrodes. Methods *33*, 312-321.

Burgess, T.L., and Kelly, R.B. (1987). Constitutive and regulated secretion of proteins. Annu Rev Cell Biol *3*, 243-293.

Burgoyne, R.D., and Morgan, A. (2003). Secretory granule exocytosis. Physiol Rev *83*, 581-632.

Chandler, D.E., and Heuser, J.E. (1980). Arrest of membrane fusion events in mast cells by quick-freezing. J Cell Biol *86*, 666-674.

Chapman, E.R., An, S., Barton, N., and Jahn, R. (1994). SNAP-25, a t-SNARE which binds to both syntaxin and synaptobrevin via domains that may form coiled coils. J Biol Chem *269*, 27427-27432.

Charlie, N.K., Schade, M.A., Thomure, A.M., and Miller, K.G. (2006). Presynaptic UNC-31 (CAPS) is required to activate the G alpha(s) pathway of the Caenorhabditis elegans synaptic signaling network. Genetics *172*, 943-961.

Chen, Y.A., and Scheller, R.H. (2001). SNARE-mediated membrane fusion. Nat Rev Mol Cell Biol *2*, 98-106.

Chow, R.H., von Ruden, L., and Neher, E. (1992). Delay in vesicle fusion revealed by electrochemical monitoring of single secretory events in adrenal chromaffin cells. Nature *356*, 60-63.

---------- Literature----------

Cole, K.S., (1968) Membranes, Ions and Impulses. University of California Press

Dietl, P., Haller, T., Mair, N., and Frick, M. (2001). Mechanisms of surfactant exocytosis in alveolar type II cells in vitro and in vivo. News Physiol Sci *16*, 239-243.

Dulubova, I., Lou, X., Lu, J., Huryeva, I., Alam, A., Schneggenburger, R., Sudhof, T.C., and Rizo, J. (2005). A Munc13/RIM/Rab3 tripartite complex: from priming to plasticity? EMBO J *24*, 2839-2850.

Dulubova, I., Sugita, S., Hill, S., Hosaka, M., Fernandez, I., Sudhof, T.C., and Rizo, J. (1999). A conformational switch in syntaxin during exocytosis: role of munc18. EMBO J *18*, 4372-4382.

Elhamdani, A., Martin, T.F., Kowalchyk, J.A., and Artalejo, C.R. (1999). Ca(2+)-dependent activator protein for secretion is critical for the fusion of dense-core vesicles with the membrane in calf adrenal chromaffin cells. J Neurosci *19*, 7375-7383.

Fasshauer, D., Eliason, W.K., Brunger, A.T., and Jahn, R. (1998a). Identification of a minimal core of the synaptic SNARE complex sufficient for reversible assembly and disassembly. Biochemistry *37*, 10354-10362.

Fasshauer, D., Sutton, R.B., Brunger, A.T., and Jahn, R. (1998b). Conserved structural features of the synaptic fusion complex: SNARE proteins reclassified as Q- and R-SNAREs. Proc Natl Acad Sci U S A *95*, 15781-15786.

Fujita, Y., Xu, A., Xie, L., Arunachalam, L., Chou, T.C., Jiang, T., Chiew, S.K., Kourtesis, J., Wang, L., Gaisano, H.Y.*, et al.* (2007). Ca2+-dependent activator protein for secretion 1 is critical for constitutive and regulated exocytosis but not for loading of transmitters into dense core vesicles. J Biol Chem *282*, 21392-21403.

Gillis, K.D., Mossner, R., and Neher, E. (1996). Protein kinase C enhances exocytosis from chromaffin cells by increasing the size of the readily releasable pool of secretory granules. Neuron *16*, 1209-1220.

Gillis, K.D., (1995) Techniques for membrane capacitance measurements. Single-Channel Recording, 2nd edition. 155-198

Grishanin, R.N., Klenchin, V.A., Loyet, K.M., Kowalchyk, J.A., Ann, K., and Martin, T.F. (2002). Membrane association domains in Ca2+-dependent activator protein for secretion mediate plasma membrane and dense-core vesicle binding required for Ca2+-dependent exocytosis. J Biol Chem *277*, 22025-22034.

Grishanin, R.N., Kowalchyk, J.A., Klenchin, V.A., Ann, K., Earles, C.A., Chapman, E.R., Gerona, R.R., and Martin, T.F. (2004). CAPS acts at a prefusion step in dense-core vesicle exocytosis as a PIP2 binding protein. Neuron *43*, 551-562.

Hammarlund, M., Palfreyman, M.T., Watanabe, S., Olsen, S., and Jorgensen, E.M. (2007). Open syntaxin docks synaptic vesicles. PLoS Biol *5*, e198.

---------- Literature----------

Hammarlund, M., Watanabe, S., Schuske, K., and Jorgensen, E.M. (2008). CAPS and syntaxin dock dense core vesicles to the plasma membrane in neurons. J Cell Biol *180*, 483-491.

Hay, J.C., and Martin, T.F. (1992). Resolution of regulated secretion into sequential MgATP-dependent and calcium-dependent stages mediated by distinct cytosolic proteins. J Cell Biol *119*, 139-151.

Hay, J.C., and Martin, T.F. (1993). Phosphatidylinositol transfer protein required for ATP-dependent priming of Ca(2+)-activated secretion. Nature *366*, 572-575.

Horrigan, F.T., and Bookman, R.J. (1994). Releasable pools and the kinetics of exocytosis in adrenal chromaffin cells. Neuron *13*, 1119-1129.

Jahn, R., Lang, T., and Sudhof, T.C. (2003). Membrane fusion. Cell *112*, 519-533.

Jahn, R., and Scheller, R.H. (2006). SNAREs--engines for membrane fusion. Nat Rev Mol Cell Biol *7*, 631-643.

James, D.J., Khodthong, C., Kowalchyk, J.A., and Martin, T.F. (2008). Phosphatidylinositol 4,5-bisphosphate regulates SNARE-dependent membrane fusion. J Cell Biol *182*, 355-366.

James, D.J., Khodthong, C., Kowalchyk, J.A., and Martin, T.F. (2009). Phosphatidylinositol 4,5-bisphosphate regulation of SNARE function in membrane fusion mediated by CAPS. Adv Enzyme Regul.

Jockusch, W.J., Speidel, D., Sigler, A., Sorensen, J.B., Varoqueaux, F., Rhee, J.S., and Brose, N. (2007). CAPS-1 and CAPS-2 are essential synaptic vesicle priming proteins. Cell *131*, 796-808.

Junge, H.J., Rhee, J.S., Jahn, O., Varoqueaux, F., Spiess, J., Waxham, M.N., Rosenmund, C., and Brose, N. (2004). Calmodulin and Munc13 form a Ca2+ sensor/effector complex that controls short-term synaptic plasticity. Cell *118*, 389-401.

Kesavan, J., Borisovska, M., and Bruns, D. (2007). v-SNARE actions during Ca(2+)-triggered exocytosis. Cell *131*, 351-363.

Lang, T., Margittai, M., Holzler, H., and Jahn, R. (2002). SNAREs in native plasma membranes are active and readily form core complexes with endogenous and exogenous SNAREs. J Cell Biol *158*, 751-760.

Leszczyszyn, D.J., Jankowski, J.A., Viveros, O.H., Diliberto, E.J., Jr., Near, J.A., and Wightman, R.M. (1990). Nicotinic receptor-mediated catecholamine secretion from individual chromaffin cells. Chemical evidence for exocytosis. J Biol Chem *265*, 14736-14737.

Liu, Y., Schirra, C., Stevens, D.R., Matti, U., Speidel, D., Hof, D., Bruns, D., Brose, N.,

and Rettig, J. (2008). CAPS facilitates filling of the rapidly releasable pool of large dense-core vesicles. J Neurosci *28*, 5594-5601.

Madison, J.M., Nurrish, S., and Kaplan, J.M. (2005). UNC-13 interaction with syntaxin is required for synaptic transmission. Curr Biol *15*, 2236-2242.

Milosevic, I., Sorensen, J.B., Lang, T., Krauss, M., Nagy, G., Haucke, V., Jahn, R., and Neher, E. (2005). Plasmalemmal phosphatidylinositol-4,5-bisphosphate level regulates the releasable vesicle pool size in chromaffin cells. J Neurosci *25*, 2557-2565.

Moser, T., and Neher, E. (1997). Rapid exocytosis in single chromaffin cells recorded from mouse adrenal slices. J Neurosci *17*, 2314-2323.

Mosharov, E.V., and Sulzer, D. (2005). Analysis of exocytotic events recorded by amperometry. Nat Methods *2*, 651-658.

Nagy, G., Reim, K., Matti, U., Brose, N., Binz, T., Rettig, J., Neher, E., and Sorensen, J.B. (2004). Regulation of releasable vesicle pool sizes by protein kinase A-dependent phosphorylation of SNAP-25. Neuron *41*, 417-429.

Neher, E. (1998). Vesicle pools and Ca2+ microdomains: new tools for understanding their roles in neurotransmitter release. Neuron *20*, 389-399.

Nofal, S., Becherer, U., Hof, D., Matti, U., and Rettig, J. (2007). Primed vesicles can be distinguished from docked vesicles by analyzing their mobility. J Neurosci *27*, 1386-1395.

Nojiri, M., Loyet, K.M., Klenchin, V.A., Kabachinski, G., and Martin, T.F. (2009). CAPS activity in priming vesicle exocytosis requires CK2 phosphorylation. J Biol Chem *284*, 18707-18714.

Parlati, F., Weber, T., McNew, J.A., Westermann, B., Sollner, T.H., and Rothman, J.E. (1999). Rapid and efficient fusion of phospholipid vesicles by the alpha-helical core of a SNARE complex in the absence of an N-terminal regulatory domain. Proc Natl Acad Sci U S A *96*, 12565-12570.

Penner, R., Neher, E., and Dreyer, F. (1986). Intracellularly injected tetanus toxin inhibits exocytosis in bovine adrenal chromaffin cells. Nature *324*, 76-78.

Pobbati, A.V., Stein, A., and Fasshauer, D. (2006). N- to C-terminal SNARE complex assembly promotes rapid membrane fusion. Science *313*, 673-676.

Renden, R., Berwin, B., Davis, W., Ann, K., Chin, C.T., Kreber, R., Ganetzky, B., Martin, T.F., and Broadie, K. (2001). Drosophila CAPS is an essential gene that regulates dense-core vesicle release and synaptic vesicle fusion. Neuron *31*, 421-437.

Rettig, J., and Neher, E. (2002). Emerging roles of presynaptic proteins in

---------- Literature----------

Ca++-triggered exocytosis. Science *298*, 781-785.

Rhee, J.S., Betz, A., Pyott, S., Reim, K., Varoqueaux, F., Augustin, I., Hesse, D., Sudhof, T.C., Takahashi, M., Rosenmund, C.*, et al.* (2002). Beta phorbol ester- and diacylglycerol-induced augmentation of transmitter release is mediated by Munc13s and not by PKCs. Cell *108*, 121-133.

Richmond, J.E., Weimer, R.M., and Jorgensen, E.M. (2001). An open form of syntaxin bypasses the requirement for UNC-13 in vesicle priming. Nature *412*, 338-341.

Rizo, J., and Rosenmund, C. (2008). Synaptic vesicle fusion. Nat Struct Mol Biol *15*, 665-674.

Rizo, J., and Sudhof, T.C. (2002). Snares and Munc18 in synaptic vesicle fusion. Nat Rev Neurosci *3*, 641-653.

Rosenmund, C., Sigler, A., Augustin, I., Reim, K., Brose, N., and Rhee, J.S. (2002). Differential control of vesicle priming and short-term plasticity by Munc13 isoforms. Neuron *33*, 411-424.

Rupnik, M., Kreft, M., Sikdar, S.K., Grilc, S., Romih, R., Zupancic, G., Martin, T.F., and Zorec, R. (2000). Rapid regulated dense-core vesicle exocytosis requires the CAPS protein. Proc Natl Acad Sci U S A *97*, 5627-5632.

Sabatini, B.L., and Regehr, W.G. (1996). Timing of neurotransmission at fast synapses in the mammalian brain. Nature *384*, 170-172.

Sadakata, T., Itakura, M., Kozaki, S., Sekine, Y., Takahashi, M., and Furuichi, T. (2006). Differential distributions of the Ca2+ -dependent activator protein for secretion family proteins (CAPS2 and CAPS1) in the mouse brain. J Comp Neurol *495*, 735-753.

Sadakata, T., Washida, M., and Furuichi, T. (2007). Alternative splicing variations in mouse CAPS2: differential expression and functional properties of splicing variants. BMC Neurosci *8*, 25.

Scales, S.J., Finley, M.F., and Scheller, R.H. (2001). Cell biology. Fusion without SNAREs? Science *294*, 1015-1016.

Schiavo, G., Benfenati, F., Poulain, B., Rossetto, O., Polverino de Laureto, P., DasGupta, B.R., and Montecucco, C. (1992). Tetanus and botulinum-B neurotoxins block neurotransmitter release by proteolytic cleavage of synaptobrevin. Nature *359*, 832-835.

Schikorski, T., and Stevens, C.F. (2001). Morphological correlates of functionally defined synaptic vesicle populations. Nat Neurosci *4*, 391-395.

Schoch, S., Castillo, P.E., Jo, T., Mukherjee, K., Geppert, M., Wang, Y., Schmitz, F.,

---------- Literature----------

Malenka, R.C., and Sudhof, T.C. (2002). RIM1alpha forms a protein scaffold for regulating neurotransmitter release at the active zone. Nature *415*, 321-326.

Sollner, T., Bennett, M.K., Whiteheart, S.W., Scheller, R.H., and Rothman, J.E. (1993). A protein assembly-disassembly pathway in vitro that may correspond to sequential steps of synaptic vesicle docking, activation, and fusion. Cell *75*, 409-418.

Sorensen, J.B. (2004). Formation, stabilisation and fusion of the readily releasable pool of secretory vesicles. Pflugers Arch *448*, 347-362.

Sorensen, J.B., Matti, U., Wei, S.H., Nehring, R.B., Voets, T., Ashery, U., Binz, T., Neher, E., and Rettig, J. (2002). The SNARE protein SNAP-25 is linked to fast calcium triggering of exocytosis. Proc Natl Acad Sci U S A *99*, 1627-1632.

Sorensen, J.B., Nagy, G., Varoqueaux, F., Nehring, R.B., Brose, N., Wilson, M.C., and Neher, E. (2003). Differential control of the releasable vesicle pools by SNAP-25 splice variants and SNAP-23. Cell *114*, 75-86.

Sorensen, J.B., Nielsen, M.S., Gudme, C.N., Larsen, E.H., and Nielsen, R. (2001). Maxi K+ channels co-localised with CFTR in the apical membrane of an exocrine gland acinus: possible involvement in secretion. Pflugers Arch *442*, 1-11.

Sorensen, J.B., Wiederhold, K., Muller, E.M., Milosevic, I., Nagy, G., de Groot, B.L., Grubmuller, H., and Fasshauer, D. (2006). Sequential N- to C-terminal SNARE complex assembly drives priming and fusion of secretory vesicles. EMBO J *25*, 955-966.

Speese, S., Petrie, M., Schuske, K., Ailion, M., Ann, K., Iwasaki, K., Jorgensen, E.M., and Martin, T.F. (2007). UNC-31 (CAPS) is required for dense-core vesicle but not synaptic vesicle exocytosis in Caenorhabditis elegans. J Neurosci *27*, 6150-6162.

Speidel, D., Bruederle, C.E., Enk, C., Voets, T., Varoqueaux, F., Reim, K., Becherer, U., Fornai, F., Ruggieri, S., Holighaus, Y., *et al.* (2005). CAPS1 regulates catecholamine loading of large dense-core vesicles. Neuron *46*, 75-88.

Speidel, D., Salehi, A., Obermueller, S., Lundquist, I., Brose, N., Renstrom, E., and Rorsman, P. (2008). CAPS1 and CAPS2 regulate stability and recruitment of insulin granules in mouse pancreatic beta cells. Cell Metab *7*, 57-67.

Speidel, D., Varoqueaux, F., Enk, C., Nojiri, M., Grishanin, R.N., Martin, T.F., Hofmann, K., Brose, N., and Reim, K. (2003). A family of Ca2+-dependent activator proteins for secretion: comparative analysis of structure, expression, localization, and function. J Biol Chem *278*, 52802-52809.

Stevens, D.R., Wu, Z.X., Matti, U., Junge, H.J., Schirra, C., Becherer, U., Wojcik, S.M., Brose, N., and Rettig, J. (2005). Identification of the minimal protein domain required for priming activity of Munc13-1. Curr Biol *15*, 2243-2248.

Steyer, J.A., Horstmann, H., and Almers, W. (1997). Transport, docking and

----------- Literature----------

exocytosis of single secretory granules in live chromaffin cells. Nature *388*, 474-478.

Studer, D., Humbel, B.M., and Chiquet, M. (2008). Electron microscopy of high pressure frozen samples: bridging the gap between cellular ultrastructure and atomic resolution. Histochem Cell Biol *130*, 877-889.

Sudhof, T.C. (1995). The synaptic vesicle cycle: a cascade of protein-protein interactions. Nature *375*, 645-653.

Sudhof, T.C., and Rothman, J.E. (2009). Membrane fusion: grappling with SNARE and SM proteins. Science *323*, 474-477.

Sutton, R.B., Fasshauer, D., Jahn, R., and Brunger, A.T. (1998). Crystal structure of a SNARE complex involved in synaptic exocytosis at 2.4 A resolution. Nature *395*, 347-353.

Tandon, A., Bannykh, S., Kowalchyk, J.A., Banerjee, A., Martin, T.F., and Balch, W.E. (1998). Differential regulation of exocytosis by calcium and CAPS in semi-intact synaptosomes. Neuron *21*, 147-154.

Toonen, R.F., Kochubey, O., de Wit, H., Gulyas-Kovacs, A., Konijnenburg, B., Sorensen, J.B., Klingauf, J., and Verhage, M. (2006). Dissecting docking and tethering of secretory vesicles at the target membrane. EMBO J *25*, 3725-3737.

Tooze, S.A., Martens, G.J., and Huttner, W.B. (2001). Secretory granule biogenesis: rafting to the SNARE. Trends Cell Biol *11*, 116-122.

Varoqueaux, F., Sigler, A., Rhee, J.S., Brose, N., Enk, C., Reim, K., and Rosenmund, C. (2002). Total arrest of spontaneous and evoked synaptic transmission but normal synaptogenesis in the absence of Munc13-mediated vesicle priming. Proc Natl Acad Sci U S A *99*, 9037-9042.

Verhage, M., and Sorensen, J.B. (2008). Vesicle docking in regulated exocytosis. Traffic *9*, 1414-1424.

Voets, T. (2000). Dissection of three Ca2+-dependent steps leading to secretion in chromaffin cells from mouse adrenal slices. Neuron *28*, 537-545.

Voets, T., Neher, E., and Moser, T. (1999). Mechanisms underlying phasic and sustained secretion in chromaffin cells from mouse adrenal slices. Neuron *23*, 607-615.

Voets, T., Toonen, R.F., Brian, E.C., de Wit, H., Moser, T., Rettig, J., Sudhof, T.C., Neher, E., and Verhage, M. (2001). Munc18-1 promotes large dense-core vesicle docking. Neuron *31*, 581-591.

Walent, J.H., Porter, B.W., and Martin, T.F. (1992). A novel 145 kd brain cytosolic protein reconstitutes Ca(2+)-regulated secretion in permeable neuroendocrine cells. Cell *70*, 765-775.

---------- Literature----------

Weber, T., Zemelman, B.V., McNew, J.A., Westermann, B., Gmachl, M., Parlati, F., Sollner, T.H., and Rothman, J.E. (1998). SNAREpins: minimal machinery for membrane fusion. Cell *92*, 759-772.

Wojcik, S.M., and Brose, N. (2007). Regulation of membrane fusion in synaptic excitation-secretion coupling: speed and accuracy matter. Neuron *55*, 11-24.

Xu, T., Rammner, B., Margittai, M., Artalejo, A.R., Neher, E., and Jahn, R. (1999). Inhibition of SNARE complex assembly differentially affects kinetic components of exocytosis. Cell *99*, 713-722.

Zhou, K.M., Dong, Y.M., Ge, Q., Zhu, D., Zhou, W., Lin, X.G., Liang, T., Wu, Z.X., and Xu, T. (2007). PKA activation bypasses the requirement for UNC-31 in the docking of dense core vesicles from C. elegans neurons. Neuron *56*, 657-669.

Curriculum Vitae

Personal Information

Name:	Yuanyuan Liu
Date of birth:	13th August 1981
Place of birth:	Hubei
Marital status:	Married
Nationality:	China

Education

2005	Master degree in Biophysics from the Institute of Biophysics and Biochemistry, Huazhong University of Science and Technology (**HUST**), Wuhan, P. R. China
2002	Bachelor degree in Biotechnology from **HUST**, Wuhan, P. R. China
1998	Primary school

Research work

Sept.2005 – Present	Ph.D. Student of Prof. Dr. Jens Rettig, Institute of Physiology, Saarland University, Homburg/Saar, Germany
Sept.2002 – July.2005	Postgraduate Student of Dr. Xu Tao, Institute of Biophysics and Biochemistry, HUST, Wuhan, P. R. China

Publications

Liu Y, Schirra C, Matti U, Rhee J, Hof D, Bruns D, Brose N, Rieger H, Stevens DR, Rettig J. ***Molecular characterization of two distinct secretory vesicle priming steps in adrenal chromaffin cells***. J Cell Biol. (in submission)

Zeniou-Meyer M, Liu Y, Begle A, Olanish M, Hanauer A, Becherer U, Rettig J, Bader MF, Vitale N. ***The Coffin-Lowry syndrome-associated protein RSK2 is implicated in calcium-regulated exocytosis through the regulation of PLD1***. Proc Natl Acad Sci U S A. 2008 June 17;105(24):8434-8439.

Liu Y, Schirra C, Stevens DR, Matti U, Speidel D, Hof D, Bruns D, Brose N, Rettig J. ***CAPS facilitates filling of the rapidly releasable pool of large dense-core vesicles***. J Neurosci. 2008 May 21;28(21):5594-5601.

Liu Y, Schirra C, Stevens DR, Matti U, Speidel D, Hof D, Bruns D, Brose N, Rettig J. ***CAPS facilitates filling of the rapidly releasable pool of large dense-core vesicles***. 52nd Annual Meeting of the Biophysical Society, Long beach, CA, USA, 2008.